2015

Functional analysis of the propanediol utilization microcompartment shell proteins PduB and PduB' in Salmonella enterica

Brent Lehman
Iowa State University

Functional analysis of the propanediol utilization microcompartment shell proteins PduB and PduB' in *Salmonella enterica*

by

Brent Lehman

A thesis submitted to the graduate faculty

in partial fulfillment of the requirements for the degree of

MASTER OF SCIENCE

Major: Biochemistry

Program of Study Committee:
Thomas A. Bobik, Major Professor
Guru Rao
Scott Nelson

Iowa State University

Ames, Iowa

2015

TABLE OF CONTENTS

LIST OF FIGURES

CHAPTER 3: AN OPEN FORM OF PDUB' AND IMPLICATIONS OF TRANSPORT

CHAPTER 4: ROLE OF THE N-TERMINUS OF PDUB

LIST OF TABLES

ACKNOWLEDGMENTS

First and foremost I would like to thank my major professor, Dr. Tom Bobik. Words can't describe how much I've learned from you, both in life as a researcher. I can't thank you enough for and how much you've mentored me throughout my time here at Iowa State, and also for paying me.

I would also like to thank my committee members, Dr. Guru Rao, and recently-tenured Dr. Scott Nelson for serving on my committee. Both are excellent leaders in the BBMB department at Iowa State University and I'm honored they could critique my work.

Additionally, I would like to thank both past and current Bobik Lab members. Particularly, Dr. Sharmistha Sinha who first trained me in the lab. I would also like to thank Dr Chiranjit Chowdhury for helping me in troubleshooting my microcompartment purifications and enzymatic assays, especially during electron microscopy.

Finally, to those in my personal life that have supported me throughout my time here. My parents, Phil and Judy and my brother Drew for always loving and supporting me. My partner, Diana Eisenberg for inspiring and making me expand my boundaries. Finally, to all my friends, both new and old, who helped me have fun over the past 3 years.

ABSTRACT

Bacterial microcompartments (MCPs) are proteinaceous sub-cellular organelles that are widely distributed among bacteria and that function in a variety of processes ranging from global carbon fixation to enteric pathogenesis. MCPs consist of metabolic enzymes encapsulated with a protein shell. The role of the MCP is to harbor a specific metabolic pathway that produces a toxic or volatile intermediate and confine that intermediate to minimize cellular toxicity and carbon loss. To date, the protein shells of MCPs have been shown to play a functional role in transport of small metabolites through selective pores and in the encapsulation of lumen enzymes through short N-or C-terminal peptide extensions. Interestingly, homologs of the propanediol utilization (Pdu) MCP shell protein PduB' have been crystallized in two forms, one that is closed and another that forms a large channel. This suggested that these proteins undergo conformational changes that allow the transport of larger enzymatic cofactor that the MCP needs to properly function. However, no mutational work has been done to examine residues that are responsible for such a large conformational change and assess its physiological significance. Charged residues (R78, K81) and Ramachandran outlier (D79), which are located at the center of the PduB', are key structural components that when substituted with alanine cause MCP instability. Interestingly, substitutions of a channel residue A53 appears to cause central pore opening. In addition, results indicate that there is a functional difference between PduB and PduB' despite the fact that they are identical in sequence except for a 37 amino acid N-terminal extension on PduB. The smaller protein, PduB', is dispensable for MCP formation but the PduB protein which contains a 37 amino acid N-terminal extension is integral to MCP assembly and formation.

CHAPTER 1: INTRODUCTION TO BACTERIAL MICROCOMPARTMENTS

Prokaryotic Organelles – Microcompartments

As a group prokaryotes synthesize a number of subcellular compartments that are able to mediate a variety of complex processes (Murat *et al.* 2010, van Niftrik and Jetten 2012, Rae *et al.* 2013, Saier and Bogdanov 2013, Chowdhury *et al.* 2014). These compartments are analogous to the organelles in eukaryotes in that they localize a particular metabolic process, and carry a specific role in the overall metabolism of the cell. One example is bacterial microcompartments (MCPs), which are a family of organelles used to optimize specific metabolic pathways (Bobik 2006, Cheng *et al.* 2008, Kerfeld *et al.* 2010, Abdul-Rahman *et al.* 2013, Jorda *et al.* 2013, Rae, *et al.* 2013, Axen *et al.* 2014, Chowdhury *et al.* 2014). MCPs differ from other organelles in that they consist of a protein shell that encapsulates metabolic enzymes and lack a lipid membrane. The sizes of MCPs range from 100-150 nm in diameter. They are polyhedral shape, and their overall mass can be more than a gigadalton. When expressed, they occupy about 10% of the bacterial cytoplasm (Figure 1) (Bobik *et al.* 1999).

The overall function of MCPs is to localize sequentially-acting metabolic enzymes, concentrate metabolic intermediates, accelerate catalysis and block unwanted side reactions (Kerfeld *et al.* 2010, Rae *et al.* 2013, Chowdhury *et al.* 2014). This is done by confining metabolic enzymes within a sophisticated protein shell. Often, the biochemical pathway sequestered within an MCP shell produces an intermediate that is toxic or volatile and poorly

retained by the cell envelope. The MCP shell is able to retain these toxic/volatile intermediates which accelerates catalysis, blocks any potential side reactions and prevents carbon loss and cellular damage.

Genomic analysis indicate that MCPs are produced by about 20% of bacteria and that there are seven or more different types and numerous subtypes (Bobik 2006, Abdul-Rahman *et al.* 2013, Jorda *et al.* 2013, Axen *et al.* 2014). The shells of varied MCPs are built from the same family of proteins but the encapsulated enzymes are diverse and impart different physiological roles. The most studied MCP to date is the carboxysome which plays a major role in carbon fixation by the Calvin cycle. Other MCPs have been found to optimize the catabolism of 1,2-propanediol (1,2-PD), ethanolamine, glycerol, rhamnose, fucose, and fucoidan (Shively *et al.* 1973, Talarico *et al.* 1988, Price and Badger 1989, Bobik *et al.* 1999, Penrod and Roth 2006, Sriramulu *et al.* 2008, Erbilgin, *et al.* 2014). In addition, sequence analysis suggests that MCPs may be involved in the metabolism of choline, ethanol, and amino alcohols (Abdul-Rahman *et al.* 2013, Jorda *et al.* 2013, Axen *et al.* 2014). It is also of note that the 1,2-PD utilization (Pdu) and ethanolamine utilization (Eut) MCPs play an important role in enteric pathogenesis (Conner *et al.* 1998, Heithoff *et al.* 1999, Winter *et al.* 2010, Thiennimitr *et al.* 2011, Winter and Baumler 2011). Thus, MCPs are widespread bacterial organelles that have many diverse and important functions in bacterial physiology.

MCP assembly and Targeting of Lumen Enzymes

The targeting of enzymes to the lumen of MCPs is required for proper function. Interestingly, a theme has emerged where short extensions on the N- or C-terminus of structural proteins and internal enzymes play important roles in both lumen enzyme encapsulation and MCP assembly. The PduD and PduP proteins have N-terminal extensions that are required for packaging into the lumen of the Pdu MCP (Figure 2) (Fan *et al.* 2010, Fan and Bobik 2011, Kinney *et al.* 2011, Yeates *et al.* 2013). Bioinformatic analysis suggests that these targeting peptides are not be exclusive to the Pdu MCP and are widely used in other MCP families (Huseby and Roth 2013, Liu *et al.* 2015). Studies have also shown that the CcmN protein of the carboxysome has a short C-terminal sequence that is essential for carboxysome formation and recruitment of lumen enzymes during MCP assembly (Kinney *et al.* 2012). It is also known that an N-terminal sequence of the PduV shell protein is capable of directing GFP to the outer surface of the Pdu MCP (Parsons *et al.* 2010). Finally, encapsulation of the PduP enzyme requires binding to C-terminal extensions of the PduA and PduJ shell proteins (Fan *et al.* 2010). So, the theme of short, terminal sequences to direct assembly in enzyme incorporation appears to play a prominent role in MCP design.

Microcompartment Shell Organization

The shells of diverse MCPs are formed almost entirely of the bacterial microcompartment (BMC)-domain family of proteins, suggesting varied MCPs operate under the same set of

functional principles that have been evolutionary maintained. The BMC family was established early on by structural studies of carboxysome shell proteins and the classification soon spread to the shell proteins of the Pdu and Eut MCPs (Price *et al.* 1993, English *et al.* 1994, Stojiljkovic *et al.* 1995, Bobik *et al.* 1999, Kofoid *et al.* 1999). The overall central feature of BMC-domain shell proteins is their distinct hexagonal shape (Figure 3 and 4). These hexagons are often cyclic hexamers but may also be pseudohexameric trimers where each monomer contains two BMC domains. Observing these hexamers and pseudohexamers along the edge gives an indication of which side faces the lumen of the MCP and which side faces the cytosol. The face that is displayed towards the cytosol has a flat appearance that is somewhat convex in shape and is relatively polar, whereas the lumen side is distinctly concave in shape, less polar, and contains flexible protein termini that are consistent with protein-protein interactions (Yeates *et al.* 2011).

A number of BMC-domain proteins have been shown to interact edge-to-edge and give rise to extended molecular sheets that are understood to form the facets of the polyhedral protein shell (Figure 3) (Kerfeld *et al.* 2005, Tsai *et al.* 2007, Dryden *et al.* 2009, Tanaka *et al.* 2009, Samborska and Kimber 2012). Examination of the make-up of these edge contacts revealed conserved lysine residues that interact in an antiparallel fashion at the lateral interface between the shell hexamers, suggesting a role in protein sheet formation (Crowley *et al.* 2010, Pang *et al.* 2012). Mutagenesis of these lysines alters the assembly of the Pdu MCP *in vivo* and hampers sheet formation *in vitro* (Sinha *et al.* 2014). Two other polar residues are often required giving rise to a triad of side chains that stabilize the edge-to-edge interactions in shell proteins. There is high sequence similarity along the edges of all BMC-domain proteins studied thus far, which suggests that varied hexamers and pseudohexamers mix-and-match to form the protein sheets

that comprise the shell. Thus, the facets that of the polyhedral shells of MCPs are thought to be mixed sheets of different types of BMC-domain proteins.

As described above, BMC domain containing hexamers and pseudohexamers tile into flat sheets that are thought to form the facets of the polyhedral shell. Arranging of these sheets into a closed icosahedron/polyhedron requires a specialized shell protein referred to as a BMV (bacterial microcompartment vertex) protein (Wheatley *et al.* 2013). BMV domain containing proteins are structurally and evolutionary distinct from BMC proteins and they fold into pentamers whose shape and size are consistent with occupying the vertex positions (Figure 3) (Tanaka *et al.* 2008, Sutter *et al.* 2013, Wheatley *et al.* 2013). The edges of these BMV domain proteins are capable of forming edge-to-edge interactions with BMC containing proteins in order to complete the shell assembly.

Molecular transport across the MCP shell

The purpose of the MCP is to confine a particular biochemical pathway, thus transport of enzyme substrates, products, and cofactors into the MCP is a necessity. To date, there is no evidence suggesting the use of direct active transport of substrates across the shell from the cytosol to the lumen of the MCP. As such, the MCP must rely on diffusion of substrates and products across the shell. This creates a paradox of needs for the MCP: on one hand, a central function of the MCP is to be a strict barrier to toxic and volatile metabolic intermediates, while on the other hand, there needs to be a constant flow of substrates and necessary cofactors into the lumen and release of products into the cytosol.

One line of reasoning is that co-localizing of sequentially acting enzymes could limit intermediate escape. In this view, preferential movement of substrates compared to intermediates would be unnecessary for as soon as the intermediate is produced, it is taken up as a substrate by the next enzyme (Reinhold *et al.* 1991, Brinsmade *et al.* 2005, Huseby and Roth 2013). This idea can be supported by mathematical models (Castellana *et al.* 2014). However, as more structural information of the shell proteins has become available, it appears that the shell can function as a selective permeability barrier. Most MCPs contain at least one classical, i.e. single BMC-domain, non-permuted homohexamers (Fig. 3 and 4). In these canonical BMC proteins, there is a small pore along the central axis that that is thought to mediate substrate transport. Furthermore, these pores appear to be tailored for the transport of particular small molecules. It the case of carboxysome shell protein CcmK2, the lining of the central pore is positively charged and which would allow the negatively charged bicarbonate ion entry while at the same time restricting the nonpolar intermediate (CO_2) from escaping (Kerfeld *et al.* 2005, Tsai *et al.* 2007). Similarly, the central pore of the PduA protein is lined with hydrophilic residues that might preferentially mediate the movement of 1,2-PD compared to propionaldehyde which is less polar (Crowley *et al.* 2010). Importantly, recent studies have shown that the PduA pore does indeed allow the selective diffusion of 1,2-PD into the Pdu MCP. In wild-type PduA, a serine residue lies at the center of the PduA pore and provides a hydrophilic environment that attracts 1,2-PD and facilitates diffusion across the shell into the lumen of the MCP. Site-directed mutagenesis showed that changing residue 40 of PduA to leucine (S40L) restricted diffusion of 1,2-PD across the MCP shell. Interestingly, in an PduA S40A mutant propionaldehyde (a toxic intermediate) escaped the lumen at a faster rate while 1,2-PD uptake was unchanged (Figure 5) (Chowdhury *et al.* 2015). These results showed that the PduA central pore is designed to allow facile 1,2-PD

influx while restricting the egress of propionaldehyde. Thus, the protein shell of bacterial MCPs are selectively permeable.

While small substrates are thought to enter MCPs through the central pores of canonical hexameric BMC-domain shell proteins, larger molecules such as enzymatic cofactors are thought to traverse the shell through larger allosterically regulated pores in pseudohexameric BMC-domain proteins. Crystal structures of the carboxysome and Eut pseudohexameric shell proteins indicate that these proteins are capable of undergoing large conformational changes that open and close a large central pore at the interface of the trimer (Klein *et al.* 2009, Sagermann *et al.* 2009, Tanaka *et al.* 2010, Cai *et al.* 2013). What triggers the conformational change between open and closed form is currently unknown as are the residues that aid in the conformational change. However, keeping the central pore open for long periods of time would likely be detrimental to the function of the MCP as more pathway intermediates would be able to escape the confines of the shell. Thus, there is probably an equilibrium of open/closed conformations would balance the need for larger cofactors and prevent the release of intermediate.

Because transport in MCPs is central to function, it is likely to be regulated through some means that relates the status of the MCP and state of the cell. The pseudohexameric BMC domain protein in the ethanolamine utilization MCP, EutL, appears to be allosterically regulated by binding of the substrate, ethanolamine, at a site distant from the central pore. Interestingly, ethanolamine binds with a much higher affinity to the closed form of the trimer and this might prevent central pore opening via steric forces that would be generated by a large conformational change that is necessary for central pore opening (Thompson *et al.* 2015). In addition, a disulfide linkage promotes central pore closure in the same protein. This suggests that the substrate and

the redox state of the cell serves as an allosteric inhibitor of central pore opening in the tandem BMC proteins. The identity of the molecules that would pass through such a large pore remains speculative at best, but it makes intuitive sense that larger cofactors such as NAD^+/NADH, B_{12}, ATP, and HS-CoA would be likely candidates for molecular transport.

While cofactor transport is clearly critical to MCP function, internal cofactor recycling is similarly important. In the case of the Pdu MCP, the lumen enzymes require NAD^+/NADH, B_{12}, ATP, and HS-CoA (Chowdhury *et al.* 2014) (Cheng, *et al.* 2012). Presumably, these would enter the Pdu MCP through the gated pores of the pseudohexameric BMC-domain shell proteins, PduB and PduB', and/or be encapsulated during assembly. In addition, recent studies indicate that NAD^+/NADH are internally recycled within the Pdu MCP (Cheng *et al.* 2012). The PduP enzyme converts NAD^+ to NADH and the PduQ enzyme converts NADH to NAD^+. A *pduQ* deletion mutant grows at about 50% of wild-type rate on 1,2-PD minimal medium due to impaired recycling and NADH to NAD^+ within the lumen of the MCP. However, the fact that a *pduQ* deletion mutant still grows at 50% of the wild-type rate shows that there is another mechanism that rapidly supplies NAD^+ to the lumen enzymes of the Pdu MCP, presumably transport of NADH across the shell followed by oxidation of NADH to NAD^+ by the electron transport chain (Cheng *et al.* 2012). Furthermore, recent studies showed that coenzyme A can also be recycled internally within Pdu MCP by the PduL and PduP enzymes. In *pduL* deletion strains growth is also about 50% than wild-type, indicating that the CoA pool in the MCP is replenished by the cytosol (Liu, *et al.* 2015). In addition, the enzymes required for Ado-B_{12} recycling are components of purified MCPs suggesting that B_{12} could be recycled internal to the MCP (Cheng and Bobik 2010, Huseby and Roth 2013). Hence, the current view is that recycling

works in conjunction with gated pores to meet the substrate/cofactor requirements of encapsulated enzymes as well as maintain homeostasis between MCPs and their host cells.

The Pdu Microcompartment

The 1,2 propanediol utilization (Pdu) MCP of *Salmonella enterica* serovar Typhimurium LT2 is used to optimize the coenzyme B_{12}-dependent catabolism of 1,2-PD when that compound is used as a growth substrate (Figure 6) (Bobik *et al.* 1999, Havemann *et al.* 2002). 1,2-PD is produced in the fermentation of rhamnose and fucose and is thought to be an important carbon source in anaerobic environments including the large intestine of higher animals, sediments, and soil depths (Obradors *et al.* 1988). Genera that can produce Pdu MCPs include *Salmonella, Klebsiella, Shigella, Yersinia, Listeria, Lactobacillus, Lactococcus, Citrobacter, Clostridium* and at least one species of *Escherichia coli* (E24377A) (Bobik 2006, Abdul-Rahman *et al.* 2013, Jorda *et al.* 2013, Axen *et al.* 2014). The ability to degrade 1,2-PD is associated with pathogenicity (Conner *et al.* 1998, Thiennimitr *et al.* 2011). In *Salmonella*, *pdu* genes are induced in host tissues, and mutations in these genes confer a virulence defect in mice (Conner *et al.* 1998, Heithoff *et al.* 1999). In *Listeria*, *pdu* genes are induced during growth in host cells and 1,2-PD degradation is correlated to pathogenesis (Buchrieser *et al.* 2003, Joseph *et al.* 2006). Finally, *Salmonella* has been found to respire 1,2-PD with tetrathionate, which is an important terminal electron acceptor in the inflamed gut (Price-Carter *et al.* 2001). During infection, *Salmonella* releases effector molecules to induce the release of reactive oxygen species by the host, which converts thiosulfate (an endogenous sulfur compound) to tetrathionate (Winter *et al.* 2010, Thiennimitr *et al.* 2011). In other words, *Salmonella* are able to utilize 1,2-PD as a carbon

source in the inflamed gut while using tetrathionate as the terminal electron acceptor in anaerobic respiration to provide an advantage in growth over competing microbes in the local environment.

As mentioned above, a MCP is used to optimize 1,2-PD degradation. The catabolism of 1,2-PD begins when the substrate crosses the protein shell from the cytosol into the lumen of the Pdu MCP where it is converted into propionaldehyde by the B_{12}-dependent diol dehydratase, PduCDE (Jeter 1990, Bobik *et al.* 1997). This intermediate is either converted to propionyl-CoA by the aldehyde dehydrogenase PduP, or to 1-propanol by the 1-propanol dehydrogenase, PduQ (Leal *et al.* 2003, Cheng *et al.* 2012). Propionyl-CoA can then be further modified by the phosphotransacylase PduL into propionyl-PO_4^{2-} (Liu *et al.* 2015). According to current models, propionyl-PO_4^{2-} and 1-propanol exit the lumen of the Pdu MCP and enter the cytoplasm. Propionyl-PO_4^{2-} can enter central metabolism via the methyl citrate pathway where it can serve as a usable carbon source for energy and growth, or it can be converted to propionate and excreted outside the cell along with 1-propanol (Obradors *et al.* 1988, Horswill and Escalante-Semerena 1997, Horswill and Escalante-Semerena 1999, Sampson and Bobik 2008). In addition to the degradative enzymes there are also three B_{12} recycling enzymes (PduGH, PduO, and PduS) that are necessary to reactivate PduCDE, which can undergo mechanism-based inactivation during catalysis (Mori *et al.* 1997, Bobik *et al.* 1999, Mori and Toraya 1999, Johnson *et al.* 2001, Johnson *et al.* 2004, Sampson *et al.* 2005, Cheng and Bobik 2010, Parsons *et al.* 2010). The function of the Pdu MCP is to mitigate propionaldehyde toxicity as well as its loss to the environment. If the shell of the Pdu MCP is compromised, there is an extended period of growth arrest due to the accumulation of high levels (15-20 mM) of propionaldehyde in the culture medium (Havemann *et al.* 2002, Sampson and Bobik 2008). In natural environments, the

levels of propionaldehyde produced by a compromised shell would be a sufficient carbon source for other microbes. Thus, the role of the Pdu MCP is to localize the pathway intermediate (propionaldehyde) so it can be rapidly converted to a usable product and to sequester this intermediate to prevent cellular damage or escape into the environment where it can be used as a carbon source for competing microbes.

The shell of the Pdu MCP

There are seven different BMC-domain containing proteins that make up the major portion of the shell of the Pdu MCP: PduA, PduB, PduB', PduJ, PduK, PduT, PduU. Of these, PduA, PduJ, PduU are single BMC domain containing peptides that form hexamers. PduA and PduJ are structurally similar hexamers that contain a central pore along their six-fold axis (Crowley *et al.* 2010). Recent studies showed that the PduA is involved in 1,2-PD transport, but the function of PduJ is currently unknown (Chowdhury *et al.* 2015). The PduU shell protein is a hexamer that contains an N-terminal β-barrel cap that blocks access to its central pore (Crowley *et al.* 2008). The β-barrel has been speculated to serve as a protein binding site but the function of PduU has not been studied. The PduT protein contains tandem BMC domain and forms pseudohexamers. Interestingly, the PduT trimer contains a 4Fe-4S cluster where the central pore would normally be found (Pang *et al.* 2011). How this cluster functions in the context of the MCP is uncertain but it has the potential to serve as an electron conduit between the cytoplasm and the MCP interior. The PduK protein is the only Pdu BMC domain containing peptide whose structure is unknown. Sequence analysis indicated it has two domains: an N-terminal BMC domain and a C-terminal domain, of which little is known.

PduB and PduB’ are the tandem-BMC shell proteins that form pseudohexameric trimers. They are expressed from overlapping genes and their only difference is a 37 amino acid N-terminal extension on PduB. The functions of PduB and PduB’ are unknown. They are however related in sequence to pseudohexameric BMC proteins proposed to have large allosterically regulated central pores used transport larger molecules such as enzyme cofactors into the MCP. For example, the EutL shell protein which is related in sequence to PduB and PduB' was crystalized in two forms: an open form and a closed form (Figure 4) suggesting a gated central pore capable of metabolite transport (Tanaka *et al.* 2010). Furthermore, the 37 amino acid N-terminal extension on the PduB protein compared to PduB' is of potential significance since recent work has shown that extensions on the termini of Pdu shell proteins and lumen enzymes are important in MCP assembly.

Herein, I will report studies on the function of the PduB and PduB' shell proteins: 1) analysis of the crystal structure of PduB’ to identify critical functional residues, 2) structure-guided mutagenesis to address the possibility that PduB' has an allosterically regulated pore and 3) studies on the role for the 37 amino acid N-terminal extension that differentiates PduB and PduB'.

Study of PduB and PduB’ in the context Pdu MCPs

The role of shell proteins can be difficult to ascertain in the study of MCPs as they are structural proteins, not enzymes, so functionality of the protein has to be done in the context of the MCP. To examine PduB', four central experiments were done: 1) growth assays on minimal

media, 2) SDS-PAGE, 3) yields, and 4) transmission electron microscopy (TEM) of purified MCPs. Growth assays can establish the growth rate of the mutant and, if growth deviates from that of wild-type, we can draw certain conclusions. Faster growth rate indicates that the 1,2-PD substrate is more accessible to the diol dehydratase enzyme and is indicative with increased permeability. SDS-PAGE allows us to examine overall protein content and compare that to wild-type. Yields of purified microcompartments can reveal whether the mutant affects the overall stability of the MCP. Finally, TEM specifies the morphology of mutant MCPs as well as hints at the overall stability of the MCP. Taken together, these experiments help demonstrate how a mutation in the shell protein affects the function of the MCP.

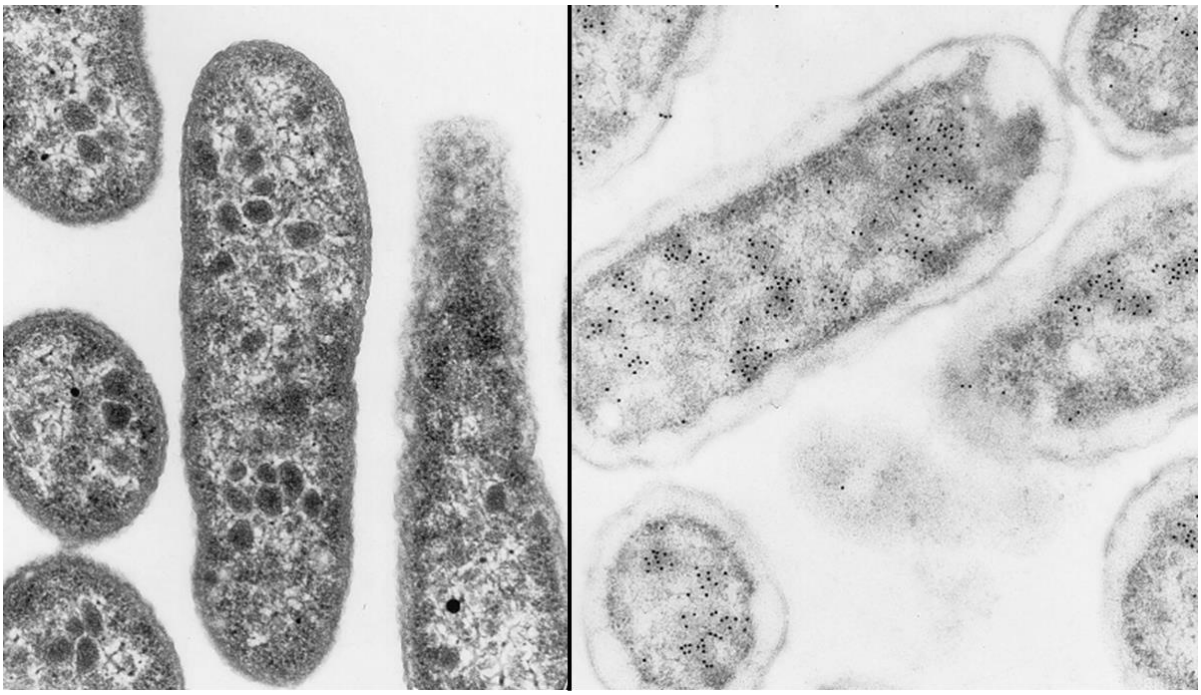

Figure 1. Electron micrograph of Pdu microcompartments made by *Salmonella enterica.* (Left) Pdu MCPs when grown on 1,2-PD media. (Right) Diol-dehydratase immunogold staining of Pdu MCPs. Adapted from (Bobik *et al.* 1999)

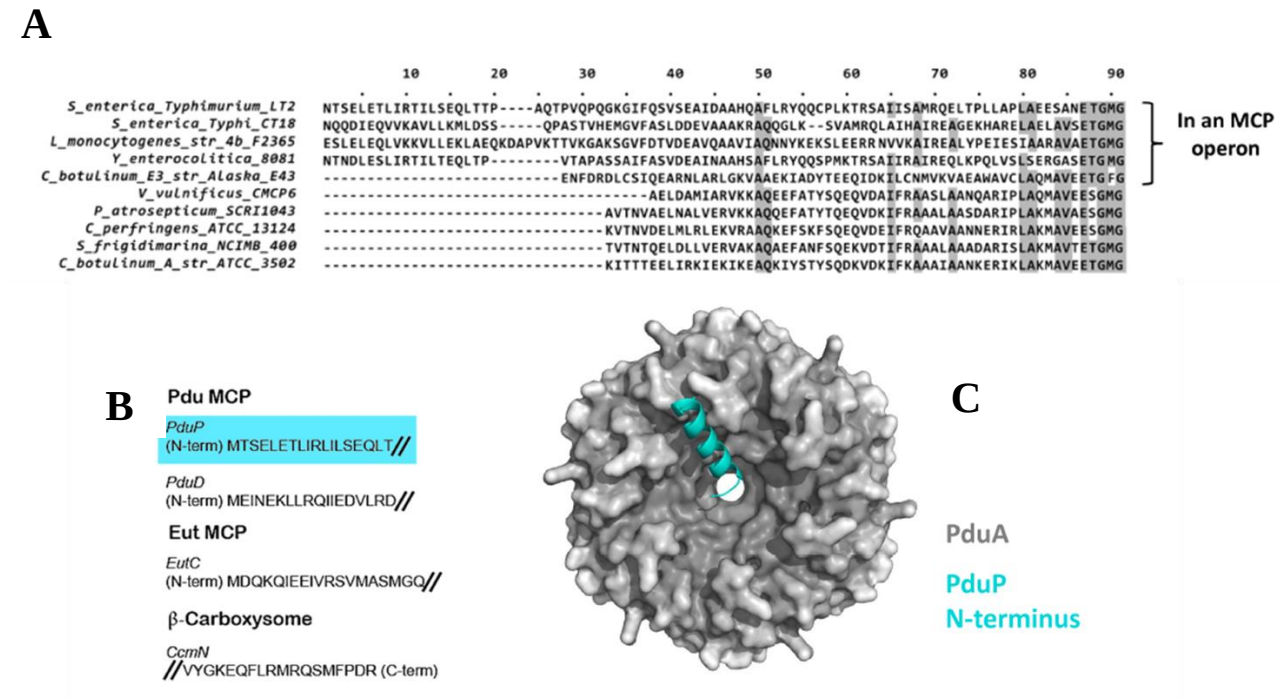

Figure 2. MCPs use terminal extensions to target lumen enzymes to the interior of the MCP. (A) An alignment of PduP homologs illustrates that enzymes encoded in an MCP operons contain an N–terminal extension compared to homologs not associated with MCPs. Adapted from (Fan *et al.* 2010, Bobik *et al.* 2015). (B) Extensions on termini are not exclusive to the Pdu MCP and have been found in both the Eut MCP and Carboxysome (Fan *et al.* 2010, Fan and Bobik 2011, Choudhary *et al.* 2012, Kinney *et al.* 2012, Lawrence *et al.* 2014, Bobik *et al.* 2015, Jorda *et al.* 2015). (C). Model for interaction between the N-terminus of PduP and the C-terminus of a PduA hexamer, an interaction that in needed for encapsulation of PduP within the Pdu MCP. Adapted from (Yeates *et al.* 2013, Bobik *et al.* 2015).

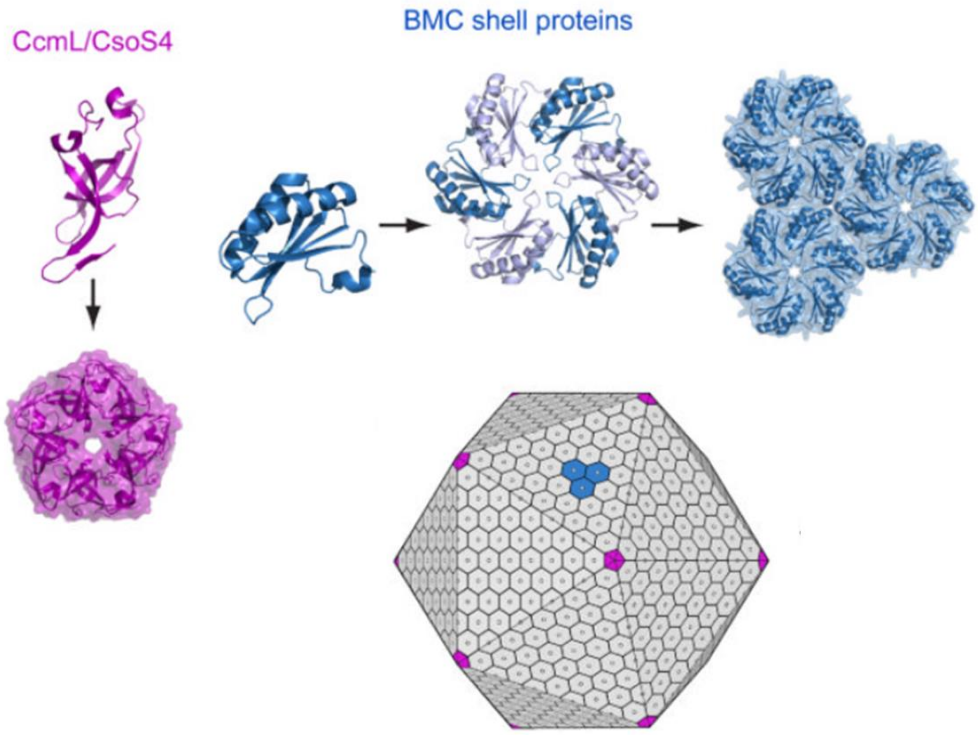

Figure 3. Arrangement of BMC and BMV proteins in the MCP shell. BMC-domain containing peptides (blue) assemble into hexamers (or pseudohexameric trimers) and form sheets that form the facets of the MCP. BMV-domain containing proteins (magenta) assemble into pentamers that form the vertices of the MCP. Figure adapted from (Yeates *et al.* 2011).

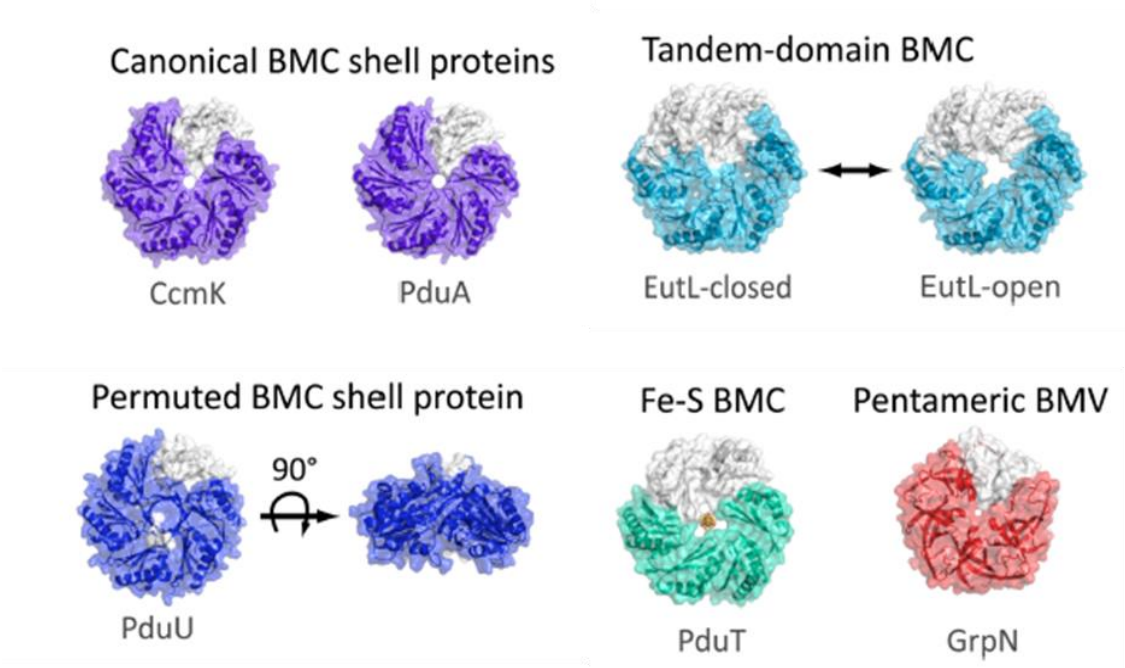

Figure 4. Shell proteins of MCPs serve diverse functions within the context of the MCP. Uncolored peptides are monomers while the colored portion shows the quaternary structure of the complete multimer. PDB identifications CcmK: 3BN4 and 2A10; PduA: 3NGK; EutL-closed: 3I82; EutL-open: 3I87; PduU: 3CGI; PduT: 3PAC; GrpN: 4I7A. Adapted from (Bobik *et al.* 2015)

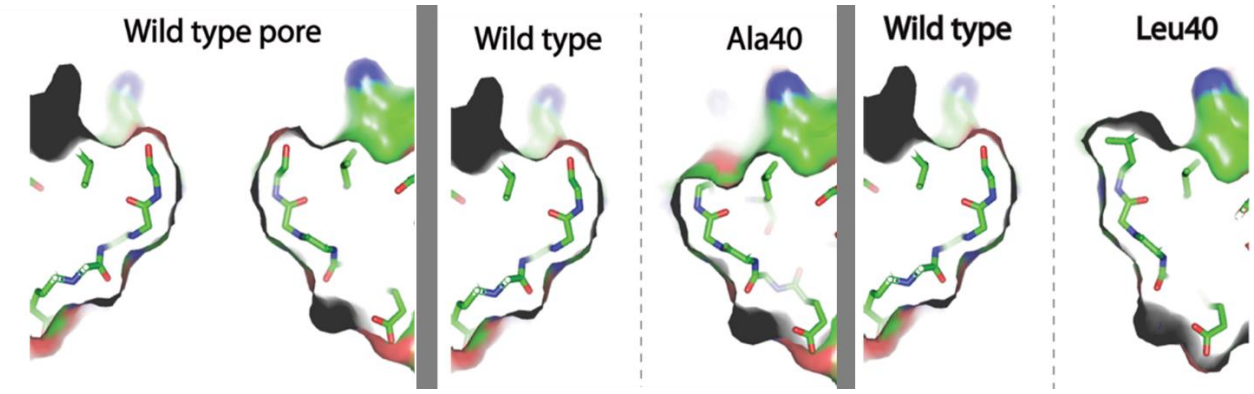

Figure 5. The central pore in PduA can be modified for selective transport. The central pore in PduA can be modified for selective transport. The wild type pore has a serine at position 40. In an S40A substitution, propionaldehyde can escape the lumen of the MCP more readily while not impeding 1,2-PD entry. In the S40L substitution, transport of 1,2-PD across the protein shell is impaired. Adapted from (Bobik *et al.* 2015)

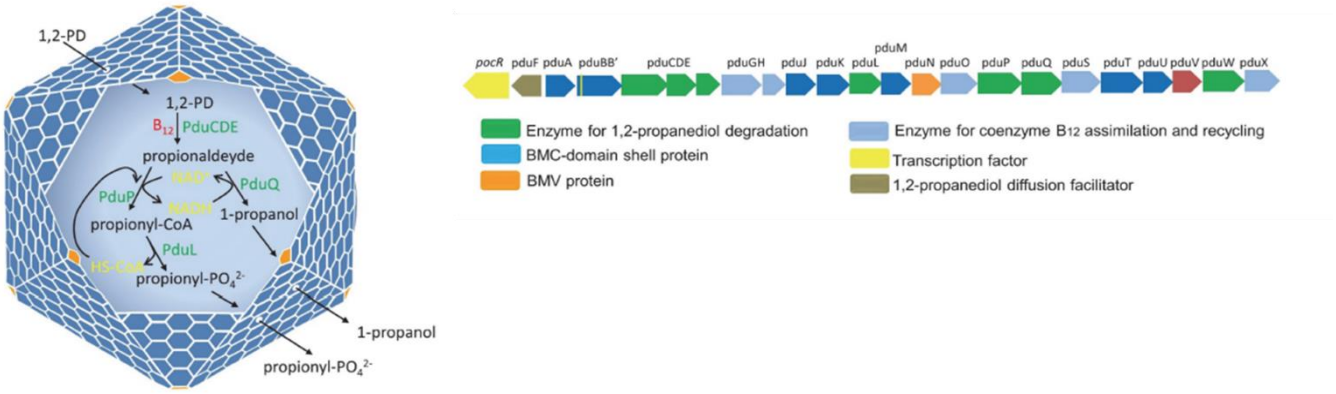

Figure 6. The Pdu MCP model for 1,2-PD degradation. (Left) Proposed metabolic pathway to take place in the lumen of the MCP. (Right) The *pdu* operon Adapted from (Chowdhury *et al.* 2014, Bobik *et al.* 2015)

Works Cited

Abdul-Rahman, F., *et al.* (2013). "The distribution of polyhedral bacterial microcompartments suggests frequent horizontal transfer and operon reassembly." J. Phylogen. Evolution. Biol. **1**(4): doi 10.4172/2329-9002.1000118

Axen, S. D., *et al.* (2014). "A taxonomy of bacterial microcompartment loci constructed by a novel scoring method." PLoS Comput. Biol. **10**(10): e1003898.

Bobik, T. A. (2006). "Polyhedral organelles compartmenting bacterial metabolic processes." Appl Microbiol Biotechnol **70**(5): 517-525.

Bobik, T. A., *et al.* (1999). "The propanediol utilization (*pdu*) operon of *Salmonella enterica* serovar Typhimurium LT2 includes genes necessary for formation of polyhedral organelles involved in coenzyme B_{12}-dependent 1, 2-propanediol degradation." J Bacteriol **181**(19): 5967-5975.

Bobik, T. A., *et al.* (2015). "Bacterial microcompartments: widespread prokaryotic organelles for isolation and optimization of metabolic pathways." Mol Microbiol **98**(2): 193-207.

Bobik, T. A., *et al.* (1997). "Propanediol utilization genes (*pdu*) of *Salmonella typhimurium*: three genes for the propanediol dehydratase." J Bacteriol **179**(21): 6633-6639.

Brinsmade, S. R., *et al.* (2005). "Minimal functions and physiological conditions required for growth of *Salmonella enterica* on ethanolamine in the absence of the metabolosome." J Bacteriol **187**(23): 8039-8046.

Buchrieser, C., *et al.* (2003). "Comparison of the genome sequences of *Listeria monocytogenes* and *Listeria innocua*: clues for evolution and pathogenicity." FEMS Immunol Med Microbiol **35**(3): 207-213.

Cai, F., *et al.* (2013). "The structure of CcmP, a tandem bacterial microcompartment domain protein from the β-carboxysome, forms a subcompartment within a microcompartment." J Biol Chem **288**(22): 16055-16063.

Castellana, M., *et al.* (2014). "Enzyme clustering accelerates processing of intermediates through metabolic channeling." Nat. Biotechnol. **32**(10): 1011-1018.

Cheng, S. and T. A. Bobik (2010). "Characterization of the PduS cobalamin reductase of *Salmonella enterica* and its role in the Pdu microcompartment." J Bacteriol **192**(19): 5071-5080.

Cheng, S., *et al.* (2012). "The PduQ enzyme is an alcohol dehydrogenase used to recycle NAD^+ internally within the Pdu microcompartment of *Salmonella enterica*." PLoS One **7**(10): e47144.

Cheng, S., *et al.* (2008). "Bacterial microcompartments: their properties and paradoxes." Bioessays **30**(11-12): 1084-1095.

Choudhary, S., *et al.* (2012). "Engineered protein nano-compartments for targeted enzyme localization." PLoS One **7**(3): e33342.

Chowdhury, C., *et al.* (2015). "Selective molecular transport through the protein shell of a bacterial microcompartment organelle." Proc Natl Acad Sci U S A **112**(10): 2990-2995.

Chowdhury, C., *et al.* (2014). "Diverse bacterial microcompartment organelles." Microbiol. Mol. Biol. Rev. **78**(3): 438-468.

Conner, C. P., *et al.* (1998). "Differential patterns of acquired virulence genes distinguish *Salmonella* strains." Proc Natl Acad Sci U S A **95**(8): 4641-4645.

Crowley, C. S., *et al.* (2010). "Structural insight into the mechanisms of transport across the *Salmonella enterica* Pdu microcompartment shell." J Biol Chem **285**(48): 37838-37846.

Crowley, C. S., *et al.* (2008). "Structure of the PduU shell protein from the Pdu microcompartment of Salmonella." Structure **16**(9): 1324-1332.

Dryden, K. A., *et al.* (2009). "Two-dimensional crystals of carboxysome shell proteins recapitulate the hexagonal packing of three-dimensional crystals." Protein Sci **18**(12): 2629-2635.

English, R. S., *et al.* (1994). "Isolation and characterization of a carboxysome shell gene from *Thiobacillus neapolitanus*." Mol. Microbiol. **12**(4): 647-654.

Erbilgin, O., *et al.* (2014). "Characterization of a planctomycetal organelle: a novel bacterial microcompartment for the aerobic degradation of plant saccharides." Appl Environ Microbiol **80**(7): 2193-2205.

Fan, C. and T. A. Bobik (2011). "The N-terminal region of the medium subunit (PduD) packages adenosylcobalamin-dependent diol dehydratase (PduCDE) into the Pdu microcompartment." J Bacteriol **193**(20): 5623-5628.

Fan, C., *et al.* (2010). "Short N-terminal sequences package proteins into bacterial microcompartments." Proc Natl Acad Sci U S A **107**(16): 7509-7514.

Havemann, G. D., *et al.* (2002). "PduA is a shell protein of polyhedral organelles involved in coenzyme B_{12}-dependent degradation of 1,2-propanediol in *Salmonella enterica* serovar typhimurium LT2." J Bacteriol **184**(5): 1253-1261.

Heithoff, D. M., *et al.* (1999). "Coordinate intracellular expression of *Salmonella* genes induced during infection." J Bacteriol **181**(3): 799-807.

Horswill, A. R. and J. C. Escalante-Semerena (1997). "Propionate catabolism in *Salmonella typhimurium* LT2: two divergently transcribed units comprise the *prp* locus at 8.5 centisomes, *prpR* encodes a member of the sigma-54 family of activators, and the *prpBCDE* genes constitute an operon." J Bacteriol **179**(3): 928-940.

Horswill, A. R. and J. C. Escalante-Semerena (1999). "*Salmonella typhimurium* LT2 catabolizes propionate via the 2-methylcitric acid cycle." J Bacteriol **181**(18): 5615-5623.

Huseby, D. L. and J. R. Roth (2013). "Evidence that a metabolic microcompartment contains and recycles private cofactor pools." J Bacteriol **195**(12): 2864-2879.

Jeter, R. M. (1990). "Cobalamin-dependent 1,2-propanediol utilization by *Salmonella typhimurium*." J Gen Microbiol **136**(5): 887-896.

Johnson, C. L., *et al.* (2004). "Purification and initial characterization of the *Salmonella enterica* PduO ATP:Cob(I)alamin adenosyltransferase." J Bacteriol **186**(23): 7881-7887.

Johnson, C. L., *et al.* (2001). "Functional genomic, biochemical, and genetic characterization of the *Salmonella pduO* gene, an ATP:cob(I)alamin adenosyltransferase gene." J Bacteriol **183**(5): 1577-1584.

Jorda, J., *et al.* (2015). "Exploring bacterial organelle interactomes: a model of the protein-protein interaction network in the Pdu microcompartment." PLoS Comput Biol **11**(2): e1004067.

Jorda, J., *et al.* (2013). "Using comparative genomics to uncover new kinds of protein-based metabolic organelles in bacteria." Protein Sci **22**(2): 179-195.

Joseph, B., *et al.* (2006). "Identification of *Listeria monocytogenes* genes contributing to intracellular replication by expression profiling and mutant screening." J Bacteriol **188**(2): 556-568.

Kerfeld, C. A., *et al.* (2010). "Bacterial microcompartments." Annu Rev Microbiol **64**: 391-408.

Kerfeld, C. A., *et al.* (2005). "Protein structures forming the shell of primitive bacterial organelles." Science **309**(5736): 936-938.

Kinney, J. N., *et al.* (2011). "Comparative analysis of carboxysome shell proteins." Photosynth Res **109**(1-3): 21-32.

Kinney, J. N., *et al.* (2012). "Elucidating essential role of conserved carboxysomal protein CcmN reveals common feature of bacterial microcompartment assembly." J Biol Chem **287**(21): 17729-17736.

Klein, M. G., *et al.* (2009). "Identification and structural analysis of a novel carboxysome shell protein with implications for metabolite transport." J Mol Biol **392**(2): 319-333.

Kofoid, E., *et al.* (1999). "The 17-gene ethanolamine (*eut*) operon of *Salmonella typhimurium* encodes five homologues of carboxysome shell proteins." J Bacteriol **181**(17): 5317-5329.

Lawrence, A. D., *et al.* (2014). "Solution structure of a bacterial microcompartment targeting peptide and its application in the construction of an ethanol bioreactor." ACS Synthetic Biology **DOI: 10.1021/sb4001118**.

Leal, N. A., *et al.* (2003). "PduP is a coenzyme-A-acylating propionaldehyde dehydrogenase associated with the polyhedral bodies involved in B_{12}-dependent 1,2-propanediol degradation by *Salmonella enterica* serovar Typhimurium LT2." Arch Microbiol **180**(5): 353-361.

Liu, Y., *et al.* (2015). "The PduL phosphotransacylase is used to recycle coenzyme A within the Pdu microcompartment." J Bacteriol **197**(14): 2392-2399.

Mori, K., *et al.* (1997). "A protein factor is essential for in situ reactivation of glycerol-inactivated adenosylcobalamin-dependent diol dehydratase." Biosci Biotechnol Biochem **61**(10): 1729-1733.

Mori, K. and T. Toraya (1999). "Mechanism of reactivation of coenzyme B_{12}-dependent diol dehydratase by a molecular chaperone-like reactivating factor." Biochemistry **38**(40): 13170-13178.

Murat, D., *et al.* (2010). "Cell biology of prokaryotic organelles." Cold Spring Harb. Perspect. Biol. **2**(10): a000422.

Obradors, N., *et al.* (1988). "Anaerobic metabolism of the L-rhamnose fermentation product 1,2-propanediol in *Salmonella typhimurium*." J Bacteriol **170**(5): 2159-2162.

Pang, A., *et al.* (2012). "Substrate channels revealed in the trimeric *Lactobacillus reuteri* bacterial microcompartment shell protein PduB." Acta Crystallogr D Biol Crystallogr **68**(Pt 12): 1642-1652.

Pang, A., *et al.* (2011). "Structure of PduT, a trimeric bacterial microcompartment protein with a 4Fe-4S cluster-binding site." Acta Crystallogr D Biol Crystallogr **67**(Pt 2): 91-96.

Parsons, J. B., *et al.* (2010). "Synthesis of empty bacterial microcompartments, directed organelle protein incorporation, and evidence of filament-associated organelle movement." Mol Cell **38**(2): 305-315.

Parsons, J. B., *et al.* (2010). "Characterisation of PduS, the *pdu* metabolosome corrin reductase, and evidence of substructural organisation within the bacterial microcompartment." PLoS One **5**(11): e14009.

Penrod, J. T. and J. R. Roth (2006). "Conserving a volatile metabolite: a role for carboxysome-like organelles in *Salmonella enterica*." J Bacteriol **188**(8): 2865-2874.

Price-Carter, M., *et al.* (2001). "The alternative electron acceptor tetrathionate supports B_{12}-dependent anaerobic growth of *Salmonella enterica* serovar Typhimurium on ethanolamine or 1,2-propanediol." J Bacteriol **183**(8): 2463-2475.

Price, G. D. and M. R. Badger (1989). "Isolation and characterization of high CO_2-requiring-mutants of the cyanobacterium *Synechococcus* PCC7942 : two phenotypes that accumulate inorganic carbon but are apparently unable to generate CO_2 within the Carboxysome." Plant. Physiol. **91**(2): 514-525.

Price, G. D., *et al.* (1993). "Analysis of a genomic DNA region from the cyanobacterium *Synechococcus* sp. strain PCC7942 involved in carboxysome assembly and function." J Bacteriol **175**(10): 2871-2879.

Rae, B. D., *et al.* (2013). "Functions, compositions, and evolution of the two types of carboxysomes: polyhedral microcompartments that facilitate CO_2 fixation in cyanobacteria and some proteobacteria." Microbiol. Mol. Biol. Rev. **77**(3): 357-379.

Reinhold, L., *et al.* (1991). "A Model for inorganic carbon fluxes and photosynthesis in cyanobacterial carboxysomes." Can J Bot **69**(5): 984-988.

Sagermann, M., *et al.* (2009). "Crystal structure of the EutL shell protein of the ethanolamine ammonia lyase microcompartment." Proc Natl Acad Sci U S A **106**(22): 8883-8887.

Saier, M. H., Jr. and M. V. Bogdanov (2013). "Membranous organelles in bacteria." J. Mol. Microbiol. Biotechnol. **23**(1-2): 5-12.

Samborska, B. and M. S. Kimber (2012). "A dodecameric CcmK2 structure suggests β-carboxysomal shell facets have a double-layered organization." Structure **20**(8): 1353-1362.

Sampson, E. M. and T. A. Bobik (2008). "Microcompartments for B_{12}-dependent 1,2-propanediol degradation provide protection from DNA and cellular damage by a reactive metabolic intermediate." J Bacteriol **190**(8): 2966-2971.

Sampson, E. M., *et al.* (2005). "Biochemical evidence that the *pduS* gene encodes a bifunctional cobalamin reductase." Microbiology **151**(Pt 4): 1169-1177.

Shively, J. M., *et al.* (1973). "Functional organelles in prokaryotes: polyhedral inclusions (carboxysomes) of *Thiobacillus neapolitanus*." Science **182**(112): 584-586.

Sinha, S., *et al.* (2014). "Alanine scanning mutagenesis identifies an asparagine-arginine-lysine triad essential to assembly of the shell of the Pdu microcompartment." J Mol Biol **426**(12): 2328-2345.

Sriramulu, D. D., *et al.* (2008). "*Lactobacillus reuteri* DSM 20016 produces cobalamin-dependent diol dehydratase in metabolosomes and metabolizes 1,2-propanediol by disproportionation." J Bacteriol **190**(13): 4559-4567.

Stojiljkovic, I., *et al.* (1995). "Ethanolamine utilization in *Salmonella typhimurium*: nucleotide sequence, protein expression, and mutational analysis of the *cchA cchB eutE eutJ eutG eutH* gene cluster." J. Bacteriol. **177**(5): 1357-1366.

Sutter, M., *et al.* (2013). "Two new high-resolution crystal structures of carboxysome pentamer proteins reveal high structural conservation of CcmL orthologs among distantly related cyanobacterial species." Photosynth Res **118**(1-2): 9-16.

Talarico, T. L., *et al.* (1988). "Production and isolation of reuterin, a growth inhibitor produced by *Lactobacillus reuteri*." Antimicrob Agents Chemother **32**(12): 1854-1858.

Tanaka, S., *et al.* (2008). "Atomic-level models of the bacterial carboxysome shell." Science **319**(5866): 1083-1086.

Tanaka, S., *et al.* (2009). "Insights from multiple structures of the shell proteins from the β-carboxysome." Protein Sci **18**(1): 108-120.

Tanaka, S., *et al.* (2010). "Structure and mechanisms of a protein-based organelle in *Escherichia coli*." Science **327**(5961): 81-84.

Thiennimitr, P., *et al.* (2011). "Intestinal inflammation allows *Salmonella* to use ethanolamine to compete with the microbiota." Proc Natl Acad Sci U S A **108**(42): 17480-17485.

Thompson, M. C., *et al.* (2015). "An allosteric model for control of pore opening by substrate binding in the EutL microcompartment shell protein." Protein Sci **24**(6): 956-975.

Tsai, Y., *et al.* (2007). "Structural analysis of CsoS1A and the protein shell of the *Halothiobacillus neapolitanus* carboxysome." PLoS Biol **5**(6): e144.

van Niftrik, L. and M. S. Jetten (2012). "Anaerobic ammonium-oxidizing bacteria: unique microorganisms with exceptional properties." Microbiol. Mol. Biol. Rev. **76**(3): 585-596.

Wheatley, N. M., *et al.* (2013). "Bacterial microcompartment shells of diverse functional types possess pentameric vertex proteins." Protein Sci. **22**(5): 660-665.

Winter, S. E. and A. J. Baumler (2011). "A breathtaking feat: to compete with the gut microbiota, *Salmonella* drives its host to provide a respiratory electron acceptor." Gut Microbes **2**(1): 58-60.

Winter, S. E., *et al.* (2010). "Gut inflammation provides a respiratory electron acceptor for *Salmonella*." Nature **467**(7314): 426-429.

Yeates, T. O., *et al.* (2013). "The shells of BMC-type microcompartment organelles in bacteria." J Mol Microbiol Biotechnol **23**(4-5): 290-299.

Yeates, T. O., *et al.* (2011). "The protein shells of bacterial microcompartment organelles." Curr Opin Struct Biol **21**(2): 223-231.

CHAPTER 2: STRUCTURAL ANALSIS OF PDUB'

Introduction

Bacterial Microcompartments (MCPs) are subcellular organelles that are found in about 20% of all bacteria (Bobik 2006, Abdul-Rahman *et al.* 2013, Axen *et al.* 2014). MCPs consist of metabolic enzymes encased within a protein shell. Hence, compared to other organelles, they are unusual in having a protein shell rather that a lipid membrane. The role of MCPs is to confine toxic or volatile metabolic intermediates that can cause DNA damage or escape the cellular envelope (Kerfeld *et al.* 2010, Rae *et al.* 2013, Chowdhury *et al.* 2014). The most studied MCPs are the carboxysome, the 1,2-propanediol utilization (Pdu), and the ethanolamine utilization (Eut) microcompartments. The metabolic pathways contained in these MCPs produce CO_2, propionaldehyde, and acetaldehyde, respectively, which are confined within the shell of the MCP to minimize toxicity and/or carbon loss (Shively *et al.* 1973, Talarico *et al.* 1988, Bobik *et al.* 1999). In addition to confining a metabolic intermediate, the shell must also allow the exit and entry of MCP substrates and products. Studies indicate that the protein shell is selectively permeable, restricting the outward diffusion of toxic/volatile intermediates while preferentially allowing the movement of substrates, products and cofactors (Kerfeld *et al.* 2005, Tsai *et al.* 2007, Crowley *et al.* 2010, Chowdhury *et al.* 2015). However, the mechanisms by which a protein barrier mediates selective permeability are not understood fully.

In *Salmonella* a MCP is used for the utilization of 1,2-PD as a carbon and energy source (Pdu MCP) (Bobik *et al.* 1999). 1,2-PD is a major byproduct of the fermentation of rhamnose and fucose and an important carbon compound in anaerobic environments such as soil depths,

sediments, and the large intestines (Obradors *et al.* 1988). Metabolism begins when the 1,2 PD crosses the protein shell and enters the lumen of the MCP where it is converted to propionaldehyde by the B_{12} dependent diol dehydratase (PduCDE) (Figure 1) (Jeter 1990, Bobik *et al.* 1997, Bobik *et al.* 1999, Havemann *et al.* 2002, Sampson and Bobik 2008). The shell of the MCP confines the propionaldehyde intermediate so it cannot cause DNA damage and escape the membrane of the cell where it can be used as a carbon source for other competing microbes (Havemann *et al.* 2002, Sampson and Bobik 2008). Once formed, propionaldehyde can be converted to 1-propanol or propionyl-CoA which is further metabolized into propionyl-PO_4 (Leal *et al.* 2003, Liu *et al.* 2007, Cheng *et al.* 2012). The products 1-propanol and propionyl-PO_4^{2-} can then escape the shell and enter the cytosol. 1-propaniol is excreted from the cell and propionyl-PO_4^{2-} feeds into central metabolism via the methylcitrate pathway to producing additional ATP and biosynthetic building blocks (Obradors *et al.* 1988, Horswill and Escalante-Semerena 1997, Sampson and Bobik 2008). How the shell can retain propionaldehyde while allowing entry of substrates and much larger enzymatic cofactors as well as product escape is a major unanswered question in the MCP field.

The primary building block of MCP shells is a family of proteins defined by the presence of a bacterial microcompartment (BMC) domain. BMC-domain proteins can assemble into hexamers or trimeric pseudohexamers, i.e. trimers where each monomer contains two BMC domains (Price *et al.* 1993, Chen *et al.* 1994, Stojiljkovic *et al.* 1995). The hexamers and pseudohexamers are thought to assembly side-by-side into mixed protein sheets that form the facets of the polyhedral shell (Figure 1) and act as a protein barrier to shield the cytosol from the toxic or volatile intermediate formed by the metabolism occurring in the MCP. In the Pdu MCP,

there are seven different BMC domain shell proteins (PduA, PduB, PduB', PduJ, PduK, PduT and PduU). Crystal structures have been determined for each Pdu BMC-domain protein except PduK (Crowley *et al.* 2008, Crowley *et al.* 2010, Pang *et al.* 2011, Pang *et al.* 2012). Each forms a hexamer or a pseudohexamer with a hexagonal shape. In addition, they have shape complementarity along their edges supporting the idea that they assemble into mixed protein sheets. An examination of the protein sheets formed by the PduA BMC domain protein shows that the major opening is a central pore across the six-fold symmetry axis (Figure 2) (Crowley *et al.* 2010). Recent studies have shown that this pore mediates 1,2-PD transport across the MCP shell (Chowdhury *et al.* 2015). In addition, single amino acid substitutions along the edge of PduA's central pore selectively alters transport to reduce 1,2-PD entry, and increase propionaldehyde escape. Thus, the pore of the PduA shell protein is designed to allow 1,2-PD entry while limiting propionaldehyde escape.

Structural studies of other Pdu shell proteins have highlighted their functional diversity although precise physiological roles have not been fully worked out. The PduT shell protein has an iron-sulfur cluster where the central pore would be found in most BMC-domain proteins (Pang *et al.* 2011). Hence, PduT was proposed to act as an electron conduit between the cytoplasm and the MCP interior, or alternatively in the repair of iron-sulfur centers found in enzyme within the MCP. The PduU protein has a beta-barrel capping and closing the central pore regions (Crowley *et al.* 2008). This barrel was is expected to be location on the outer surface of the Pdu MCP and may provide a binding site for interaction with other cellular proteins. The PduJ protein is a typical hexameric BMC-domain protein but its function is unknown while

PduK contains both a BMC domain as well as a C-terminal domain (about 60 amino acids in length) about which little in known.

Two of the major components of the Pdu MCP shell are the pseudohexameric BMC-domain proteins PduB and PduB'. Together they compromise ~50% of the total protein in the Pdu MCP shell (Havemann and Bobik 2003). PduB and PduB' are identical in amino acid sequence except that PduB is 37 amino acid longer at its N-terminus. PduB' is translated from and internal start site within the PduB gene (Bobik *et al.* 1999). PduB and PduB' were identified by proteomics studies (Chen *et al.* 1995, Daniel *et al.* 1998, Bobik *et al.* 1999, Havemann and Bobik 2003). Mutations that delete PduB and PduB, prevent MCP formation but the specific functional roles of PduB and PduB' have not been determined (Cheng *et al.* 2011, Cheng *et al.* 2012). Several homologs of the *Salmonella* PduB protein have been crystalized and their structures are known (Tsai *et al.* 2007, Heldt *et al.* 2009, Tanaka *et al.* 2010, Pang *et al.* 2012). In three cases (EutL, CcmP and CsoS1D) PduB’ homologs were crystalized in two forms: one which has an occluded central pore and another that has an open central much larger than the pores found hexameric BMC-domain proteins (Figure 3, D and E) (Klein *et al.* 2009, Tanaka *et al.* 2010, Cai *et al.* 2013). Consequently, it was proposed that EutL and homologs might function as a gated pore for the selective transport of larger metabolites (such as enzymatic cofactors) into bacterial MCPs (Tanaka *et al.* 2010). It was also suggested that the ability to form gated metabolite conduits might be a general property of the pseudohexameric BMC-domain proteins (Cai *et al.* 2013). Further structural studies showed that the EutL pseudohexamer binds ethanolamine (the substrate in this case) in a manner expected to stabilize the closed form (Thompson, *et al.* 2015). Based on these studies, it was proposed that the EutL pore was

allosterically regulated by the substrate of the Eut MCP. One rationale here would be that ethanolamine binding reduces the activity of the Etu MCP at high levels of substrate moderating aldehyde production (Thompson *et al.* 2015). However, to date, no genetic or physiological studies have been reported that address the physiological relevance of pore regulation or whether the pore is even capable of assuming both open and closed conformation under physiological conditions (as opposed to within the constraints of a crystal lattice). To this end, our lab recently determined the crystal structure of *Salmonella enterica* PduB' as an aid in structure-guided mutagenesis to dissect the in vivo function of the PduB and PduB' proteins.

Results

Structural analysis of PduB'

The structure of PduB' from *Salmonella enterica* closely resembles the PduB structure of *Lactobacillus* and the EtuB structure of the ethanol MCP (Heldt *et al.* 2009, Pang *et al.* 2012). The shape of PduB' is a pseudohexamer with the overall geometry of a hexagon and made up of three individual subunits (Figure 3 A, B and C). Along the central axis on the trimer interface lays a collection of coiled residues. The central pore is closed. However, it is this area that is proposed to open wide after a large conformational change (Figure 3D and E) (Klein *et al.* 2009, Tanaka *et al.* 2010, Cai *et al.* 2013, Thompson *et al.* 2015). A number of residues in this area are very well conserved among PduB' homologs and may play a role in central pore function (Figure 4). Of these, one residue stands out that happens to be an outlier in the Ramachandran plot of the PduB' structure: D79 (Figure 5A and B). The outlier is not exclusive to the *Salmonella* PduB' and is seen in the PduB homologs in *Lactobaccilus* and EtuB (Heldt *et al.* 2009, Pang *et al.*

2012). In addition, there is a coordinating residue that helps maintain the Ramachandran outlier conformation, R50, which is also highly conserved among PduB' homologs. Because of this, D79 was proposed by others to contain the potential energy required for central pore opening. Accordingly, we used site-directed mutagenesis to examine the role of PduB' D79 and R50.

Structure-guided mutagenesis of Ramachandran outlier D79 of PduB'

Mutagenesis of the central pore residues revealed the importance of D79 and R50 to overall PduB' structure and thus MCP stability. Alanine substitution of R50 and D79 results in faster growth on 1,2-PD at limiting B_{12} compared to wild-type *Salmonella* (Figure 5C). Prior studies established that faster growth on minimal 1,2-PD medium is indicative of a damaged MCP shell that is impaired as a diffusion barrier. This results in increased substrate availability to the MCP lumen enzymes which leads to faster growth. It is interesting that amino acid substitutions other than alanine at the above positions give similar growth phenotypes indicating that there is a high degree of amino acid specificity at the D79 position. Next, we purified MCPs from R50A and D79A and observed their respective band patterns on SDS-PAGE. Interestingly, the band pattern of the mutants was comparable to wild-type suggesting normally formed MCPs (Figure 6A). However, MCP yields (g MCP/g cells) were decreased to 30% for both mutants and indicated a loss of stability during purification. Transmission electron microscopy of the D79A mutant revealed that the microcompartments produced from the mutation are properly formed and look like that which is typically seen with wild-type (Figure 6C). We also looked at production of recombinant D79A using a T7 expression system. Poor production was observed suggesting reduced protein stability.

Taken together, these results indicate that the Ramachandran outlier, D79, is important for PduB' stability. Substitutions at D79 destabilized the MCP as overall yields were much lower perhaps due to lower PduB' availability as a consequence of instability. In addition, R50 is a specific electrostatic partner of D79. Neutralizing the charge at R50 showed a similar growth phenotype to D79A and MCP yields were comparable between the two mutants. Next, we attempted to introduce competition of the R50 positive charge by designing a K81D mutant. The rationale for this was to attempt to modestly reduce the electrostatic interaction between D79 and R50 and open the central pore because K81 is proximal to both R50 and D79 in the crystal structure of PduB'. Unfortunately, competition of R50 was not evident. Growth assays of the K81D mutant showed growth similar to that of wild-type (data not shown) and purified MCP were obtained from the K81D mutant with yields and a SDS-PAGE banding pattern similar to wild-type (Figure 6B). This suggests that the R50-D79 electrostatic interaction is specific and promotes PduB' stability. Also, these results indicated the tolerance of the K81 residue as substituting with an opposite charge (K81D) showed no phenotype.

Electrostatic residues R78 and K81

Two ionic residues lie at the center of the pore on the convex side: R78 and K81 (Figure 7A). Of these, R78 is the most evolutionary conserved (Figure 4C). Alanine mutagenesis of these residues showed increased growth on minimal media for the R78A mutant, but not as fast as the D79A mutant. Growth of the K81A mutant was similar to wild-type (Figure 7B). Purified MCPs showed a similar band pattern to wild-type (LT2), but overall yields were 40% for R78A and 100% for K81A (Figure 7C). Another substitution at the R78 position, R78C, showed similar

growth to R78A (data not shown). These results indicate that the R78 position, like that of D79, is an integral electrostatic residue at the trimer interface that helps stabilize PduB'.

Glycine-rich motif in the PduB' pore

The section of PduB' that rearranges during pore opening/closing contains a glycine rich region that is highly conserved among PduB' homologs (Figure 4B). If a large central pore exists in PduB' as it does in the EutL homolog, a large conformational change would need to occur to open the central pore, and, since glycine is the least restricted amino acid in terms of motion, we explored how substituting different amino acids in this region would affect the function of PduB' (Klein *et al.* 2009, Tanaka *et al.* 2010, Cai *et al.* 2013). The residues in this region range from G82 to G87 (Figure 3B), and several of these residues are well conserved (Figure 4C). A variety of mutations were made at all positions along this motif with emphasis on G82, G83, G85, and G87. At the G82 position, a number of substitutions were made: G82A, G82C, G82I, G82L, G82L, G82S, and G82V. None of these mutants showed a fast growth phenotype on 1,2-PD minimal medium under low B_{12} conditions, suggesting that intact MCPs are formed. Interestingly, however, the G82V mutant showed slower growth under medium B_{12} (50 nm) levels (Figure 8A). Wanting to test this slow growth mutant, microcompartments were purified from the G82V. Yields of the mutant had compared to wild-type and showed no obvious structural abnormalities in SDS-PAGE or in electron microscopy (Figure 8C and D). We also found that purified G82V MCPs have DDH and PduP activities similar to LT2 (DDH: 27.6 $\mu mol \cdot min^{-1} \cdot mg^{-1}$ compared to 27.2 $\mu mol \cdot min^{-1} \cdot mg^{-1}$; PduP: 7.5 $\mu mol \cdot min^{-1} \cdot mg^{-1}$ compared to 6.8 $\mu mol \cdot min^{-1} \cdot mg^{-1}$). None of the tests we did the G82V mutant suggested that the central pore

in PduB' was occluded to 1,2-PD or any other cofactor. The slow growth exhibited by the G82V mutant is a special case because the only other instance of seeing slower growth on minimal media due to a mutation of a shell protein is in the S40L mutant of the PduA pore. This may be due to the valine substitution hindering the PduB' central pore opening and closing transition. However, this slow growth phenotype has been somewhat difficult to reproduce and we are trying to define the growth condition more carefully. These results indicate that the G82 residue is a tolerant residue capable of a wide range of substitutions which is interesting considering it is one of the more evolutionary conserved residues in the region (93%) (Figure 4C).

Other glycine substitutions at positions G83, G85, and G87 had fast growth phenotypes. G85A, G85M, G85D, and G85K somewhat faster that wild-type (Figure 8B). Interestingly, G87A grew similar to LT2 while the G87N mutant much faster indicated a broken MCP shell. G83A showed similar growth to LT2. Due to the faster growth on minimal media, these results suggest that the mutants at G85 produce unstable MCPs, thus G85 is a position that is an obligate glycine. Supporting this is the multiple sequence alignment that shows G85 is 100% conserved among all PduB' homologs (Figure 4C). Interestingly, the G87A mutant showed growth similar to LT2 even though the G87 position is a glycine across PduB homologs, while the G87N mutant showed faster growth indicative of an unstable MCP. Mutagenesis at the G83 position showed no growth phenotype (G83A) indicating that substitutions at this position are not as debilitating as the G85 or G87 positions. Taken together, mutations at G82 and G83 produced stable MCPs, while mutations at the G85 and G87 mutations produced unstable MCPs.

Concave side of the PduB' trimer

The pore region of the PduB shell protein found on the inner surface of the MCP shell is vastly different than that of the cytoplasmic (convex) side. Amino acid residues of the lumen side are much less conserved than those of the cytoplasmic side indicating a tolerance for more drastic amino acid substitutions (Figure 9A and B). Immediately noticeable in the structure are three phenylalanines, one from each trimer, that come together in the center of the pore. The Phe residues are also present in PduB' homologs in EtuB and PduB' (Heldt *et al.* 2009, Pang *et al.* 2012). Pi-Pi interaction among these residue might stabilize the closed form of the pore and bulky phenylalanine side chains might be needed for full closure. Extensive mutagenesis of this area was done (F188A, F188R, F188C, F188P, and F188W). Surprisingly, the growth phenotypes of these mutants did not differ from LT2 (Figure 9C). In addition, purified MCPs from mutagenesis at F188 showed similar SDS-PAGE banding patterns and had similar yields to LT2 (Figure 9D, E, and F).

Interestingly, of seven mutants made on the lumen side of the pore, only E191 was found to play an essential role using alanine mutagenesis. This site was selected because it is 100% conserved among all pduB' homologs and it was in a position that was close to the central pore. Curiously, the side chain sticks into a channel of a PduB' monomer in the crystal structure. Seeing as it was an evolutionary conserved residue and was near the central pore of PduB', it was selected for mutagenesis to probe its potential function. The E191A mutant grew much faster than LT2 in growth assays, suggesting that an incomplete shell is being formed. MCPs purified from E191A showed similar SDS-PAGE banding pattern to LT2 (Figure 9F), including all major shell proteins. The only difference between microcompartment purifications of E191A

and wild-type were overall yields of MCPs as the yield of E191A MCPs were much lower than LT2 (30%). This indicates that the E191A mutant produces an unstable MCP. Other mutations done in this region were H184A and N190A. The growth phenotypes and MCPs purified from these were comparable to LT2 (data not shown).

From this work on the concave side of the pore, there were fewer residues that affected the overall stability of the trimer compared to mutagenesis studies on the convex side. This may be correlated to the low level of conserved residues across this side of the pore (Figure 9B). However, the flexibility of the F188 position is extremely interesting, as disruption of the hydrophobic patch (F188A), introduction of a trp (F188W), adding a potential re-dox reactive site (F188C), and changing the hydrophobic environment to an electrostatic one (F188R) have no discernable phenotypes. Because these mutants do not show any growth phenotypes and the overall yield of the MCPs are comparable to LT2, it indicates that mutations at the F188 residue is not affecting the overall stability of the MCP and, presumably, PduB'.

Discussion

The rationale for this work was to identify essential residues in PduB' and how mutations of those residues affect the overall MCP function *in vivo and in vitro*. Because this is the first work looking at single amino acid positions in PduB', most residues were selected based on their location in the PduB' structure and how conserved they were among PduB' homologs. To evaluate a residues contribution to the overall function of PduB', two assays were primarily done: growth assays on minimal media and purified microcompartment yields and banding pattern on SDS-PAGE (protein content). Prior studies demonstrated that faster growth on 1,2-PD minimal medium at limiting B_{12} levels is indicative of mutations that impairs that ability of the

MCP shell to act as a diffusion barrier (Havemann, *et al.* 2002, Cheng *et al.* 2012, Sinha *et al.* 2014, Chowdhury *et al.* 2015, Liu *et al.* 2015). The yield and protein content of purified MCPs was used as an indicator of stability during purification and assembly.

Residues examined in this study were primarily central pore residues meaning that they are within the region of PduB' that opens to form the large central pore. This region was targeted to address the function of the pore. In most cases, mutation of highly conserved residues reduced MCP yields during purification indicating reduced MCP stability or impaired assembly. Conversely, substitutions as less conserved sites usually lacked obvious phenotypes and gave normal MCP yields. For all mutant MCPs that were purified, bands seen on SDS-PAGE gels were nearly identical to wild-type controls. All major shell proteins were present and the shell was still able to encapsulate lumen enzymes. This is indicative of normally assembled MCPs. The only difference in purification between control and mutant MCPs was the overall yield. Low yields of purified MCPs indicated that mutant MCPs were unstable during purification or that fewer MCPs were formed. The yield of purified MCPs corresponded well with the growth assays, i.e. lower MCP yield correlated with faster growth than wild-type on 1,2-PD minimal medium. This supported the idea that mutagenesis at these conserved residues altered PduB' in such a way that MCPs are unstable during purification and that the MCP lumen enzymes have increased access to their substrates and cofactors in vivo. It cannot be discerned whether lumen enzymes have increased substrate access due to a "leaky" MCP shell, misassembled MCPs or an open central pore that forms a large channel into the MCP.

Another surprising result of the mutagenesis was that F188 was tolerant to a wide variety of changes without apparent phenotype. It appears that the pi-pi interactions of the phenylalanine

rings are not inherently important to PduB' stability and that changing this bulky phe side chain with a methyl group (ala) does not influence shell permeability or stability. It is also of note that F188C mutations may be used further to cross-link the central pore locking it in the closed position). Furthermore, F188R mutations demonstrate that the central pore can be changed from a hydrophobic environment to a charged environment with no effect on overall MCP stability of function. Finally, the F188W mutant could play a role in future *in vitro* work like using trp fluorescence as a sensor for central pore opening and closing. PduB has no native trp residues.

These findings described above, to our knowledge, are the first to show the effect of individual amino acid substitutions of PduB and PduB' *in vivo.* Although the finding that most PduB' mutants likely reduced protein stability are admittedly underwhelming, they are an important stepping stone to understand how PduB' and its homologs work as an individual protein, as a trimer, and in the overall context of the MCP. Findings here can be used to further address transport across the central pore and to actively study PduB' *in vivo*.

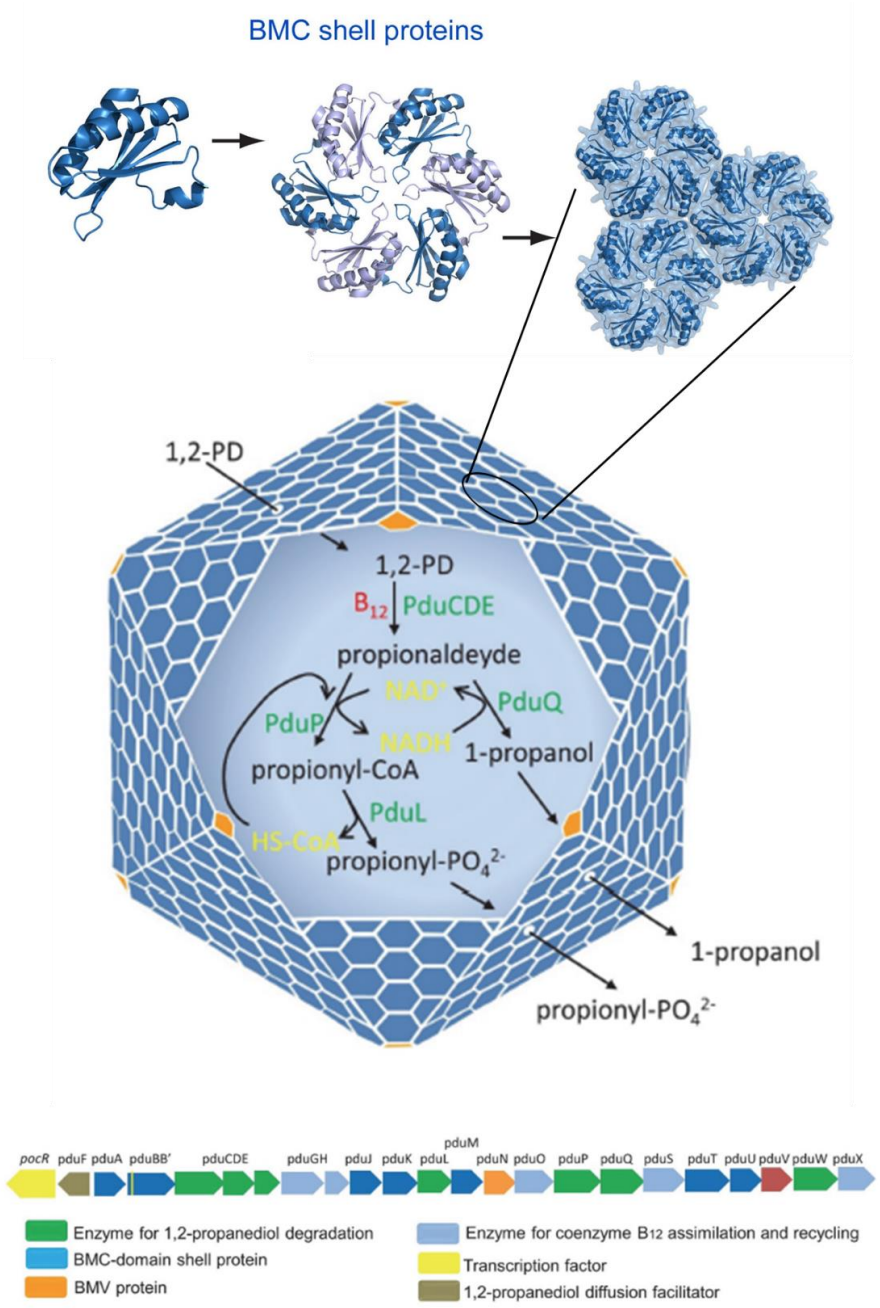

Figure 1. Current model of Pdu MCP metabolism. BMC domain containing peptides assemble into hexamers or pseudohexamers and come together along the edges to form the facets of the MCP. The shell then encapsulates the metabolic process of 1,2-PD degradation. Adapted from Yeates, *et al.* 2001 and Bobik *et al.* 2015.

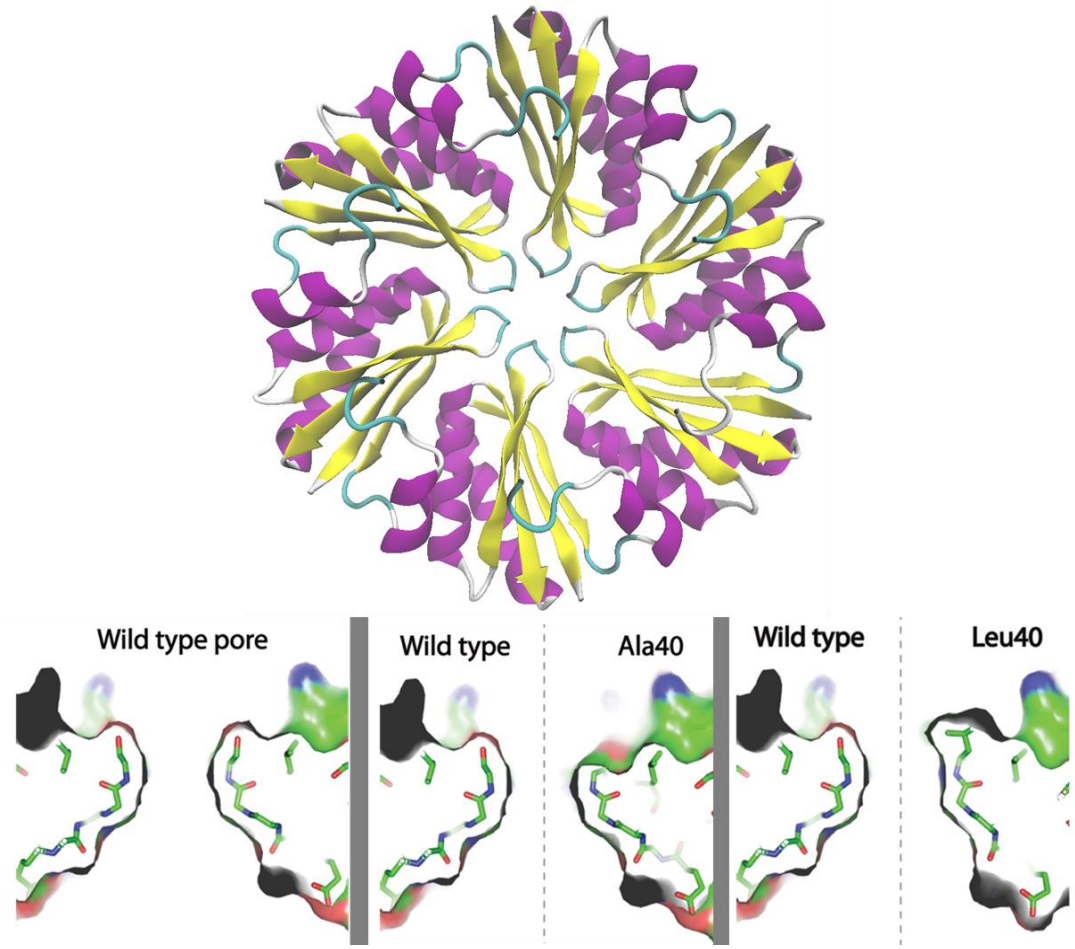

Figure 2. Transport across the PduA shell protein can be altered. (Top) structure of the PduA hexamer (PDB ID: 3NGK). (Bottom) Amino acid substitutions along the central pore can alter transport of metabolites. Left panel: wild-type pore; Middle panel: the S40A substitution promote propionaldehyde escape from the lumen of the MCP; Right panel: an S40L substitution occludes 1,2-PD from entering the MCP. Adapted from (Bobik *et al* 2015)

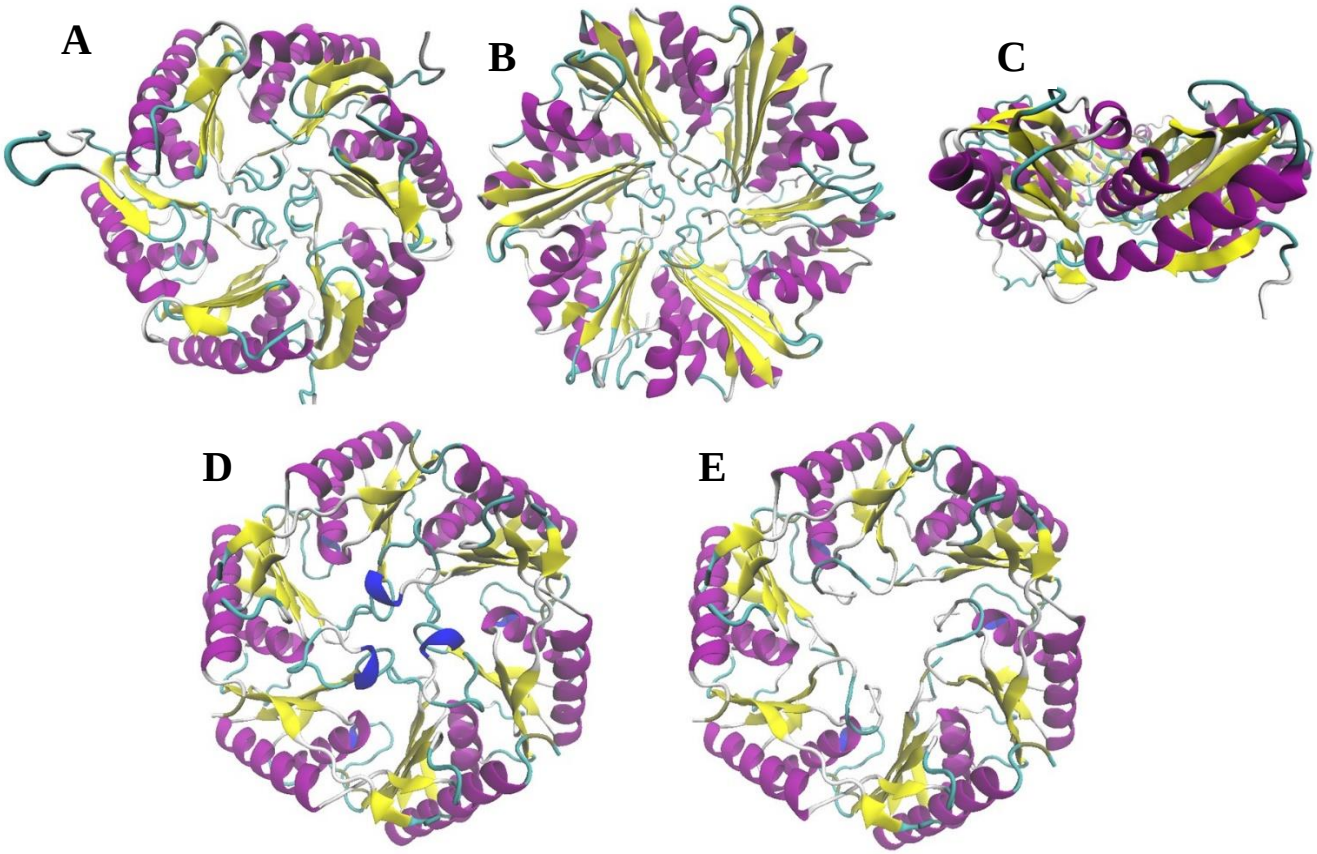

Figure 3.Strucutre of PduB’ PduB’ structure facing the (A) convex side, (B) concave side, and (C) view from the side. EutL in closed (D) and open (E) forms (PDB entries 3I82 and 3I87, respectively) (Tanaka *et al.* 2010). Visualization was done using VMD.

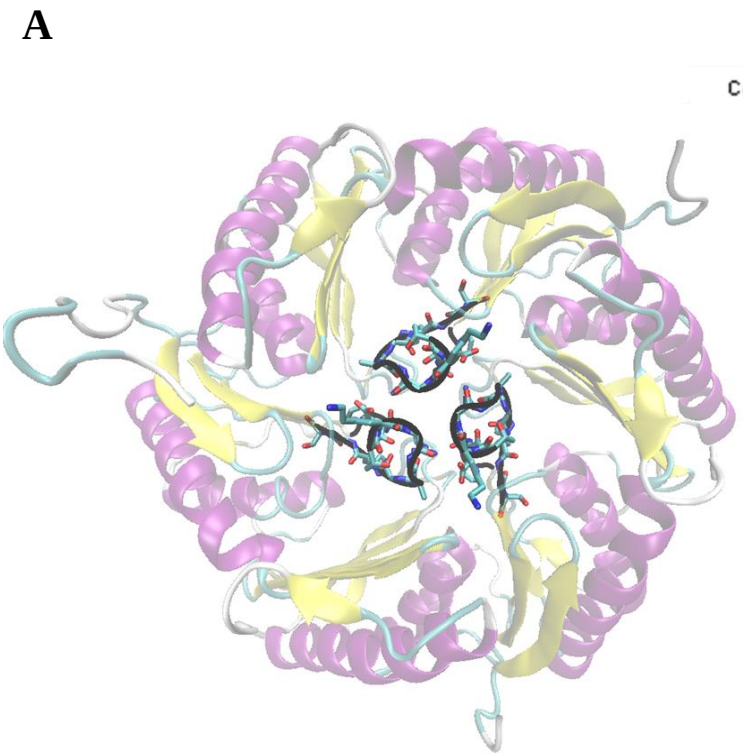

C

Residue	% Identity
P77	73
R78	99
D79	100
T80	94
K81	83
G82	96
G83	86
A84	77
G85	100
H86	95
G87	100
S88	82

Figure 4. Important residues on the convex side of the PduB' trimer. (A) Convex side of PduB' with highlighted residues corresponding to the Multiple Sequence Alignment in (B). Residues atop the MSA in (B) are highlighted if they contain >83% sequence identity with other PduB homologs. The row below the sequence is conservation of the alignment that doesn't contain gaps. The row line below the sequence is the quality score based on the BLOSUM62 values for that residue. The final row is the consensus sequence based on the input of the alignment. In all rows, the height of the bars indicate a higher score for that particular residue. (C) Table showing residues highlighted in structure and MSA and their % identity among PduB' homologs. Visualization of PduB' was done using VMD; MSA was done using Jalview and the alignment was done using clustalomega

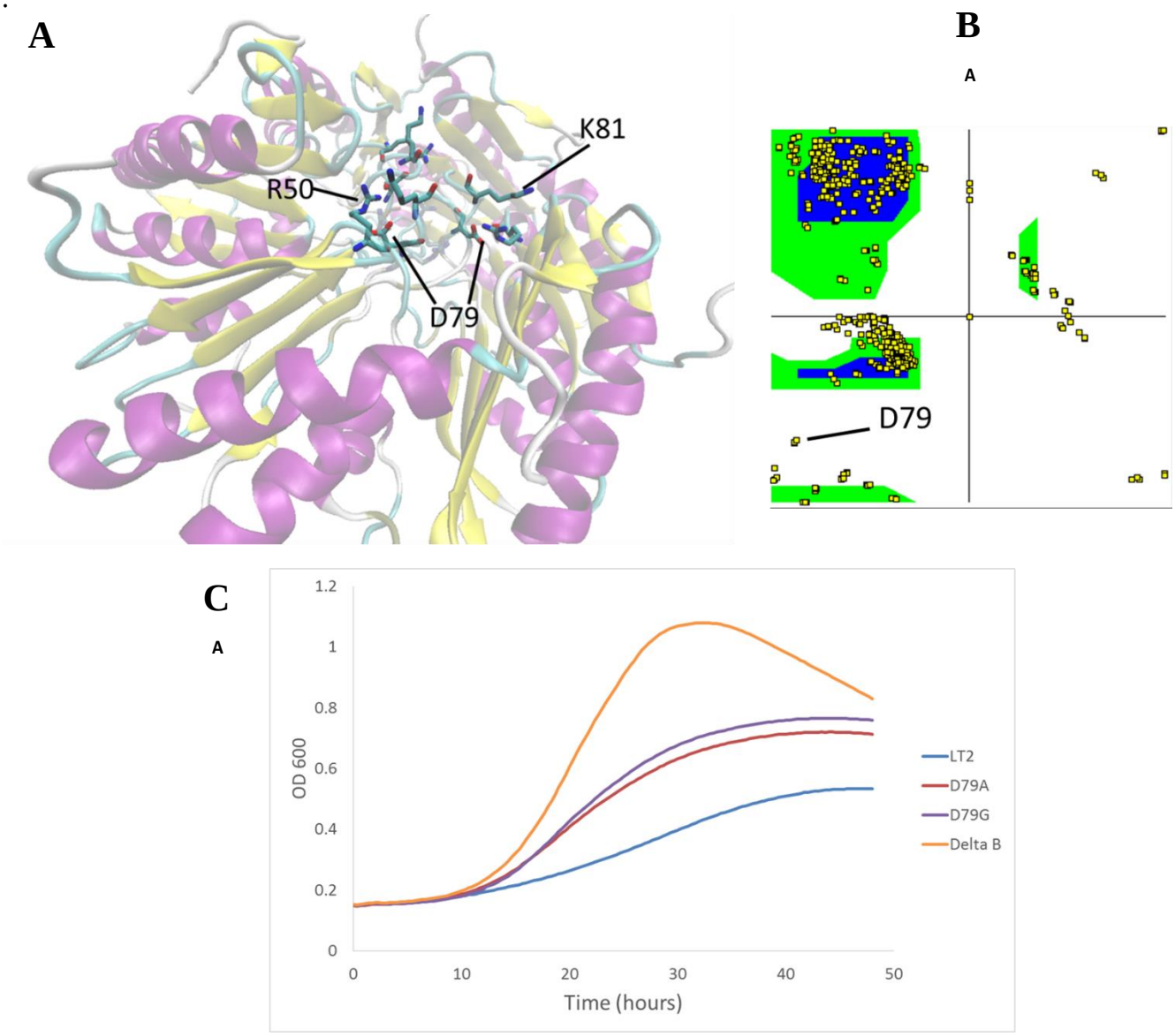

Figure 5. Location and importance of D79. (A) Structure of PduB' with highlighted residues, specifically the Ramachandran outlier D79 which can be observed in (B). (C) Growth curve of wild-type (LT2) and mutant strains on minimal media.

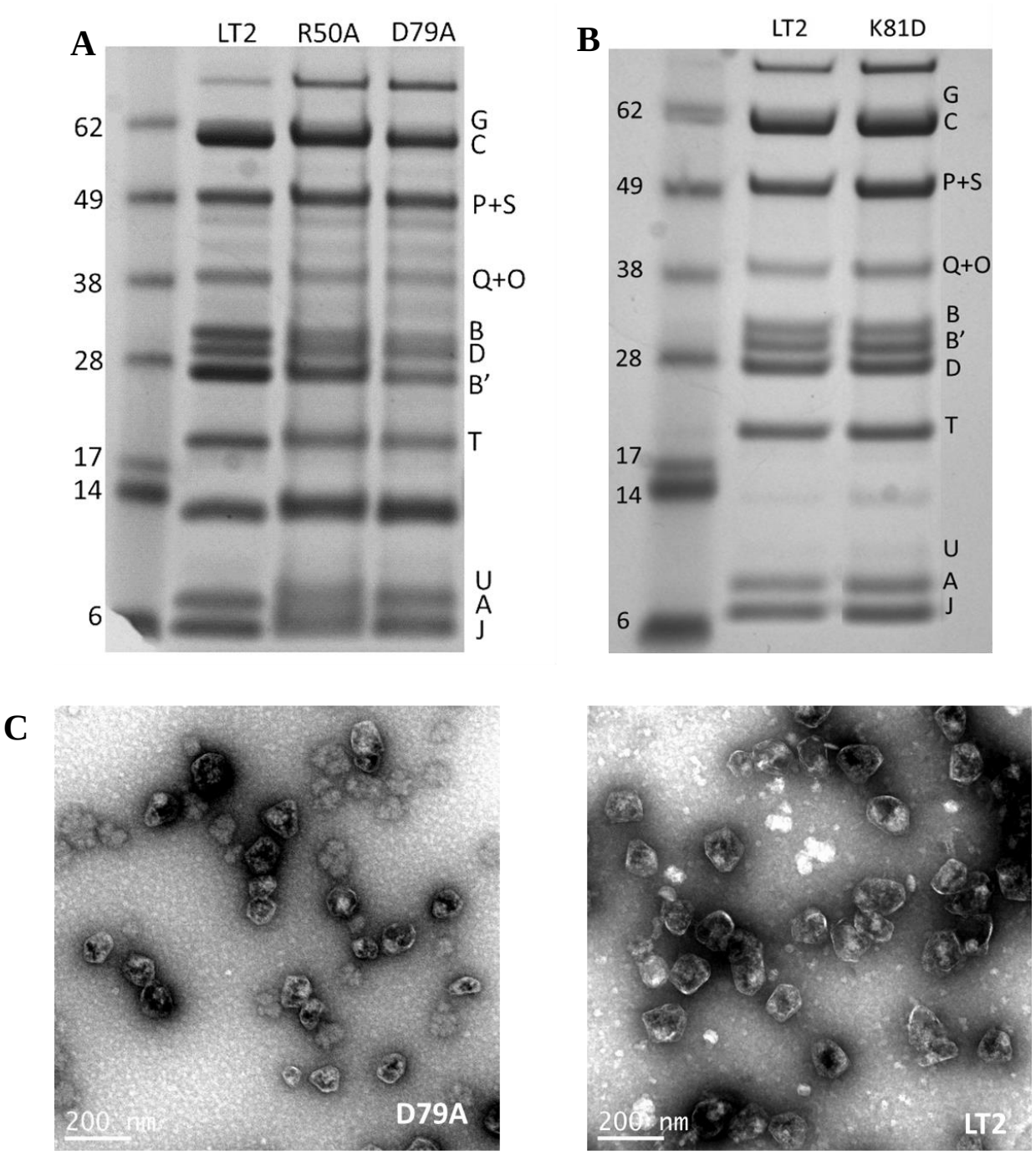

Figure 6. Microcompartments of D79A, R50A, and K81D. (A and B) SDS-PAGE gels of purified microcompartments from labeled strain. Wild-type: LT2. The numbers to the left of each gel indicate the sizes of molecular mass markers while the letter on the right side indicate particular Pdu proteins. (C and D) Transmission electron microscopy image of purified MCPs of the D79A mutant (left) and of LT2 (right).

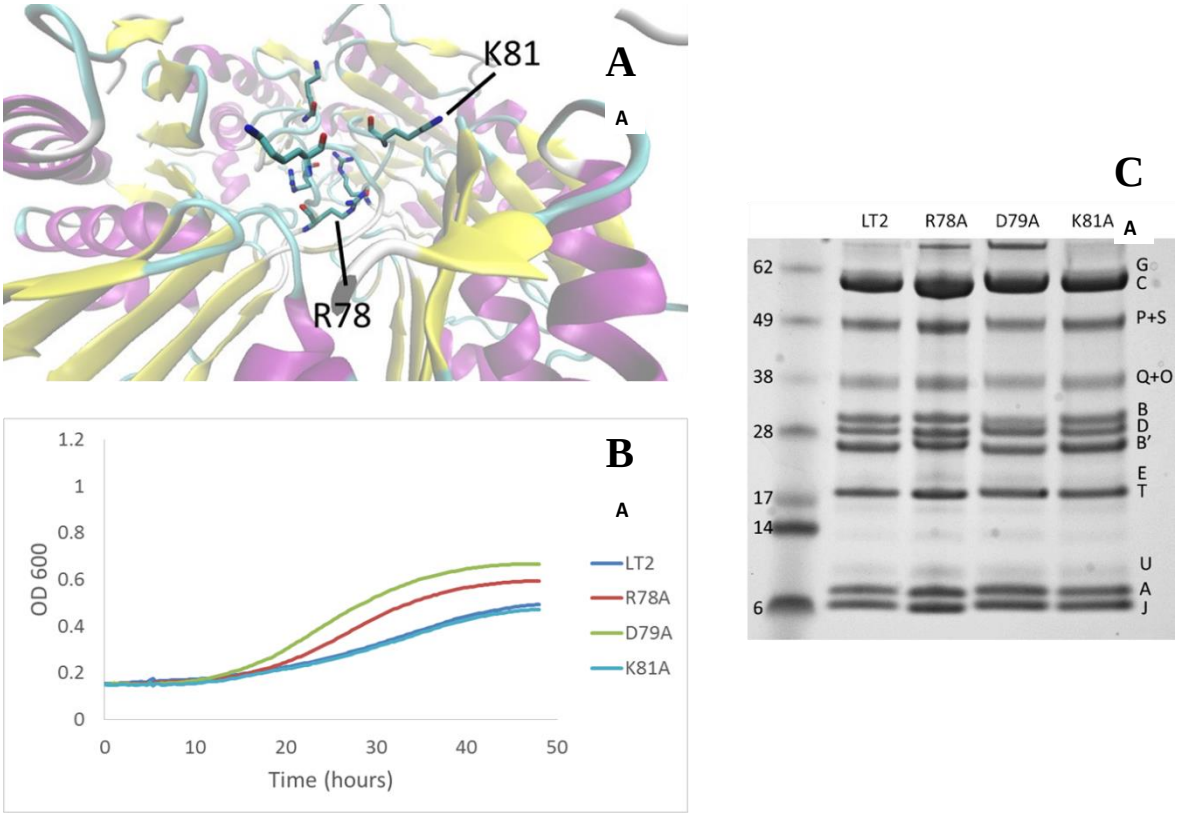

Figure 7. Electrostatic mutants on the convex side of the PduB' pore. (A) Positively charged residues at the center on the cytoplasmic side of the PduB' trimer. (B) Growth of wild type (LT2) and PduB mutants on 1,2-PD minimal media. (C) Protein content of the purified MCPs by SDS-PAGE. The numbers to the left of each gel indicate the sizes of molecular mass markers while the letter on the right side indicate particular Pdu protein

A

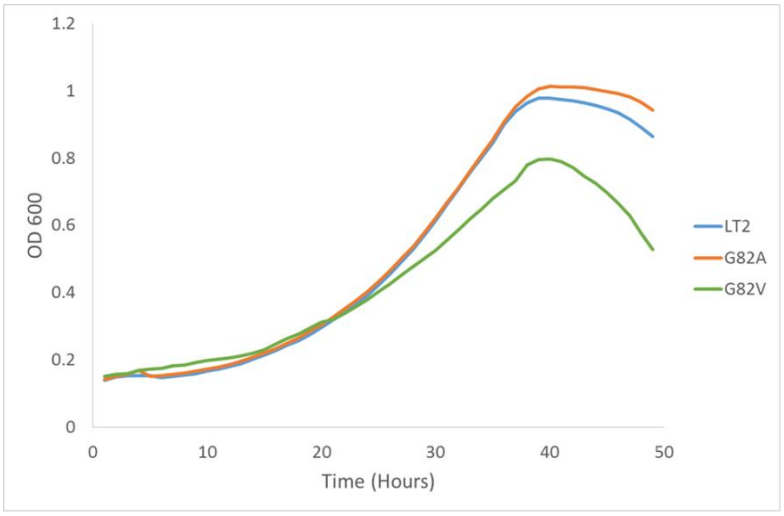

B

Residue	Mutation	Growth Phenotype (20nM B12)
G82	A	Normal
	C	Normal
	I	Normal
	L	Normal
	S	Normal
	V	Slow
G83	A	Normal
G85	A	Fast
	D	Fast
	M	Fast
	K	Fast
G87	A	Normal
	N	Fast

C

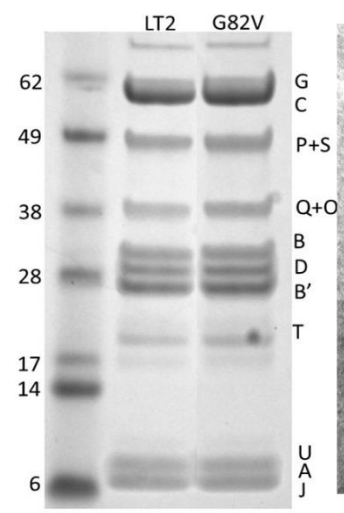

D

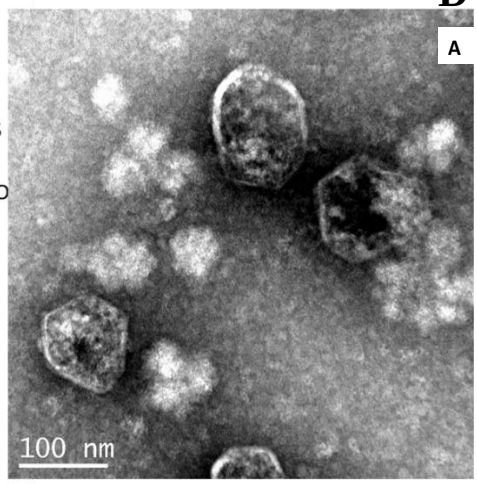

Figure 8. G82V growth and microcompartments. (A) Growth assay on 1,2-PD minimal media (50 nm CN). Wild-type (LT2) and strains with particular PduB' mutations are indicated. (B) Table of glycine-rich motif mutants generated with their growth phenotype under low B_{12} conditions. Normal growth indicates that the strain grew similar to wild-type. (C) SDS-PAGE of 15µg purified MCPs from wild-type and the G82V mutant. The numbers to the left of each gel indicate the sizes of molecular mass markers while the letter on the right side indicate particular Pdu protein. (D) Transmission electron microscopy of G82V microcompartments.

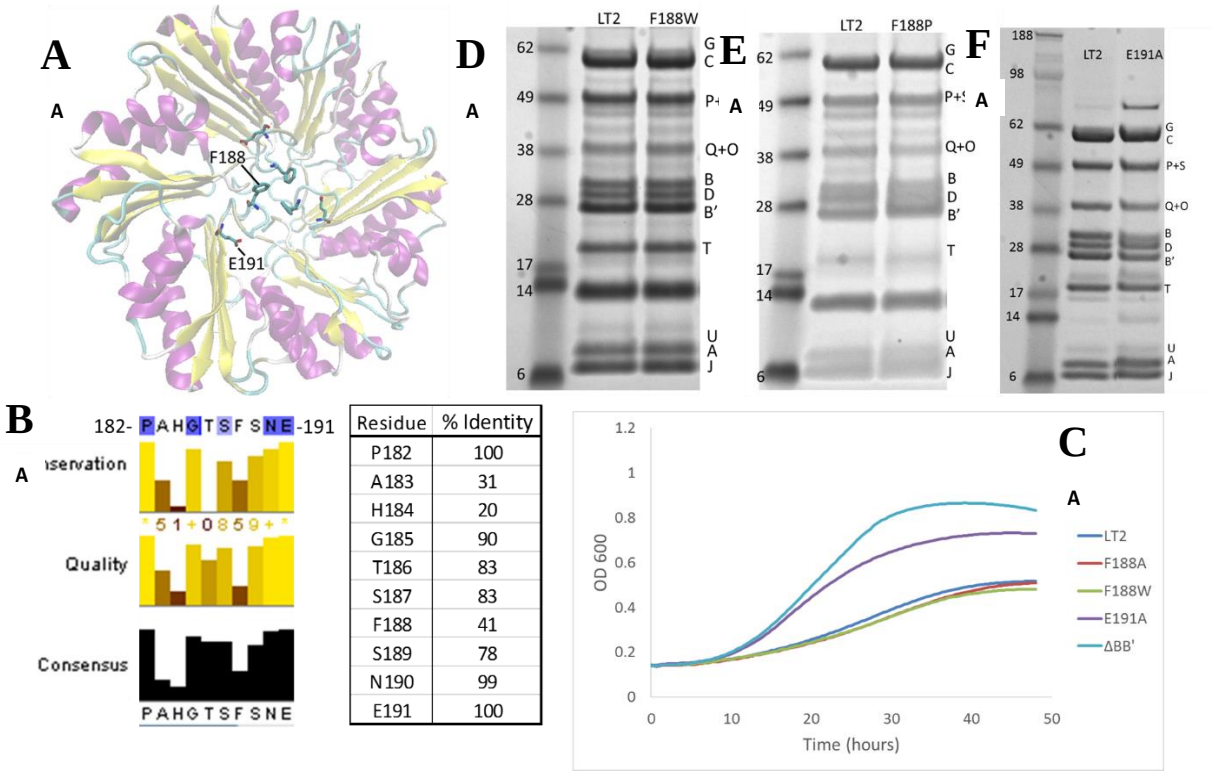

Figure 9. Mutants along the concave side of the PduB' pore. (A) Structure of PduB' highlighting residues F188 and E191. (B) Multiple sequence analysis of PduB' with same parameters as Figure 2B. Each residue is labeled with a percent identity compared to all other PduB' homologs. (C) Growth assay of selected mutants on 1,2-PD minimal media (20 nm OH-B_{12}). Wild-type strain is LT2. (D, E, and F) Purified MCPs of selected mutants and wild-type (LT2). The numbers to the left of each gel indicate the sizes of molecular mass markers while the letter on the right side indicate particular Pdu protein

Materials and Methods

Multiple Sequence Alignment

The sequence of the PduB' crystal structure was inputted into NCBI PSI-Blast algorithm tool to searching the Reference Proteins (refseq_protein) database excluding *Salmonella enterica* (taxid:28901). The blast search was run for three cycles. 106 sequences were pulled together and a multiple sequence alignment was made using clustalomega and visualized using Jalview.

Generating chromosomal mutants

Forward and reverse Sac-Cat construct oligos were designed in a fashion there were 70bp of homology to the gene of interest and 20bp of homology to the Sac-Cat gene. Sac-Cat genes were taken from pCS693 of our lab collection. Sac-Cat gene amplification was done via PCR in an Eppendorf AG thermocycler with the following conditions: Step 1) 95°C for 2 min; Step 2) 95°C for 30 sec, 50°C for 30 sec, 72°C for 2:30 min, for 30 cycles; Step 3)70°C 10min. Amplified DNA was purified using a Promega Wizard PCR cleanup kit using directions given by the supplier. DNA was then added to a 1% agarose gel and ran at 140V for 20min where the band of appropriate size (~2.3Kb) was excised and purified using a Qaigen Gel Extraction kit. Restriction Digest of DNA was then done using DpnI digestion for 4 hours at 37°C. DNA was applied to a 1% agarose gel and band was excised after 20 min at 140V. 100ng of DNA was then added to cells with an OD_{600} of 50-100 expressing the Lambda Phage Red Recombinase from the pKD46 plasmid. DNA was transformed via electroporation. Cells recovered at 37°C in SOC for 1 hour where they were then plated on a TYE-Cam 20ug/µL plate. Colonies observed were screened for sucrose sensitivity and chloramphenicol resistance. Positive colonies were then subject to colony PCR where insertion of the Sac-Cat at the desired position at the 5' and 3' ends was done using primers flanking the gene of interest and primers internal to the Sac-Cat. Colony PCR protocol was Step1) 95°C for 10 min; Step 2) 95°C for 30sec, 50°C for 30sec, and 70°C for 2:30min, repeated 30 times; Step 3) 70°C for 10 minutes. Positive colonies were then grown and the pKD46 plasmid was transformed back into the cells. 100ng of an oligo containing the desired mutation as well as flanking regions to the area of the gene that's encompassed by the Sac-Cat was then electroporated into competent cells with an OD_{600} of 50-100 containing the Sac-Cat and expressing the lambda phage red recombinase. Cells would then recover in 1mL SOC media at 37°C and plated on a TYE-10% Sucrose plate. Colonies observed were screened for chloramphenicol sensitivity. Positive colonies from the screen were subject to colony PCR using primers flanking the entire gene of interest. Bands were excised and sent for DNA sequencing.

Chromosomal Oligos

All oligos used in this study were purchased from IDT

Sac-Cat Insertion oligo	Sequence
pduBSC_343_354F	gaagcggtgaaagccaccaacaccgaagtggtcagcattgagctgccg aatacattcaaatatgtatccg
pduBSC_343_354R	gaaacgtcgttaccgcctaaaataatcagcgaaccgtggcccgcgccgcc ttacgccccgccctgccactc
pduBSC 663-684F	gatggccgataccgcgctgaagtcagccaacgttgaagtcgtggcgtacagctctccggcg aatacattcaaatatgtatccgctcatga
pduBSC 663-684R	cgggcggaggtcaccgcctgacggaccgcgccggagtcgccggaaatcaccagaatagc ttacgccccgccctgccactcatcgcagtac
pduB' 49-55SC_F	ctggacgcga tgaaacttga gaagcgctat cgttccatcg gcattctcgg caatacattcaaatatgtatccg
pduB' 49-55SC_R	accacttcggtgttggtggctttcaccgcttcgtccgccgccataatgtg ttacgccccgccctgccactc
Chromosomal Mutation oligo	**Sequence**
pduB'_R78A	aagccaccaacaccgaagtggtcagcattgagctgccggccgataccaaaggcggcgcgggccacggttcgctgattatt
pduB'_D79N	aagccaccaacaccgaagtggtcagcattgagctgccgcgcaataccaaaggcggcgcgggccacggttcgctgattatt
pduB'_D79A	aagccaccaacaccgaagtggtcagcattgagctgccgcgcgctaccaaaggcggcgcgggccacggttcgctgattatt
pduB'_K81A	aagccaccaacaccgaagtggtcagcattgagctgccgcgcgataccgcaggcggcgcgggccacggttcgctgattatt
pduB' F188A	aagtcgtggcgtacagctctccggcgcacggcaccagcgctagtaacgaagctattctggtgatttccggcgactccggc
PduB' H184A	aagtcgtggcgtacagctctccggcggccggcaccagctttagtaacgaagctattctggtgatttccggcgactccggc
PduB' E191A	aagtcgtggcgtacagctctccggcgcacggcaccagctttagtaacgcagctattctggtgatttccggcgactccggc
pduB' F188W	aagtcgtggcgtacagctctccggcgcacggcaccagctggagtaacgaagctattctggtgatttccggcgactccggc
pduB' R50A	gaagcgctatcgttccatcggcattctcggcgccgccaccggcgcaggcccgcacattatggcggcggacgaagcggtga
pduB' N190A	aagtcgtggcgtacagctctccggcgcacggcaccagctttagtgccgaagctattctggtgatttccggcgactccggc
pduB' F188C	aagtcgtggcgtacagctctccggcgcacggcaccagctgtagtaacgaagctattctggtgatttccggcgactccggc
pduB' F188R	aagtcgtggcgtacagctctccggcgcacggcaccagcagaagtaacgaagctattctggtgatttccggcgactccggc
pduB'_D79G	aagccaccaacaccgaagtggtcagcattgagctgccgcgcggtaccaaaggcggcgcgggccacggttcgctgattatt
pduB' K81D	aagccaccaacaccgaagtggtcagcattgagctgccgcgcgataccgaaggcggcgcgggccacggttcgctgattatt
pduB' G82C	aagccaccaacaccgaagtggtcagcattgagctgccgcgcgataccaaatgcggcgcgggccacggttcgctgattatt
pduB' R78C	aagccaccaacaccgaagtggtcagcattgagctgccgtgcgataccaaaggcggcgcgggccacggttcgctgattatt
pduB' G82L	aagccaccaacaccgaagtggtcagcattgagctgccgcgcgataccaaactcggcgcgggccacggttcgctgattatt
pduB' G82S	aagccaccaacaccgaagtggtcagcattgagctgccgcgcgataccaaatccggcgcgggccacggttcgctgattatt
pduB' G82V	aagccaccaacaccgaagtggtcagcattgagctgccgcgcgataccaaagtcggcgcgggccacggttcgctgattatt
pduB' G82I	aagccaccaacaccgaagtggtcagcattgagctgccgcgcgataccaaaatcggcgcgggccacggttcgctgattatt
pduB' G82A	aagccaccaacaccgaagtggtcagcattgagctgccgcgcgataccaaagccggcgcgggccacggttcgctgattatt
pduB' G83A	caccgaagtggtcagcattgagctgccgcg cgataccaaaggcgccgcgggccacggttcgctgattattttaggcggta
pduB' G87A	accaacaccgaagtggtcagcattgagctgccgcgcgataccaaaggcggcgcgggccacgcttcgctgattattttaggcggtaacgac
pduB' G87N	accaacaccgaagtggtcagcattgagctgccgcgcgataccaaaggcggcgcgggccacaattcgctgattattttaggcggtaacgac
pduB' G85D	accaacaccgaagtggtcagcattgagctgccgcgcgataccaaaggcggcgcggaccacggttcgctgattattttaggcggtaacgac
pduB' G85A	accaacaccgaagtggtcagcattgagctgccgcgcgataccaaaggcggcgcggcccacggttcgctgattattttaggcggtaacgac
pduB' G85K	accaacaccgaagtggtcagcattgagctgccgcgcgataccaaaggcggcgcgaaacacggttcgctgattattttaggcggtaacgac

Growth assay on minimal media

Growth assays were done in accordance with Liu *et. al.* (2007), with the modification that sterile ddH_2O was used instead of sterile dH_2O

Microcompartment Purification

MCP purification were done in accordance with Sina *et. al.* (2012), with the following modifications: 4mL of overnight LB culture was used as an inoculum, and final resuspension volume was dependent on the size of the pellet. For unstable MCPs, as little as 40µL was used to resuspend the final MCP pellet.

DDH and PduP assays

Enzymatic assays involving purified MCPs were done in accordance with Chowdhury *et. al.* 2015.

Strains used in study

Strains used that were previously generated		
Name	Genotype	Lab Strain Number
LT2	wild-type salmonella lab strain LT2	
LT2/pKD46	LT2/pKD46	BE293
ΔBB'	LT2 ΔBB'	SS23
SC	p41a-Sac-Cat	CS693

Strains Generated In This Study			
Name	Genotype	Mother/Father	BL Strain Number
343-354SC	pduB-SC 342-354	BE293/SC oligo 343-354	39
343-354SC/pKD46	pduB-SC 342-354/pKD46	BL39/pKD46	40
D79N	PduB' D79N	BL40/ oligo PduB'_D79N	41
D79A	PduB' D79A	BL40/ oligo PduB'_D79A	42
R78A	PduB' R78A	BL40/ oligo PduB'_R78A	43
K81A	PduB' K81A	BL40/Ioligo PduB'_K81AA	44
663-664SC	pduB-SC 663-684	BE293/SC oligo 663-684	45
663-664SC/pKD46	pduB-SC 663-684/pkD46	BL45/pKD46	48
H184A	pduB' H184A	BL48/oligo PduB' H184A	49
F188A	pduB' F188A	BL48/oligo PduB' F188A	50
F188W	pduB' F188W	BL48/oligo PduB' F188W	51
E191A	pduB' E191A	BL48/oligo PduB' E191A	52
G85M	pduB' G85M	BL40/ oligo PduB G85M	59
49-55SC	pduB' SC 49-55	BE293/SC oligo 49-55	69
N190A	pduB' N190A	BL48/oligo PduB' N190A	75
49-55SC/pKD46	pduB' SC 49-55/pKD46	BL69/pKD46	78
R50A	PduB' R50A	BL78/oligo PduB' R50A	79
F188C	pduB' F188C	BL48/oligo PduB' F188C	82
F188R	pduB' F188R	BL48/oligo PduB' F188R	83
D79G	pduB' D79G	BL40/ oligo PduB' D79G	84
R78C	pduB' R78C	BL40/ oligo PduB' R78C	86
K81D	pduB' K81D	BL40/ oligo PduB' K81D	87
G82C	pduB' G82C	BL40/ oligo PduB' G82C	88
G82A	pduB' G82A	BL40/ oligo PduB' G82A	96
G82L	pduB' G82L	BL40/ oligo PduB' G82L	98
G82S	pduB' G82S	BL40/ oligo PduB' G82S	99
G82V	pduB' G82V	BL40/ oligo PduB' G82V	100
G83A	pduB' G83A	BL40/ oligo PduB' G83A	127
F188P	pduB' F188P	BL48/oligo PduB' F188P	129
G85D	pduB' G85D	BL40/ oligo PduB' G85D	134
G87A	pduB' G87A	BL40/ oligo PduB' G87A	135
G87N	pduB' G87N	BL40/ oligo PduB' G87N	136
G85A	pduB' G85A	BL40/ oligo PduB' G85A	140
G85K	pduB' G85K	BL40/ oligo PduB' G85K	141

Works Cited

Abdul-Rahman, F., *et al.* (2013). "The distribution of polyhedral bacterial microcompartments suggests frequent horizontal transfer and operon reassembly." J. Phylogen. Evolution. Biol. **1**(4): doi 10.4172/2329-9002.1000118

Axen, S. D., *et al.* (2014). "A taxonomy of bacterial microcompartment loci constructed by a novel scoring method." PLoS Comput. Biol. **10**(10): e1003898.

Bobik, T. A. (2006). "Polyhedral organelles compartmenting bacterial metabolic processes." Appl Microbiol Biotechnol **70**(5): 517-525.

Bobik, T. A., *et al.* (1999). "The propanediol utilization (*pdu*) operon of *Salmonella enterica* serovar Typhimurium LT2 includes genes necessary for formation of polyhedral organelles involved in coenzyme B_{12}-dependent 1, 2-propanediol degradation." J Bacteriol **181**(19): 5967-5975.

Bobik, T. A., *et al.* (1997). "Propanediol utilization genes (*pdu*) of *Salmonella typhimurium*: three genes for the propanediol dehydratase." J Bacteriol **179**(21): 6633-6639.

Cai, F., *et al.* (2013). "The structure of CcmP, a tandem bacterial microcompartment domain protein from the β-carboxysome, forms a subcompartment within a microcompartment." J Biol Chem **288**(22): 16055-16063.

Chen, P., *et al.* (1995). "Five promoters integrate control of the *cob*/*pdu* regulon in *Salmonella typhimurium*." J Bacteriol **177**(19): 5401-5410.

Chen, P., *et al.* (1994). "The control region of the *pdu*/*cob* regulon in *Salmonella typhimurium*." J Bacteriol **176**(17): 5474-5482.

Cheng, S., *et al.* (2012). "The PduQ enzyme is an alcohol dehydrogenase used to recycle NAD^+ internally within the Pdu microcompartment of *Salmonella enterica*." PLoS One **7**(10): e47144.

Cheng, S., *et al.* (2011). "Genetic analysis of the protein shell of the microcompartments involved in coenzyme B_{12}-dependent 1,2-propanediol degradation by *Salmonella*." J Bacteriol **193**(6): 1385-1392.

Chowdhury, C., *et al.* (2015). "Selective molecular transport through the protein shell of a bacterial microcompartment organelle." Proc Natl Acad Sci U S A **112**(10): 2990-2995.

Chowdhury, C., *et al.* (2014). "Diverse bacterial microcompartment organelles." Microbiol. Mol. Biol. Rev. **78**(3): 438-468.

Crowley, C. S., *et al.* (2010). "Structural insight into the mechanisms of transport across the *Salmonella enterica* Pdu microcompartment shell." J Biol Chem **285**(48): 37838-37846.

Crowley, C. S., *et al.* (2008). "Structure of the PduU shell protein from the Pdu microcompartment of Salmonella." Structure **16**(9): 1324-1332.

Daniel, R., *et al.* (1998). "Biochemistry of coenzyme B_{12}-dependent glycerol and diol dehydratases and organization of the encoding genes." FEMS Microbiol Rev **22**(5): 553-566.

Havemann, G. D. and T. A. Bobik (2003). "Protein content of polyhedral organelles involved in coenzyme B_{12}-dependent degradation of 1,2-propanediol in *Salmonella enterica* serovar Typhimurium LT2." J Bacteriol **185**(17): 5086-5095.

Havemann, G. D., *et al.* (2002). "PduA is a shell protein of polyhedral organelles involved in coenzyme B_{12}-dependent degradation of 1,2-propanediol in *Salmonella enterica* serovar typhimurium LT2." J Bacteriol **184**(5): 1253-1261.

Heldt, D., *et al.* (2009). "Structure of a trimeric bacterial microcompartment shell protein, EtuB, associated with ethanol utilization in Clostridium kluyveri." Biochem J **423**(2): 199-207.

Horswill, A. R. and J. C. Escalante-Semerena (1997). "Propionate catabolism in *Salmonella typhimurium* LT2: two divergently transcribed units comprise the *prp* locus at 8.5 centisomes, *prpR* encodes a member of the sigma-54 family of activators, and the *prpBCDE* genes constitute an operon." J Bacteriol **179**(3): 928-940.

Jeter, R. M. (1990). "Cobalamin-dependent 1,2-propanediol utilization by *Salmonella typhimurium*." J Gen Microbiol **136**(5): 887-896.

Kerfeld, C. A., *et al.* (2010). "Bacterial microcompartments." Annu Rev Microbiol **64**: 391-408.

Kerfeld, C. A., *et al.* (2005). "Protein structures forming the shell of primitive bacterial organelles." Science **309**(5736): 936-938.

Klein, M. G., *et al.* (2009). "Identification and structural analysis of a novel carboxysome shell protein with implications for metabolite transport." J Mol Biol **392**(2): 319-333.

Leal, N. A., *et al.* (2003). "PduP is a coenzyme-A-acylating propionaldehyde dehydrogenase associated with the polyhedral bodies involved in B_{12}-dependent 1,2-propanediol degradation by *Salmonella enterica* serovar Typhimurium LT2." Arch Microbiol **180**(5): 353-361.

Liu, Y., *et al.* (2015). "The PduL phosphotransacylase is used to recycle coenzyme A within the Pdu microcompartment." J Bacteriol **197**(14): 2392-2399.

Liu, Y., *et al.* (2007). "PduL is an evolutionarily distinct phosphotransacylase involved in B_{12}-dependent 1,2-propanediol degradation by *Salmonella enterica* serovar Typhimurium LT2." J Bacteriol **189**(5): 1589-1596.

Obradors, N., *et al.* (1988). "Anaerobic metabolism of the L-rhamnose fermentation product 1,2-propanediol in *Salmonella typhimurium*." J Bacteriol **170**(5): 2159-2162.

Pang, A., *et al.* (2012). "Substrate channels revealed in the trimeric Lactobacillus reuteri bacterial microcompartment shell protein PduB." Acta Crystallogr D Biol Crystallogr **68**(Pt 12): 1642-1652.

Pang, A., *et al.* (2012). "Substrate channels revealed in the trimeric *Lactobacillus reuteri* bacterial microcompartment shell protein PduB." Acta Crystallogr D Biol Crystallogr **68**(Pt 12): 1642-1652.

Pang, A., *et al.* (2011). "Structure of PduT, a trimeric bacterial microcompartment protein with a 4Fe-4S cluster-binding site." Acta Crystallogr D Biol Crystallogr **67**(Pt 2): 91-96.

Price, G. D., *et al.* (1993). "Analysis of a genomic DNA region from the cyanobacterium *Synechococcus* sp. strain PCC7942 involved in carboxysome assembly and function." J Bacteriol **175**(10): 2871-2879.

Rae, B. D., *et al.* (2013). "Functions, compositions, and evolution of the two types of carboxysomes: polyhedral microcompartments that facilitate CO_2 fixation in cyanobacteria and some proteobacteria." Microbiol. Mol. Biol. Rev. **77**(3): 357-379.

Sampson, E. M. and T. A. Bobik (2008). "Microcompartments for B_{12}-dependent 1,2-propanediol degradation provide protection from DNA and cellular damage by a reactive metabolic intermediate." J Bacteriol **190**(8): 2966-2971.

Shively, J. M., *et al.* (1973). "Functional organelles in prokaryotes: polyhedral inclusions (carboxysomes) of *Thiobacillus neapolitanus*." Science **182**(112): 584-586.

Sinha, S., *et al.* (2014). "Alanine scanning mutagenesis identifies an asparagine-arginine-lysine triad essential to assembly of the shell of the Pdu microcompartment." J Mol Biol **426**(12): 2328-2345.

Stojiljkovic, I., *et al.* (1995). "Ethanolamine utilization in *Salmonella typhimurium*: nucleotide sequence, protein expression, and mutational analysis of the *cchA cchB eutE eutJ eutG eutH* gene cluster." J. Bacteriol. **177**(5): 1357-1366.

Talarico, T. L., *et al.* (1988). "Production and isolation of reuterin, a growth inhibitor produced by *Lactobacillus reuteri*." Antimicrob Agents Chemother **32**(12): 1854-1858.

Tanaka, S., *et al.* (2010). "Structure and mechanisms of a protein-based organelle in *Escherichia coli*." Science **327**(5961): 81-84.

Thompson, M. C., *et al.* (2015). "An allosteric model for control of pore opening by substrate binding in the EutL microcompartment shell protein." Protein Sci **24**(6): 956-975.

Tsai, Y., *et al.* (2007). "Structural analysis of CsoS1A and the protein shell of the *Halothiobacillus neapolitanus* carboxysome." PLoS Biol **5**(6): e144.

CHAPTER 3: AN OPEN FORM OF PDUB' AND IMPLICATIONS OF TRANSPORT

Introduction

Controlled transport of molecules between cells and organelles is a fundamental concept of biology that remains extremely complex. Although it appears simple, movement of ions and small molecules is a quintessential necessity of cellular homeostasis (Doyle *et al.* 1998). Understanding this complexity has engulfed a wide range of scientific disciplines from biophysics to cell biology so much so that a new membrane biophysics field is beginning to emerge (Luckey 2014). The core principles of transport: diffusion, facilitated diffusion, and active transport across a membrane are taught in introductory courses across the world. However, there is a much less studied system in nature that also requires transport of these small molecules that may be more abundant than originally thought. Almost 20% of all bacteria produce proteinaceous organelles known as microcompartments (MCPs) that have no lipid component to them (Bobik 2006, Abdul-Rahman *et al.* 2013, Jorda *et al.* 2013, Axen *et al.* 2014). MCPs consist of metabolic enzymes encapsulated within a protein shell and their function required the transport of enzyme substrates, products and cofactors across their outer protein shell. (Kerfeld *et al.* 2005, Yeates *et al.* 2011, Abdul-Rahman *et al.* 2013, Jorda *et al.* 2013, Chowdhury *et al.* 2015).

MCPs have been shown to carry out diverse metabolic processes ranging from CO_2 fixation to bacterial pathogenesis (Bobik 2006, Abdul-Rahman *et al.* 2013, Rae *et al.* 2013). Their general function is to optimize a metabolic pathways that have toxic or volatile intermediate (Bobik 2006, Cheng *et al.* 2008, Kerfeld *et al.* 2010, Abdul-Rahman *et al.* 2013, Jorda *et al.* 2013, Rae *et al.* 2013, Axen *et al.* 2014, Chowdhury *et al.* 2014). Accordingly, MCPs typically sequester a specific metabolite pathway that produce a toxic or volatile intermediate. The protein shell of the MCP prevents the toxic/volatile intermediate from escaping (Kerfeld *et al.* 2010, Rae, *et al.* 2013, Chowdhury *et al.* 2014). This minimizes cell damage, accelerates catalysis, and prevents the loss of valuable carbon to the environment. However, as mentioned above, the shell must also allow for entry of substrates and cofactors needed by the lumen enzymes as the egress of pathway products.

Although MCPs have a diverse array of metabolic functions, their shells have a common ancestor and are primarily built from a conserved family of proteins that contain the bacterial microcompartment (BMC) domain. BMC domain proteins assemble into hexamers or pseudohexamers that tile into extended protein sheets of the MCP shell. In recent years, structural studies of multiple BMC-domain shell proteins have given clues as to how they function in molecular transport (Tsai *et al.* 2007, Dryden *et al.* 2009, Tanaka *et al.* 2009, Crowley *et al.* 2010, Tanaka *et al.* 2010, Yeates *et al.* 2011, Samborska and Kimber 2012). The hexameric BMC domain proteins typically have small narrow cavities that function in the transport of small molecules (Kerfeld *et al.* 2005, Tsai *et al.* 2007, Crowley *et al.* 2010, Chowdhury *et al.* 2015). In addition, a number of pseudohexameric shell proteins have been crystallized in pore-open and pore-closed conformations suggesting a gated pore (Klein *et al.*

2009, Tanaka *et al.* 2010, Cai *et al.* 2013). Notably, when open, the central pore of the pseudohexameric shell proteins is large enough to accommodate the transport of enzymatic cofactors such as NAD/H, coenzyme B_{12}, coenzyme A, and ATP which are too large to move through the small pores that traverse the hexameric BMC-domain proteins.

One of the best studied MCPs (the Pdu MCP) is used to optimize the B_{12}-dependent degradation of 1,2-PD as a carbon and energy source (Bobik *et al.* 1999, Havemann *et al.* 2002). 1,2-PD enters the Pdu MCP where it is converted to propionaldehyde by the B_{12}-dependent diol dehydratase enzyme (PduCDE) (Jeter 1990, Bobik *et al.* 1997). Propionaldehyde can then be converted to 1-propanol or propionyl-CoA (Leal *et al.* 2003, Cheng *et al.* 2012). Propionyl CoA is then converted to propionyl-PO_4^{2-} (Liu *et al.* 2007). The 1-propanol and propionyl-PO_4^{2-} then leave the shell and enter the cytosol where they can be further metabolized (Horswill and Escalante-Semerena 1997, Horswill and Escalante-Semerena 1999, Palacios *et al.* 2003, Sampson and Bobik 2008). A primary function of the Pdu MCP is to sequester propionaldehyde and prevent cytotoxicity and DNA damage (Havemann *et al.* 2002, Sampson and Bobik 2008). Hence, the shell of the Pdu MCP has to prevent escape of the propionaldehyde intermediate while allowing for the transport of substrate, products and enzymatic cofactors including 1,2-PD, 1-propanol, propionyl-PO_4^{2-}, NAD/H, ATP, ADP and coenzyme B_{12}.

The shell of the Pdu MCP is comprised of seven different BMC-containing proteins, PduA, PduB, PduB', PduJ, PduK, PduT and PduU. Recently, it was shown that the PduA can selectively transport 1,2-PD across the shell through its central pore (Chowdhury *et al.* 2015). Site-directed mutations central pore that altered the specificity of the pore impeding 1,2-PD transport or enhancing propionaldehyde egress. The PduB and PduB' proteins are

pseudohexamers and thus related to BMC-domain proteins that have been crystallized in pore open and pore closed conformations (Klein *et al.* 2009, Tanaka *et al.* 2010, Cai *et al.* 2013). This raised the possibility the PduB and PduB' might be involved in regulated uptake of enzymatic cofactors. However, no studies have 1) looked into essential residues that could open the central pore via site-directed mutagenesis and 2) investigated how an open pore would act *in vivo* within the context of the MCP.

Work on EutL, a protein that crystallized in open and closed forms, showed that there were three channels, one contributed from each monomer, in the closed form (Figure 1) (Tanaka *et al.* 2010, Thompson *et al.* 2015). These channels are also present in the recent structure of PduB' as well as PduB' homologs. The structural makeup of these channels show that there is a polar and a non-polar side along the walls that make up the channel with a restriction point in the center that impedes entry of small molecules (Thompson *et al.* 2015). Hence, they are unlikely to be used for substrate transport. Interestingly, in the case of EutL, ethanolamine can bind within these channels and when it does, the general free motion of the trimer is decreased. In addition, modeling of EutL reveals that these channels provide the space into which the carbon backbone of Eut must move when its central pore opens (Thompson *et al.* 2015). Hence, if ethanolamine is bound to the channel, the central pore could not be opened due to the ethanolamine molecule occupying the space coiled residues would normally occupy in the open form. In other words, binding of the ethanolamine to these channels should impede central pore opening. In addition, there is also evidence that binding of ethanolamine is enhanced under oxidative conditions due to the presence of two cysteines (Thompson *et al.* 2015). Furthermore, the pduB' structure we determined has a glycerol molecule in one of these channels and glycerol is very similar to the

structure to 1,2-PD (Figure 2A). Whether this is biologically relevant or an artifact from the cryoprotectant used in crystallography is unclear.

In this study we sought to use the recently solved structure of *Salmonella enterica* PduB' to design mutants that would have amino acid side chains in these small channels that would prevent 1,2-PD binding analogous to ethanolamine binding in EutL, and perhaps promote the open form of the PduB' trimer.

Results

Screen of Channel Residues

Mutagenesis of many positions along the small pores of PduB' was used to attempt to prevent potential 1,2 PD binding and opening of the central pore channel (figure 2A). The criteria for mutagenesis was to generate mutations along the walls of the channel and see if a viable rotamer with minimal collisions was feasible that could block the small pore using PyMol's mutagenesis software. Using these guidelines, four residues were selected for further analysis: A53, G85, H86, and E191 (Figure 2). Next, because we hypothesized that these mutations would open the pore, we screened these mutants using our growth assay to observe their phenotypes. Interestingly, all mutants had faster growth than wild-type except for the H86A, H86R, and H86Q mutations (Figure 2B). Growth of A53 mutants on minimal media can be seen in Figure 4A and 4B. If the mutation caused opening of the central pore in PduB', then we would anticipate faster growth of the mutant on minimal media under low B_{12} conditions. The rationale is that a permanently open central pore would allow for more diffusion of substrates, products, and cofactors across the shell. Prior studies showed that this circumstance

leads to faster growth on 1,2-PD minimal medium. However, this is much different than the classical interpretation of faster growth which is due to a broken or leaky MCP shell (Crowley *et al.* 2010). Because the classical explanation might also be valid, we then purified MCPs for all mutants and calculated the overall yield (grams MCP/ grams cell) and compared it to wild-type to assess MCP stability. Strikingly, only mutations at the A53 position showed normal MCP yield (Figure 2B). Other mutations that that caused faster growth had lower MCP yields indicating that the fast growth phenotype was caused by destabilization of the MCP shell. Thus, the small channels of PduB' might be allosteric binding sites and mutagenesis of only one residue showed faster growth and had a normal yield of purified MCPs: A53.

MCP Enzymatic Activity of A53 Substitutions

Next, we did enzymatic assays of the purified MCPs of the pduB' A53 point mutants, A53D, A53F, A53L, A53R, A53S, and A53W. Two assays were done, one that probed the function of the dioldehydratase enzyme (PduCDE) and the other examined the enzyme PduP. These assays are used done to assess access of the dioldehydratase (DDH) and dehydrogenase (PduP), which are encapsulated within the MCP shell, to their respective substrate *in vitro*. DDH is catalyzes the conversion of 1,2-PD to propionaldehyde in a B_{12} dependent manner (Bobik *et al.* 1997). PduP converts propionaldehyde to Propionyl-CoA while utilizing NAD^+ and coenzyme A as cofactors (Leal *et al.* 2003). Recent work involving the PduA shell protein demonstrates that occluding the PduA pore to 1,2-PD lowers the specific activity of the DDH enzyme while the PduP activity remains constant, indicating that these assays are appropriate to asses pore function of shell proteins of the Pdu MCP (Chowdhury *et al.* 2015). Interestingly, both DDH and PduP

activities of purified A53 MCPs showed higher values than LT2 (Figure 3A). In addition, all A53 point mutants show a similar SDS-PAGE banding pattern compared to LT2 and the A53F and A53R MCPs have no obvious morphological deformities visualized under electron microscopy (Figure 3B and C). Together, these results indicate that the A53 substitutions produce normal, stable MCPs that have faster DDH and PduP activities compared to LT2. This is consistent with enhanced permeability of the MCP shell due to the PduB pore being bias toward the open form in the A53 mutant strains. The *in vitro* enzymatic results also complement those of the growth assays that showed faster growth than wild-type on 1,2-PD minimal medium which was previously shown to result from increased permeability of the MCP shell to enzyme substrate and cofactors.

A53 substitutions can transport large cofactors

Prior studies indicated that enzymatic cofactors such as NAD/H and coenzyme A are both transported through the MCP shell and internally recycled. The PduQ and PduL are lumen enzymes that recycle NAD/H and HS-CoA inside the MCP (Liu *et al.* 2007, Cheng *et al.* 2012). Strains with Δ*pduQ* and Δ*pduL* mutations grow at 50% of the wild-type rate on 1,2-PD minimal medium due to internal cofactor limitation (Figure 4A, 4C, and 4D) (Cheng *et al.* 2012, Liu *et al.* 2015). However, 50% of the growth rate of wild-type still requires that cofactors rapidly cross the shell of the MCP in the Δ*pduQ* and Δ*pduL* mutants which are no longer capable of internal cofactor recycling. Hence, MCPs are presumed to have transport systems that allow for cofactor movement across the shell. The large central pores of PduB and PduB' are currently the most likely conduits for cofactor transport across the shell of the Pdu MCP shell since they are the

only pseudohexamers, i.e. BMC proteins capable of forming large pores, present in the shell of the Pdu MCP.

The A53 substitutions we generated have increased growth on minimal media and have higher enzymatic activity in *in vitro* assays. To test if these A53 substitutions could rescue the slow growth phenotypes of the Δ*pduQ* and Δ*pduL* strains we generated double mutants and observed growth on 1,2-PD minimal medium under low B_{12} conditions. All A53 substitutions were paired with a Δ*pduQ* mutation and corrected the growth phenotype brought on by the Δ*pduQ* lesion (Figuure 4A and D). In the case of A53F/Δ*pduQ* and A53W/Δ*pduQ* complete rescue was seen to levels of LT2 while in the others, recovery was partial. Under high B_{12} conditions (>100nm) a period of growth arrest was observed in Δ*pduQ* and A53/Δ*pduQ* strains (Figure 4C) The arrest is thought to be due to the escape of propionaldehyde from the lumen of the MCP (Havemann *et al.* 2002, Cheng *et al.* 2012). Interestingly, the doubling times of Δ*pduQ* strains had an effect on wild-type background, but not with the A53 background (Table 1). This suggests that the Δ*pduQ* phenotype has a greater effect on wild-type than the A53 mutants, indicating that NAD/H can more readily cross the shell in the A53 strains. In addition, two double mutants were made that contained the Δ*pduL* gene: A53F/Δ*pduL* and A53R/ Δ*pduL*. It was found that these mutations could rescue the Δ*pduL* phenotype (Figure 4E). Similar to the Δ*pduQ* mutants, doubling times of Δ*pduL* were lowered with the A53 background (Table 1). These results suggest that the A53 substitutions change the permeability of the shell of the Pdu MCP in a manner that increase the transport of NAD/H and coenzyme A. The PduQ enzyme recycles NAD/H within the MCP and, when deleted, NAD/H can no longer be recycled in the MCP, it has to be recycled in the cytosol, and so slower growth is observed. In the A53/Δ*pduQ*

double mutants, growth is similar to that of wild-type, suggesting that there is more rapid exchange of NAD/H across the MCP shell. In the case of the A53F/Δ*pduL* and A53R/Δ*pduL* double mutants growth is only partially rescued, but it still suggests that coenzyme A can more readily cross the MCP shell.

Tryptophan Fluorescence of A53F

Finally, we sought to test whether the pore of the A53 mutants is biased toward the open conformation using tryptophan fluorescence. To this end, we designed a PduB' protein that contained the A53F mutation together with a tryptophan residue at position F188 (F188W) Native PduB' has no tryptophans and F188 is expected move to a new position when the pore opens. From previous work, the F188W mutation produced normal yield of MCPs, and had similar growth compared to LT2 so we were confident that the Trp mutation would not impair the overall structure or stability of PduB'. Measuring the trp fluorescence of PduB' F188W and PduB' A53F/F188W show two distinct trp peaks: one at 380nm and 330nm, respectively (Figure 5A). This is indicative of a different trp environment and thus, overall conformation between wild type PduB' and PduB' A53F.

However, a 380 nm trp emission peak is extremely unusual and may be an artifact whose basis we have not uncovered. Controls showed that this peak is lost when PduB' F188W is denatured and a typical trp peak at about 350 nm is observed. Furthermore this 380 nm peak is dependent on the presence of PduB' F188W. Thus, if it is an artifact its nature is obscure.

Another unusual observation relative to the 380 nm emission is that during the purification of PduB' F188W, the trp emission changes form 330 nm to 380 nm when the protein

is desalted following Ni-Nta chromatography (Figure 5B). This suggests that initially, PduB' exhibits the 330 nm peak, but the behavior changes once the protein exchanges into a different buffer (from 50 mM Tris pH 8, 300 mM NaCl, 500mM imidazole, to 50mM HEPES pH 7.5, 50mM KCl). Accounting for potential inner-filter effects showed no change in the emission spectra as there was minimal absorbance from 295nm to 600 nm in the sample. However, whether the 380 peak represents a legitimate conformation in the protein needs further work.

Discussion

A key question about MCP function is how substrates and cofactors traverse the shell while toxic or volatile intermediates are retained inside. Current models propose that pseudohexameric BMC-domain proteins have allosterically gated pores that open to allow cofactor transport when needed. However, no in vivo or biochemical studies that test this hypothesis have been reported. Here we constructed several mutants designed to interfere with allosteric regulation.

Results presented here indicated that mutagenesis at the A53 position may bias the central pore of PduB' to the open position. A53 MCPs were purified with similar yield to wild-type indicating that stable MCPs are formed. MCPs run on SDS-PAGE show a similar band pattern to LT2, were purified similar yields to LT2, and show the same overall shape and integrity under electron microscopy. These finding further indicated that the A53 MCPs are normally assembled and stable. *In Vitro* assays on purified MCPs showed increased DDH activity and slightly higher PduP activity compared to LT2. This suggests that lumen enzymes are more exposed to their substrates in the A53 mutants MCPs, due to an open PduB' central

pore. Growth assays done on minimal media show a faster growth than LT2 indicating that the 1,2-PD substrate is more accessible to the diol dehydratase enzyme (PduCDE).

We also found that A53F and A53W fully corrected the Δ*pduQ* growth phenotype under low B_{12} conditions suggesting that the NAD/H cofactor can readily cross the shell. In Δ*pduQ* strains, growth is impaired because NAD/H can no longer be recycled inside the MCP. Rescuing the growth to levels of LT2 by the A53F and A53W mutants suggest that NAD/H can more readily cross the MCP shell. This is the first evidence that cofactors can traverse the large pore of a pseudohexameric BMC-domain protein. In addition, partial correction of the Δ*pduL* phenotype by A53F/Δ*pduL* and A53R/Δ*pduL* suggests that CoA can travel across the shell. Interestingly, A53F/Δ*pduL* corrected the Δ*pduL* phenotype slightly better than the A53R/Δ*pduL*. Finally, purified PduB' A53F/F188W behaves differently than PduB' F188W under trp fluorescence. Together, this suggests that the PduB' A53 mutants have an open PduB' central pore.

This study shows that the shell proteins in the shell of MCPs are capable of transporting large cofactors such as NAD/H, coenzyme A, and perhaps B_{12} and ATP. Not surprisingly, it appears that 1,2-PD can cross the central pore of PduB' as well, suggesting that the open PduB' central pore is not specific for a particular cofactor, substrate, or product, but rather it acts as a nonspecific channel. In other words, it allows cofactors, substrates, and products to go down their concentration gradients between the lumen of the MCP and the cytosol. This study reinforces that diffusion is the main force in metabolite transport across the MCP shell. However, PduB' does play a role in maintaining concentration gradients as it prevents cofactor escape when the central pore is closed down. Finally, the work here suggests that an open PduB' central pore does not damage the integrity of the shell or the capacity of lumen enzymes to function.

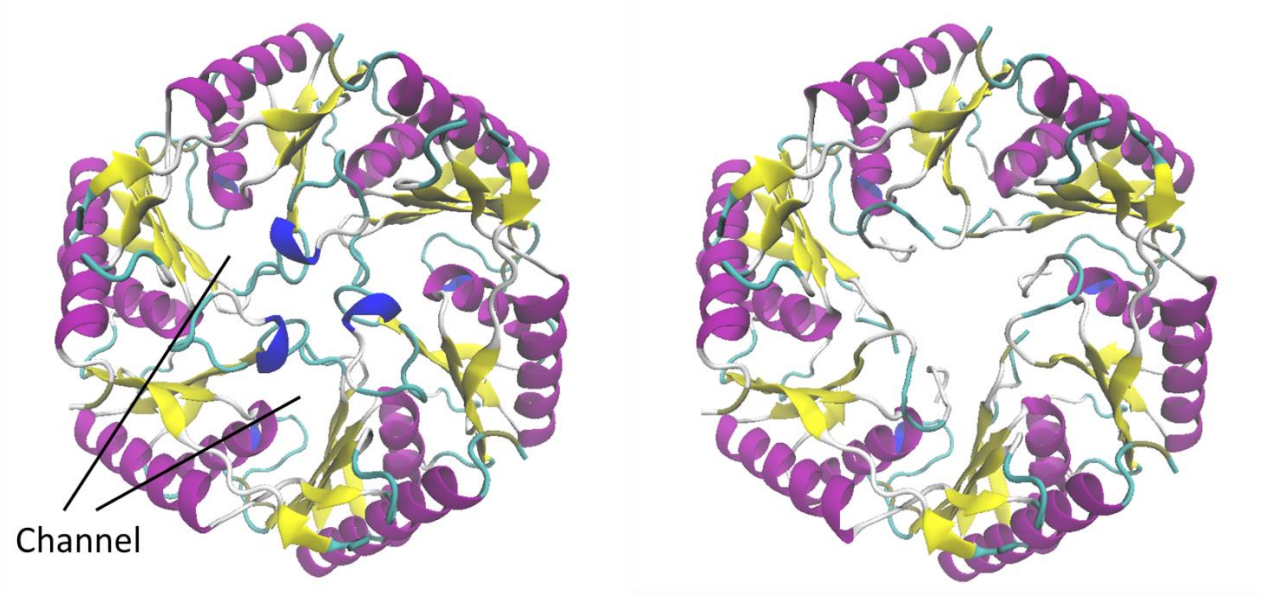

Figure 1. Open central pore of the PduB' homolog EutL. The closed (left) and open (right) structure of EutL (PDB entries 3I82 and 3I87, respectively) (Tanaka, Sawaya *et al.* 2010). Channels that have been proposed to bind ethanolamine are highlighted. These channels are occluded in the open form.

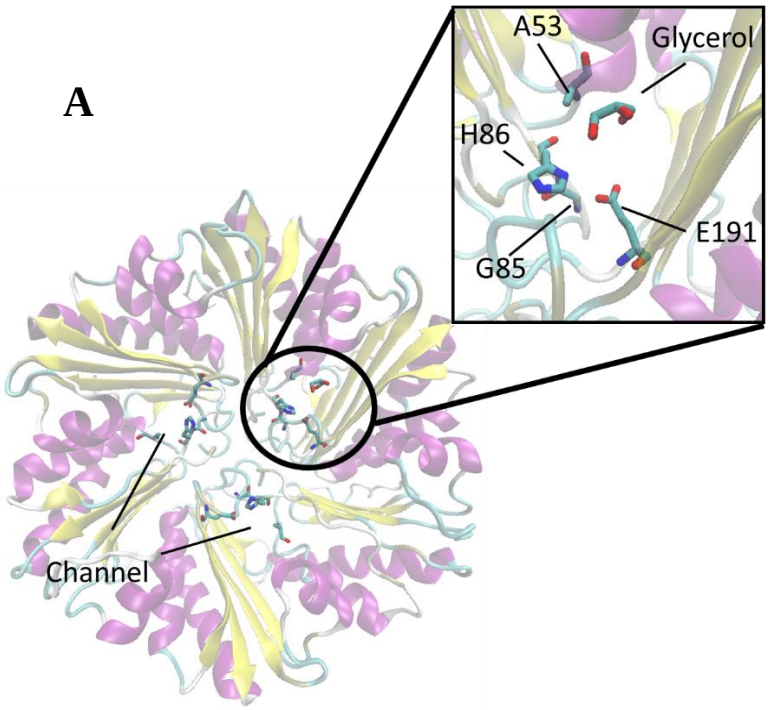

B

Residue	Mutation	Growth Phenotype (20nM B12)	MCP Yield (%)
A53	D	Fast	100
	F	Fast	100
	L	Fast	97
	R	Fast	100
	S	Fast	98
	W	Fast	99
G85	M	Fast	34
H86	A	Normal	85
	D	Fast	51
	F	Fast	26
	Q	Normal	78
	R	Normal	85
E191	A	Fast	30

Figure 2. Selected channel residues for mutational analysis. (A) Structure of PduB' with highlighted residues in the inset. Labeled residues were viable candidates that could block the small channels of PduB'. In the crystal structure, a glycerol molecule is seen in these channels. (B) Substitutions at each residue and their phenotypes on minimal media and MCP yield.

A

Strain	DDH Specific Activity (μmol·min-1·mg-1)	PduP Specific Activity (μmol·min-1·mg-1)
LT2	27.2 ± 0.6	8.7 ± 0.4
A53D	29.2 ± 0.5	9.8 ± 0.6
A53F	32.7 ± 0.3	12.7 ± 1.2
A53L	30.9 ± 0.8	9.3 ± 0.7
A53R	31.1 ± 1.0	11.9 ± 0.9
A53S	29.8 ± 0.9	9.6 ± 0.4
A53W	32.0 ± 0.7	10 ± 0.8

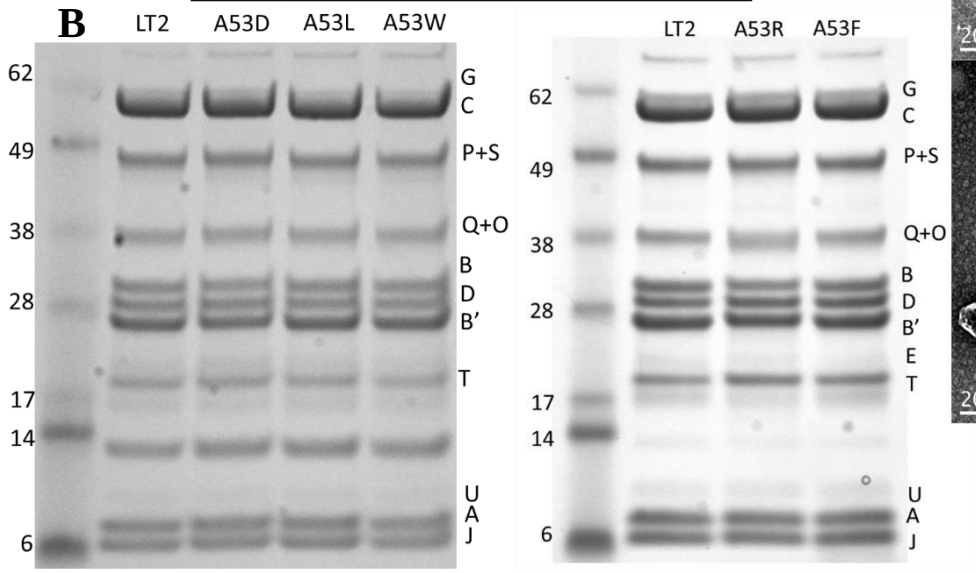

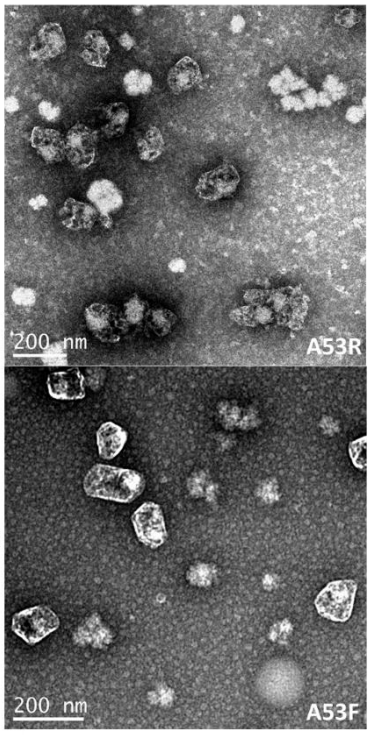

Figure 3. A53 microcompartments. (A) Enzymatic activities of A53 substitutions (B) MCPs of labeled strains. Left of the gel is the standard (in KDa) and the right is the labeled Pdu component with how they appear in wild-type (LT2). (C) Transmission electron microscopy of purified MCPs of A53R (top) and A53F (bottom) with a 200nm scale bar in the lower left hand corner.

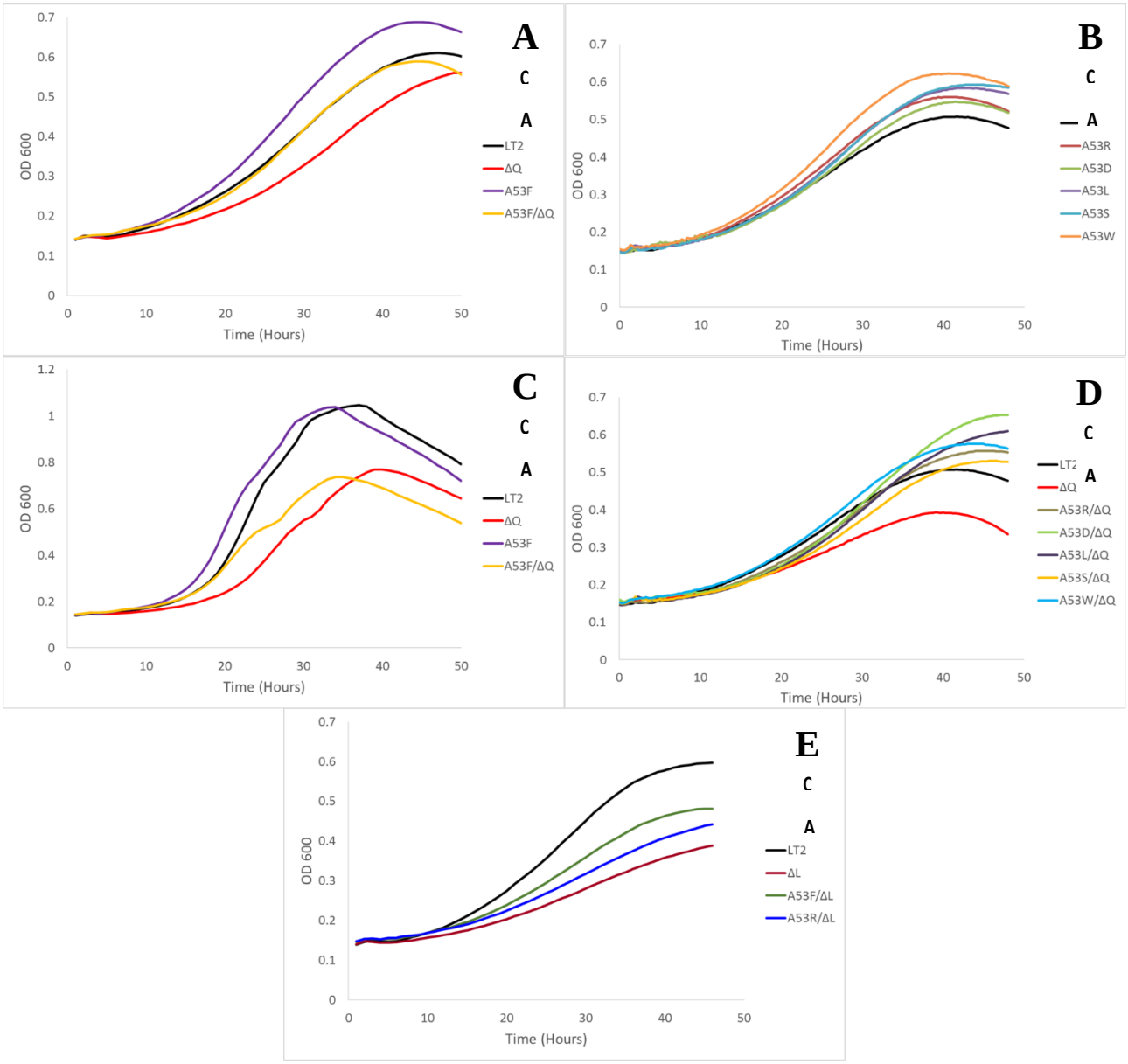

Figure 4. Growth assays of A53 mutants and double mutants. Growth assays of labeled mutants on minimal media (30nm CN-B_{12} for A, 20nm CN-B_{12} for B, D, and E, 150nm CN-B_{12} for C). Wilt-type is LT2.

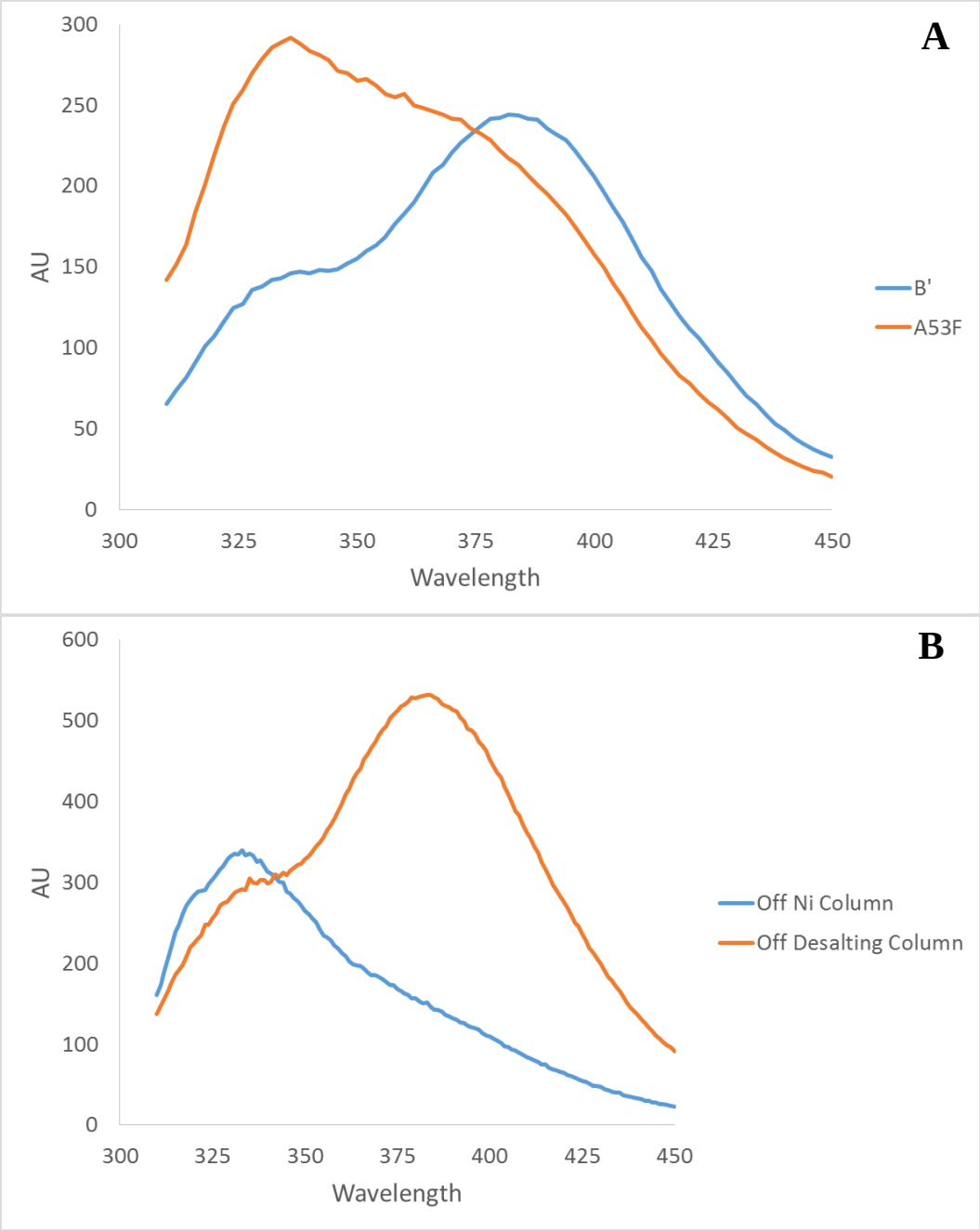

Figure 5. Tryptophan fluorescence of the PduB' F188W and PduB' A53F/F188W proteins. (A) Emission spectra of 1uM PduB' vs PduB' A53F (K65A/K170A/F188W). (B) Emission spectra of PduB' before (blue line) and after (orange line) desalting. Excitation λ: 295nm. Excitation and emission slits: 10nm.

Table 1. Doubling times of A53 mutants and double mutants. Doubling times of growth curves taken in Figure 4A (Top), Figure 4B and 4D (Middle), and Figure 4E (Bottom), wild-type is LT2. Doubling times calculated from Stanier *et al.* (1976).

Strain	Doubling Time	Ratio (ΔQ/Strain)
LT2	11.9	1.4
ΔQ	16.8	
A53F	11.6	1.0
A53F/ΔQ	11.9	

Strain	Doubling Time	Ratio (ΔQ/Strain)
LT2	12.2	1.5
ΔQ	18.0	
A53R	11.9	1.1
A53R/ΔQ	12.8	
A53D	12.1	1.0
A53D/ΔQ	12.2	
A53L	11.9	1.1
A53L/ΔQ	12.7	
A53S	11.9	1.2
A53S/ΔQ	14.3	
A53W	11.6	1.1
A53W/ΔQ	13.0	

Strain	Doubling Time	Ratio (ΔL/Strain)
LT2	12.2	1.7
ΔL	20.3	
A53F	11.7	1.3
A53F/ΔL	15.5	
A53R	11.9	1.5
A53R/ΔL	18.4	

Materials and Methods

Generating chromosomal mutations

The same method was used as described in Chapter 2.

Growth assay on minimal media

The same method was used as described in Chapter 2.

Microcompartment Purification

The same method was used as described in Chapter 2.

DDH and PduP assays

The same method was used as described in Chapter 2.

Doubling Time Calculation

Done in accordance with formulas in page 276 of The Microbial World by Stanier *et al.*

$$g = \frac{0.693}{(\frac{(logZ - logZ_0)2.303}{t - t_0})}$$

Where Z and Z_0 correspond to the amount of bacterial component of the culture at times *t* and t_o, respectively.

Generating the F188W gene fragment

The pduB' gene was cloned from our lab BE collection. The strain that contained the template was BE1832, which harbors the plasmid which we ordered the PduB' (K65A/K170A) from GenScript.

The F188W mutant was generated using fusion PCR using the plasmid from BE1832 as a template. Afterwards, the gene fragment contained was: BglII-H6-pduB'-HindIII. This fragment was then cloned into a pet41a overexpression vector and put into the lab overexpression strain BE100.

Overexpression and Purification of PduB' (K65A/K170A/F188W) and mutants

400mL of LB was inoculated with a starter culture of the BE100/p41a-H6-pduB'(K65A/K170A) and grown to an OD of 0.5 at 37°C at 275 RPM where it was induced with 500mM IPTG and placed at 16°C at 125 RPM overnight. Cells were then spun down and washed with 50mM Tris

pH 8 300mM NaCl, and then spun down again. The pellets were weighed and then resuspended in 5x lysis buffer (50mM Tris pH 8, 300mM NaCl, 5mM imidazole, 400µM AEBSF, 1mM DTT) where x is the pellet weight in grams. After resususpension, cells were put into a Thermo French pressure cell and lysed at 20,000 PSI, and then spun at 20,000xg for 30 minutes. Once spun, the supernatant was passed through a 0.45µm filter and loaded onto a Ni^{2+} agarose resin column that was pre-equilibrated with lysis buffer. Once the supernatant flowed through the column, it was reapplied to the resin. The column was then washed with lysis buffer, containing 10mM, 25mM, and 50mM imidazole. 500mM imidazole was used to elute the column. After elution, the sample was desalted using a 5mL packed Sephadex G-25 column. The protein sample was exchanged into Reaction Buffer (50mM HEPES pH 7.5, 50mM KCl, 1mM DTT) where the protein was then concentrated down to ~1mL volume. The protein was further diluted down to 1µM in a quartz cuvette with Reaction Buffer where the fluorescence of the protein was measured with λ_{ex} of 295nm. The emission spectra was observed from 310nm to 450nm. The sample was then places in an UV_{Vis} where the O.D was measured from 295 to 450. Corrected fluorescence (Fcorr) was then measured using the formula: $Fcorr = Fobs \times 10^{\frac{ODex+ODem}{2}}$.

DNA oligos used in this study

All oligos were ordered from IDT

Sac-Cat Insertion oligos	Sequence
pduBSC_343_354F	gaagcggtgaaagccaccaacaccgaagtggtcagcattgagctgccg aatacattcaaatatgtatccg
pduBSC_343_354R	gaaacgtcgttaccgcctaaaataatcagcgaaccgtggcccgcgccgcc ttacgccccgccctgccactc
pduBSC 663-684F	gatggccgataccgcgctgaagtcagccaacgttgaagtcgtggcgtacagctctccggcg aatacattcaaatatgtatccgctcatga
pduBSC 663-684R	cgggcggaggtcaccgcctgacggaccgcgccggagtcgccggaaatcaccagaatagc ttacgccccgccctgccactcatcgcagtac
pduB' 49-55SC_F	ctggacgcga tgaaacttga gaagcgctat cgttccatcg gcattctcgg caatacattcaaatatgtatccg
pduB' 49-55SC_R	accacttcggtgttggtggctttcaccgcttcgtccgccgccataatgtg ttacgccccgccctgccactc
Chromosomal Mutation oligos	**Sequence**
PduB' E191A	aagtcgtggcgtacagctctccggcgcacggcaccagctttagtaacgcagctattctggtgatttccggcgactccggc
pduB' A53F	gaagcgctatcgttccatcggcattctcggcgcccgcaccggctttggcccgcacattatggcggcggacgaagcggtga
pduB'_H86A	accaacaccgaagtggtcagcattgagctgccgcgcgataccaaaggcggcgcgggcgccggttcgctgattattttaggcggtaacgac
pduB' A53R	gaagcgctatcgttccatcggcattctcggcgcccgcaccggccgaggcccgcacattatggcggcggacgaagcggtga
pduB' H86Q	accaacaccgaagtggtcagcattgagctgccgcgcgataccaaaggcggcgcgggccagggttcgctgattattttaggcggtaacgac
pduB' H86D	accaacaccgaagtggtcagcattgagctgccgcgcgataccaaaggcggcgcgggcgacggttcgctgattattttaggcggtaacgac
pduB' H86R	accaacaccgaagtggtcagcattgagctgccgcgcgataccaaaggcggcgcgggccgcggttcgctgattattttaggcggtaacgac
pduB' H86F	accaacaccgaagtggtcagcattgagctgccgcgcgataccaaaggcggcgcgggctcggttcgctgattattttaggcggtaacgac
pduB' A53D	gaagcgctatcgttccatcggcattctcggcgcccgcaccggcgatggcccgcacattatggcggcggacgaagcggtga
pduB' A53L	gaagcgctatcgttccatcggcattctcggcgcccgcaccggcctgggcccgcacattatggcggcggacgaagcggtga
pduB' A53S	gaagcgctatcgttccatcggcattctcggcgcccgcaccggcagcggcccgcacattatggcggcggacgaagcggtga
pduB' A53W	gaagcgctatcgttccatcggcattctcggcgcccgcaccggctggggcccgcacattatggcggcggacgaagcggtga
Fusion PCR oligos	**Sequence**
RCfPCR1_A53F	tgtgcgggccaaagccggtgcg
FWfPCR2_A53F	cgcaccggctttggcccgcacattat
NdeI-H6-pduB'_F	gccgcccatatgcatcatcaccaccaccat gcagaaaaaagctgcagtttaacggaattt
PduBB'(R)HindIII	gccgccaagctttcagatgtaggacggacgatcgtttttcggttcagaacc

Strains used in this study

Lab Strains Used In this Study		
Name	**Genotype**	**Lab Strain Number**
LT2	wild-tpye *Salmonella enterica* lab strain LT2	
LT2/pKD46	LT2/pKD46	BE293
SC	p41a-Sac-Cat	CS693
ΔQ	ΔPduQ	2225
ΔL	ΔPduL	188
G85M	pduB' G85M	59
49-55SC	pduB' SC 49-55	69

Strains Generated In This Study			
Name	**Genotype**	**Mother/Father**	**BL Strain Number**
343-354SC	pduB-SC 342-354	BE293/SC oligo 343-354	39
343-354SC/pKD46	pduB-SC 342-354/pKD46	BL39/pKD46	40
663-664SC	pduB-SC 663-684	BE293/SC oligo 663-684	45
663-664SC/pKD46	pduB-SC 663-684/pkD46	BL45/pKD46	48
E191A	pduB' E191A	BL48/oligo PduB' E191A	52
G85M	pduB' G85M	BL40/ oligo PduB G85M	59
49-55SC	pduB' SC 49-55	BE293/SC oligo 49-55	69
B' F188W plasmid	DH5a/p41a-(BglII) pduB' F188W K65A K170A (HindIII)	DH5a/p41a-F188W fusion PCR	77
49-55SC/pKD46	pduB' SC 49-55/pKD46	BL69/pKD46	78
B' F188W	BL21 (Lucigen)/P41a-(BglII) pduB'-65/170 F188W (HindIII)	BL21 (Lucigen)/pBL77	81
A53F	pduB' A53F	BL/78/oligo PduB' A53F	89
H86A	pduB' H86A	BL40/oligo PduB' H86A	112
A53R	pduB' A53R	BL78/oligo PduB' A53R	139
H86D	pduB' H86D	BL40/ oligo PduB' D79G	147
H86F	pduB' H86F	BL40/ oligo PduB' R78C	148
H86Q	pduB' H86Q	BL40/ oligo PduB' K81D	149
H86R	pduB' H86R	BL40/ oligo PduB' G82C	150

Strains Generated In This Study			
Name	**Genotype**	**Mother/Father**	**BL Strain Number**
B' A53F/F188W plasmid	NEB-10/p41a-(NdeI) H6 pduB' A53F/F188W/K65A/170A (HindIII)	NEB-10/p41a-A53F/F188W fusion PCR	195
B' A53F/F188W	BE100/p41a-(NdeI) H6 pduB' A53F/F188W/K65A/170A (HindIII)	BE100/pBL195	198
A53F/ΔQ	PduB' A53F/ΔQ	BE2225/BL89	199
A53R/ΔQ	PduB' A53R/ΔQ	BE2225/BL139	200
ΔL/pkD46	ΔL/pkD46	BE188/pkD46	207
ΔL/49-55SC	ΔL/pduB 49-55SC	BE188/SC oligo 49-55	134
ΔL/49-55SC/pKD46	ΔL/pduB 49-55SC/pkD46	BL134/pKD46	135
A53F/ΔL	pduB' A53F/ΔL	BL135/oligo PduB' A53F	136
A53R/ΔL	pduB' A53R/ΔL	BL135/oligo PduB' A53R	140
A53D	pduB' A53D	BL78/oligo PduB' A53D	214
A53L	pduB' A53L	BL78/oligo PduB' A53L	215
A53S	pduB' A53S	BL78/oligo PduB' A53S	216
A53W	pduB' A53W	BL78/oligo PduB' A53W	217
A53D/ΔQ	pduB' A53D/ΔQ	BE2225/BL214	218
A53L/ΔQ	pduB' A53L/ΔQ	BE2225/BL215	219
A53S/ΔQ	pduB' A53S/ΔQ	BE2225/BL216	220
A53W/ΔQ	pduB' A53W/ΔQ	BE2225/BL217	221

Works Cited

Abdul-Rahman, F., *et al.* (2013). "The distribution of polyhedral bacterial microcompartments suggests frequent horizontal transfer and operon reassembly." J. Phylogen. Evolution. Biol. **1**(4): doi 10.4172/2329-9002.1000118

Axen, S. D., *et al.* (2014). "A taxonomy of bacterial microcompartment loci constructed by a novel scoring method." PLoS Comput. Biol. **10**(10): e1003898.

Bobik, T. A. (2006). "Polyhedral organelles compartmenting bacterial metabolic processes." Appl Microbiol Biotechnol **70**(5): 517-525.

Bobik, T. A., *et al.* (1999). "The propanediol utilization (*pdu*) operon of *Salmonella enterica* serovar Typhimurium LT2 includes genes necessary for formation of polyhedral organelles involved in coenzyme B_{12}-dependent 1, 2-propanediol degradation." J Bacteriol **181**(19): 5967-5975.

Bobik, T. A., *et al.* (1997). "Propanediol utilization genes (*pdu*) of *Salmonella typhimurium*: three genes for the propanediol dehydratase." J Bacteriol **179**(21): 6633-6639.

Brinsmade, S. R., *et al.* (2005). "Minimal functions and physiological conditions required for growth of *Salmonella enterica* on ethanolamine in the absence of the metabolosome." J Bacteriol **187**(23): 8039-8046.

Cai, F., *et al.* (2013). "The structure of CcmP, a tandem bacterial microcompartment domain protein from the β-carboxysome, forms a subcompartment within a microcompartment." J Biol Chem **288**(22): 16055-16063.

Cheng, S., *et al.* (2012). "The PduQ enzyme is an alcohol dehydrogenase used to recycle NAD^+ internally within the Pdu microcompartment of *Salmonella enterica*." PLoS One **7**(10): e47144.

Cheng, S., *et al.* (2008). "Bacterial microcompartments: their properties and paradoxes." Bioessays **30**(11-12): 1084-1095.

Chowdhury, C., *et al.* (2015). "Selective molecular transport through the protein shell of a bacterial microcompartment organelle." Proc Natl Acad Sci U S A **112**(10): 2990-2995.

Chowdhury, C., *et al.* (2014). "Diverse bacterial microcompartment organelles." Microbiol. Mol. Biol. Rev. **78**(3): 438-468.

Crowley, C. S., *et al.* (2010). "Structural insight into the mechanisms of transport across the *Salmonella enterica* Pdu microcompartment shell." J Biol Chem **285**(48): 37838-37846.

Crowley, C. S., *et al.* (2008). "Structure of the PduU shell protein from the Pdu microcompartment of Salmonella." Structure **16**(9): 1324-1332.

Doyle, D. A., *et al.* (1998). "The structure of the potassium channel: molecular basis of K+ conduction and selectivity." Science **280**(5360): 69-77.

Dryden, K. A., *et al.* (2009). "Two-dimensional crystals of carboxysome shell proteins recapitulate the hexagonal packing of three-dimensional crystals." Protein Sci **18**(12): 2629-2635.

Gehrmann, W. and M. Elsner (2011). "A specific fluorescence probe for hydrogen peroxide detection in peroxisomes." Free Radic Res **45**(5): 501-516.

Havemann, G. D., *et al.* (2002). "PduA is a shell protein of polyhedral organelles involved in coenzyme B_{12}-dependent degradation of 1,2-propanediol in *Salmonella enterica* serovar typhimurium LT2." J Bacteriol **184**(5): 1253-1261.

Heldt, D., *et al.* (2009). "Structure of a trimeric bacterial microcompartment shell protein, EtuB, associated with ethanol utilization in Clostridium kluyveri." Biochem J **423**(2): 199-207.

Horswill, A. R. and J. C. Escalante-Semerena (1997). "Propionate catabolism in *Salmonella typhimurium* LT2: two divergently transcribed units comprise the *prp* locus at 8.5 centisomes, *prpR* encodes a member of the sigma-54 family of activators, and the *prpBCDE* genes constitute an operon." J Bacteriol **179**(3): 928-940.

Horswill, A. R. and J. C. Escalante-Semerena (1999). "*Salmonella typhimurium* LT2 catabolizes propionate via the 2-methylcitric acid cycle." J Bacteriol **181**(18): 5615-5623.

Jeter, R. M. (1990). "Cobalamin-dependent 1,2-propanediol utilization by *Salmonella typhimurium*." J Gen Microbiol **136**(5): 887-896.

Jorda, J., *et al.* (2013). "Using comparative genomics to uncover new kinds of protein-based metabolic organelles in bacteria." Protein Sci **22**(2): 179-195.

Kerfeld, C. A., *et al.* (2010). "Bacterial microcompartments." Annu Rev Microbiol **64**: 391-408.

Kerfeld, C. A., *et al.* (2005). "Protein structures forming the shell of primitive bacterial organelles." Science **309**(5736): 936-938.

Klein, M. G., *et al.* (2009). "Identification and structural analysis of a novel carboxysome shell protein with implications for metabolite transport." J Mol Biol **392**(2): 319-333.

Leal, N. A., *et al.* (2003). "PduP is a coenzyme-A-acylating propionaldehyde dehydrogenase associated with the polyhedral bodies involved in B_{12}-dependent 1,2-propanediol degradation by *Salmonella enterica* serovar Typhimurium LT2." Arch Microbiol **180**(5): 353-361.

Liu, Y., *et al.* (2015). "The PduL phosphotransacylase is used to recycle coenzyme A within the Pdu microcompartment." J Bacteriol **197**(14): 2392-2399.

Liu, Y., *et al.* (2007). "PduL is an evolutionarily distinct phosphotransacylase involved in B_{12}-dependent 1,2-propanediol degradation by *Salmonella enterica* serovar Typhimurium LT2." J Bacteriol **189**(5): 1589-1596.

Luckey, M. (2014). Membrane Structural Biology: With Biochemical and Biophysical Foundations. Cambridge, Cambridge Univ Press.

Palacios, S., *et al.* (2003). "Propionyl coenzyme A is a common intermediate in the 1,2-propanediol and propionate catabolic pathways needed for expression of the *prpBCDE* operon during growth of *Salmonella enterica* on 1,2-propanediol." J Bacteriol **185**(9): 2802-2810.

Pang, A., *et al.* (2012). "Substrate channels revealed in the trimeric *Lactobacillus reuteri* bacterial microcompartment shell protein PduB." Acta Crystallogr D Biol Crystallogr **68**(Pt 12): 1642-1652.

Pang, A., *et al.* (2011). "Structure of PduT, a trimeric bacterial microcompartment protein with a 4Fe-4S cluster-binding site." Acta Crystallogr D Biol Crystallogr **67**(Pt 2): 91-96.

Penrod, J. T. and J. R. Roth (2006). "Conserving a volatile metabolite: a role for carboxysome-like organelles in *Salmonella enterica*." J Bacteriol **188**(8): 2865-2874.

Rae, B. D., *et al.* (2013). "Functions, compositions, and evolution of the two types of carboxysomes: polyhedral microcompartments that facilitate CO_2 fixation in cyanobacteria and some proteobacteria." Microbiol. Mol. Biol. Rev. **77**(3): 357-379.

Samborska, B. and M. S. Kimber (2012). "A dodecameric CcmK2 structure suggests β-carboxysomal shell facets have a double-layered organization." Structure **20**(8): 1353-1362.

Sampson, E. M. and T. A. Bobik (2008). "Microcompartments for B_{12}-dependent 1,2-propanediol degradation provide protection from DNA and cellular damage by a reactive metabolic intermediate." J Bacteriol **190**(8): 2966-2971.

Stanier, R. Y., Adelberg, Edward A., Ingraham, John (1976). The Microbial World. Englewood Cliffs, New Jersey, Prentice-Hall, Inc.

Tanaka, S., *et al.* (2009). "Insights from multiple structures of the shell proteins from the β-carboxysome." Protein Sci **18**(1): 108-120.

Tanaka, S., *et al.* (2010). "Structure and mechanisms of a protein-based organelle in *Escherichia coli*." Science **327**(5961): 81-84.

Thompson, M. C., *et al.* (2015). "An allosteric model for control of pore opening by substrate binding in the EutL microcompartment shell protein." Protein Sci **24**(6): 956-975.

Tsai, Y., *et al.* (2007). "Structural analysis of CsoS1A and the protein shell of the *Halothiobacillus neapolitanus* carboxysome." PLoS Biol **5**(6): e144.

Yeates, T. O., *et al.* (2011). "The protein shells of bacterial microcompartment organelles." Curr Opin Struct Biol **21**(2): 223-231.

CHAPTER 4: ROLE OF THE N-TERMINUS OF PDUB

Introduction

Bacterial microcompartments (MCPs) are organelles made entirely of protein that has a shell that encapsulates a particular metabolic reaction (Bobik 2006, Kerfeld *et al.* 2010, Abdul-Rahman *et al.* 2013, Jorda *et al.* 2013, Rae *et al.* 2013, Axen *et al.* 2014, Chowdhury *et al.* 2014). To date, all metabolic pathways associated with MCPs have been shown to aid in produce a toxic or volatile intermediate. The role of the shell is to prevent this intermediate from escaping the confines of the MCP where encapsulated enzymes can act on it without causing harm or escaping the cell (Kerfeld *et al.* 2010, Rae *et al.* 2013, Chowdhury *et al.* 2014). Recent work has shed some insight as to how the MCP shell proteins can encapsulate lumen enzymes.

A central theme in MCP design is the termini of varied MCP proteins provide binding sites that are important to assembly. The termini of shell proteins can aid in localization of their cognate lumen enzymes. In the Pdu system, it has been shown that the N-terminus of the lumen enzyme PduP interacts with C-terminal regions of the shell proteins PduA and PduJ (Fan *et al.* 2012). This interaction occurs through a helix-helix interaction and is necessary and sufficient for the localization of PduP to the MCP lumen. Another case involves the N-terminal extension of the medium subunit of the diol dehydratase, PduD (Fan and Bobik 2011). Deletion of this N-terminus region prevents encapsulation of the diol dehydratase enzyme (PduCDE) and addition of the extension to GFP promotes incorporation of GFP into the MCP shell. The cognate shell protein for this interaction is not currently known. Other roles of the termini of shell proteins have been examined. The N-terminus of PduV can direct GFP to the surface of the MCP

(Parsons *et al.* 2010). In the carboxysome, the CcmN protein function as an adaptor between the lumen enzyme and the carboxysome shell (Kinney *et al.* 2012). The N-terminus of CcmN interacts with CcmM and the C-terminus binds to the shell proteins CcmK and is essential for carboxysome assembly. Thus, protein termini play varied roles in MCP assembly.

The PduB and PduB' proteins are trimeric BMC domain proteins that together make up about 50% of the shell of the Pdu MCP (Havemann and Bobik 2003). Both are expressed from overlapping genes, and are identical in sequence except that PduB has a 37 amino acid N-terminal extension. (Figure 1A) (Bobik *et al.* 1999).

Results

Multiple Sequence Analysis of PduB

PSI-BLAST was used to identify PduB homologs in GenBank. To ensure that only PduB proteins were selected and not PduB', we used the first 53 amino acids of PduB as the query sequence. Multiple sequence analysis indicates that residues L6 to V18 of the N-terminal region are very well conserved but residues A18 to E35 are not (Figure 1A). Though the exact tertiary structure of the N-terminus remains uncertain, the small peptide structure prediction software PEP-FOLD predicts that it contains an α-helix (L6 - V18) followed by a linker region (A18 – E35) that connects the extension to the core structure of PduB' (Figure 1B). The predicted α-helix that is very well conserved among all PduB homologs, while the linker region is more variable.

N-terminal Deletions

To investigate the role of the N-terminal extension of PduB a series of deletion mutants were constructed and analyzed (Figure 2A). Deleted regions are 1) PduB Δ3-33, an almost complete deletion of the N-terminus that keeps intact a native ribosome binding site in the chromosome; 2) PduB Δ6-12, a deletion that encompasses half of the highly conserved predicted α-helix; 3) PduB Δ11-25, a truncation of the N-terminus by 15 of the 37 amino acids; 4) PduB Δ27-32, a deletion in a proline rich area of the linker region; 5) PduB M38A, a single amino acid substitution that changed the start codon of PduB' to alanine such that only PduB is produced, although with an M38A mutation.

Effect of N-terminal PduB deletions on MCP assembly

Prior studies showed that *Salmonella* mutants unable to properly assembly the Pdu MCP grow faster that wild-type on 1,2-PD minimal medium with limiting B_{12} (Havemann *et al.* 2002, Cheng *et al.* 2012, Sinha *et al.* 2012, Sinha *et al.* 2014). This phenotype is due to increased access of the lumen enzymes to their substrates. Therefore, growth rate at limiting B_{12} provides a test for the structural integrity of the Pdu MCP. Growth Assays of the deletion mutants described above showed a range of growth rates (Figure 2B). Deletions of the entire N terminus (PduB Δ3-33), truncation of the N-terminus (PduB Δ11-25), and deletion of the α-helical region (PduB Δ6-12) exhibit growth phenotypes that are characteristic of severe MCPs assembly defects (broken MCPs). Strikingly, the PduB Δ6-12 growth phenotype was similar to that of PduB Δ3-33 and Δ*pduBB'* mutation, suggesting that this small region of the N-terminal helix plays a key role in

MCP assembly. In contrast, deletion of a portion of the linker region PduB Δ27-32 grew similar to wild-type. Interestingly, PduB M38A mutant, which expresses only PduB and not PduB' has a minimal growth defect indicating the PduB' protein is dispensable for MCP formation.

To further test the PduB Δ27-32 and PduB M38A mutants for MCP assembly defects, we purified MCPs from each deletion mutant. The PduB M38A and PduB Δ27-32 mutants gave reasonably good overall MCP yields of purified MCPs relative to wild type, 70% and 50% respectively. The presence deletions in each mutant was confirmed by the SDS-PAGE banding pattern of purified MCPs (Figure 3). As expected, the PduB M38A has a missing PduB' band due to the start codon of PduB' being mutated to an alanine. Interestingly, this is the only band that appeared to be affected as every lumen enzyme and shell protein is accounted for in the PduB M38A lane. Likewise, deletion in the linker region of the N-terminus, PduB Δ27-32, showed a similar banding pattern to wild-type LT2. The only difference was the PduB band migrating lower than LT2 due to the five amino acid deletion. In both mutants, all lumen enzymes appear to be present as evidenced by their bands in the SDS-PAGE gel. To further test this, we performed a dioldehydratase (DDH) activity assay on the purified MCPs. DDH activities of the PduB M38A (24.3±1.2 μmol·min^{-1}·mg^{-1}) and PduB Δ27-32 (23.8±1.1 μmol·min^{-1}·mg^{-1}) mutants showed similar activity to wild-type LT2 (25.4±0.8 μmol·min^{-1}·mg^{-1}) indicating that the DDH enzyme in the PduB deletions was intact and transport of 1,2-PD across the shell was not impaired.

The other N-terminal deletions mutants analyzed (PduB Δ3-33, PduB Δ11-25, and PduB Δ6-12) all showed severe growth phenotypes indicative of a broken MCP shell (Figure 2B). To further examine the effects of these mutations, we purified MCPs of each and observed evaluated

their protein content by SDS-PAGE gels. Figure 3 shows the protein bands present in wild-type and mutant MCPs. Focusing on the lumen enzyme bands (PduG, PduC, PduP, PduQ+O, and PduD) the deletion mutants showed drastic band patterns changes compared to wild-type LT2. In the PduB Δ3-33 lane, almost no discernable bands are observed, suggesting that the N-terminal portion of PduB is required for MCP shell assembly. Interestingly, in both the PduB Δ11-25 and PduB Δ6-12 lanes, the lumen enzyme content is greatly reduced, but the major shell proteins are observed. This suggests that there is a functional region within the N-terminus of PduB that aids in lumen enzyme recruitment. Yields of MCPs was also drastically lowered compared to that of wild-type as only a 6%, 9%, and 20% recovery was seen for PduB Δ3-33, PduB Δ6-12, and PduB Δ11-25, respectively. On the surface, the low MCP yields may indicate that the MCPs formed are unstable, but the lack of lumen enzymes drastically lowers the total MCP protein, which affects yield calculations. We also measured the DDH activity in the purified deletion mutant MCPs. The values determined were below detection, 2.3 $\mu mol \cdot min^{-1} \cdot mg^{-1}$, and 2.4 $\mu mol \cdot min^{-1} \cdot mg^{-1}$ for PduB Δ3-33, PduB Δ6-12, and PduB Δ11-25, respectively. There was no PduP present in the PduB Δ3-33 and PduB Δ11-25 SDS gels. In the case of the PduB Δ6-12 mutant, there appears to be a PduP band present in the purified MCP, but the specific activity was 0.2 $\mu mol \cdot min^{-1} \cdot mg^{-1}$, which is about 100-fold lower than wild-type. Thus, PduB is extremely important for the association of the lumen enzyme with the shell of the Pdu MCP.

Point Mutants in the N-terminal α-helix

The deletion mutants described above showed that the predicted α-helical region of pduB (residues L6 to V18) is essential to MCP assembly. To further investigate its role, point mutations along the predicted helix were constructed. Interestingly, modeling of the helix using

the PEP-FOLD software indicates that there is a hydrophobic and hydrophilic face. All positions on the helix were examined for functional roles by changing amino acid side chains from polar to non-polar i.e. changing leucine to threonine and alanine to serine. These point mutants encompass the majority of the helix and include: PduB L6T, V7T, E8A, Q9A, I10T, M11S, A12S, Q13A, V14T, and I15T.

Because the PduB Δ6-12 has a broken MCP phenotype when grown on 1,2-PD minimal medium, any point mutation that showed a similar phenotype would be indicative of a key functional residue on the helix. The PduB mutations L6T, E8A, Q9A, A12S, Q13A, and I15T grew similarly to wild-type LT2 on 1,2-PD minimal medium with low B_{12} (Figure 4A). This suggests that these residues do not play a critical functional role on the N-terminal helix. Conversely, the mutations of V7T, I10T, M11S, and V14T showed faster growth than that of wild-type, and in the case of I10T, approached the same growth phenotype as the α-helix deletion (PduB Δ6-12) (Figure 4B) suggesting an essential functional role in the helix. Purified MCPs of three of the four faster growing mutants (V7T, I10T, and M11S) had a lower yield than wild-type LT2; 60%, 40%, and 50% respectively (Figure 5A) perhaps suggestive of MCP instability. On the other hand, all MCP bands, including lumen enzymes, were visible on SDS-PAGE indicating that even though the MCPs were unstable they had normal protein content. Interestingly, models of the N-terminal α-helix show that PduB V7, I10, M11, and V14 (all of which are required for MCP assembly) form a hydrophobic face, suggesting some form of functionality at this specific region of the helix (Figure 5B).

Discussion

Taken together, the data described above indicate an important role for the N-terminus of PduB in assembly of the Pdu MCP and also show that the PduB' shell protein has a less critical role. Production of the PduB’ shell protein was eliminated by changing its start codon to GCG (M38A). This resulted in a strain the expressed only PduB. Interestingly, the M38A mutant showed only a slight increase in growth rate on 1,2-PD minimal medium compared to wild-type LT2. In addition, MCP purified from the M38A mutant had near wild-type yield and normal protein content, including all major shell proteins and lumen enzymes. Thus, we conclude that PduB' is largely dispersible for MCP function and assembly and that there is no inherent functional property in PduB’ has that PduB does not also have.

In contrast, to the minimal phenotypes described above, truncation of the terminus (PduB Δ11-25) and deletion of the helix (PduB Δ6-12) resulted in much faster growth on 1,2-PD minimal medium compared to wild-type. This indicated that residues in the 6-25 region of PduB are essential for MCP assembly. Additionally, these results were substantiated by SDS-PAGE of purified MCPs which showed that these mutants lacked or had a very low content of lumen enzymes, essentially empty MCP shells were obtained by the standard MCP purification protocol (Figure 3). Thus, two independent lines of evidence showed that residues 6-25 are essential for proper MCP assembly. We feel it's unlikely that these mutations cause misfolding of the PduB protein. Prior crystallography studies demonstrated that the PduB' protein is normally folded and expressed even though it lacks the entire N-terminal extension. Furthermore, the PduB Δ11-25 and Δ6-12 mutants still interacted with other MCP shell protein based on SDS-PAGE which would be consistent with normal folding (Figure 3).

The studies presented here also indicated that a hydrophobic patch on the N-terminal α-helix of PduB is required for MCP assembly (V7, I10, M11, and V14). When hydrophilic substitutions are made in this region, it increased the growth rate on 1,2-PD minimal medium almost to levels of a broken MCP. In addition, yields of MCPs during purification were decreased most likely due to MCP destabilization. However, in all substitutions made, lumen enzymes are still present in purified MCPs as evidenced by SDS-PAGE and the activities of DDH and PduP in purified MCPs. Thus, unlike the deletion mutations described above changes at V7, I10, M11, and V14 did not impair lumen enzyme targeting.

The finding that certain PduB deletion mutants are defective in the encapsulation lumen enzymes would appear to contradict earlier studies that indicated the PduP enzyme is encapsulated via binding to the PduA shell protein. In the Δ6-12 and Δ11-25 SDS-PAGE gels, there is a very prominent PduA band, but no PduP band or PduP activity in the MCPs. This suggests that association of PduP with the shell may require interaction with both PduA and PduB and that both interactions are required for its encapsulation. Alternatively, it may suggest that PduB must initiate MCP assembly before the PduA and PduP interaction can occur.

Overall, studies indicated that a short predicted α-helix at the N-terminus of PduB is crucial to MCP assembly (residues 6-12). This appears to extend the theme that terminal extensions on MCP proteins guide assembly. Prior studies showed that in PduD, an N-terminal extension is required for encapsulation into the MCP. PduP has an N-terminal extension that not only is required for directory into the lumen, but also has been shown to interact with the C-terminal extension of the shell proteins PduA and PduJ.

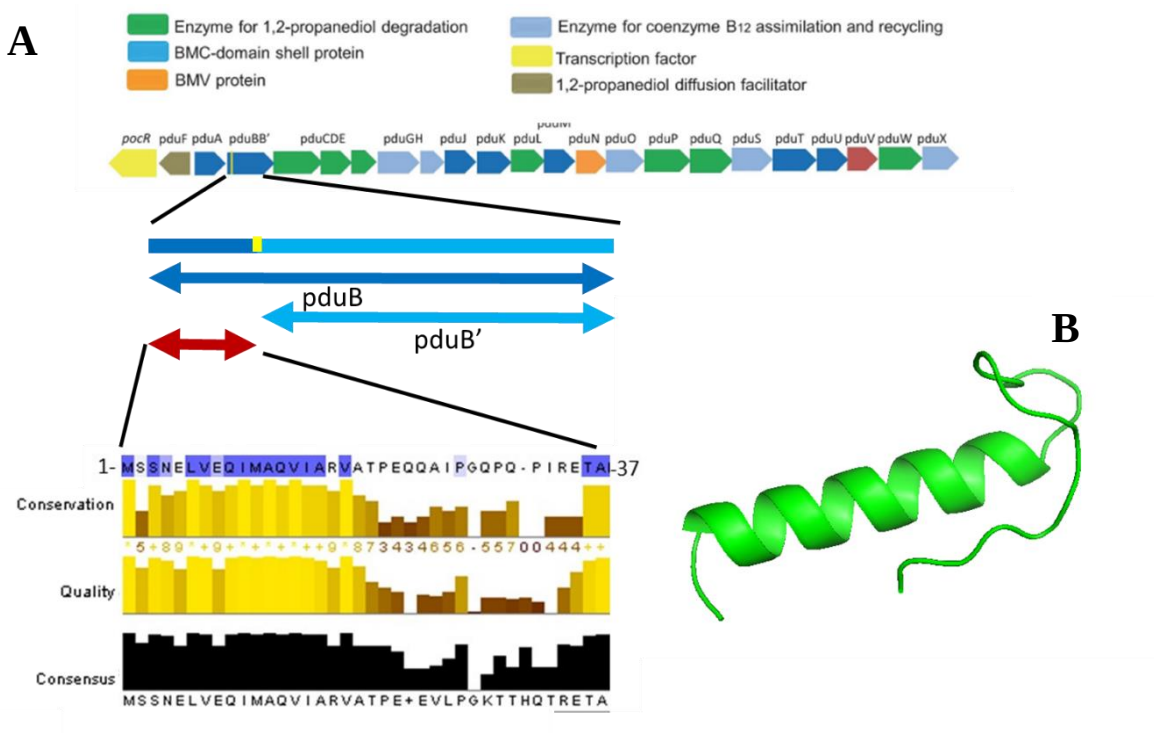

Figure 1. The N-terminal extension of PduB. (A) The N-terminal extension of PduB in the context of the *pdu* operon and a multiple sequence alignment. The residues atop the alignment are highlighted if they contain >80% sequence identity with other PduB homologs. The conservation row scores the alignment that doesn't contain gaps. The Quality row scores residues based on the BLOSUM62 values for that residue. The Consensus row is the consensus sequence based on the input of the alignment. In all rows, the height of the bars indicate a higher score for that particular residue. Visualization of MSA was done using Jalview and the alignment was done using clustalomega. (B) Model of the N-terminus using the PEP-FOLD software. The predicted structure is an α-helix region followed by a linker region.

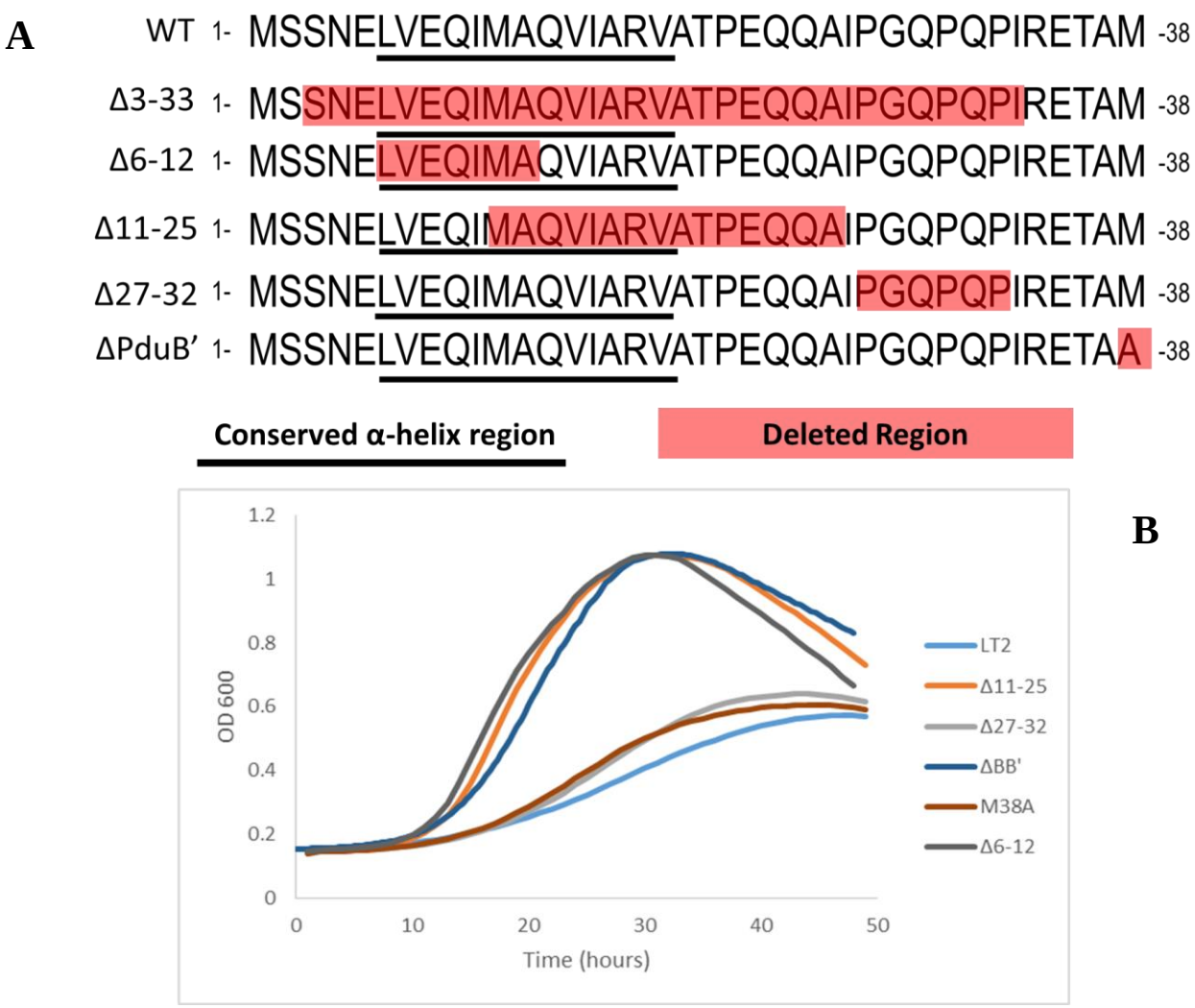

Figure 2. N-terminal deletions and growth phenotypes. (A) Schematic of N-terminal deletions. Residues underlined indicate the evolutionary conserved portion of the N-terminus. Residues highlighted in red are deleted residues in the strain (or altered in the case of ΔPduB') Wild-type (WT) sequence is included at the top for reference. (B) Growth curve of deletion mutants under minimal media (0.6% 1,2 –PD, 50uM Fe, 30nm CN-B12). The LT2 strain is the wild-type strain.

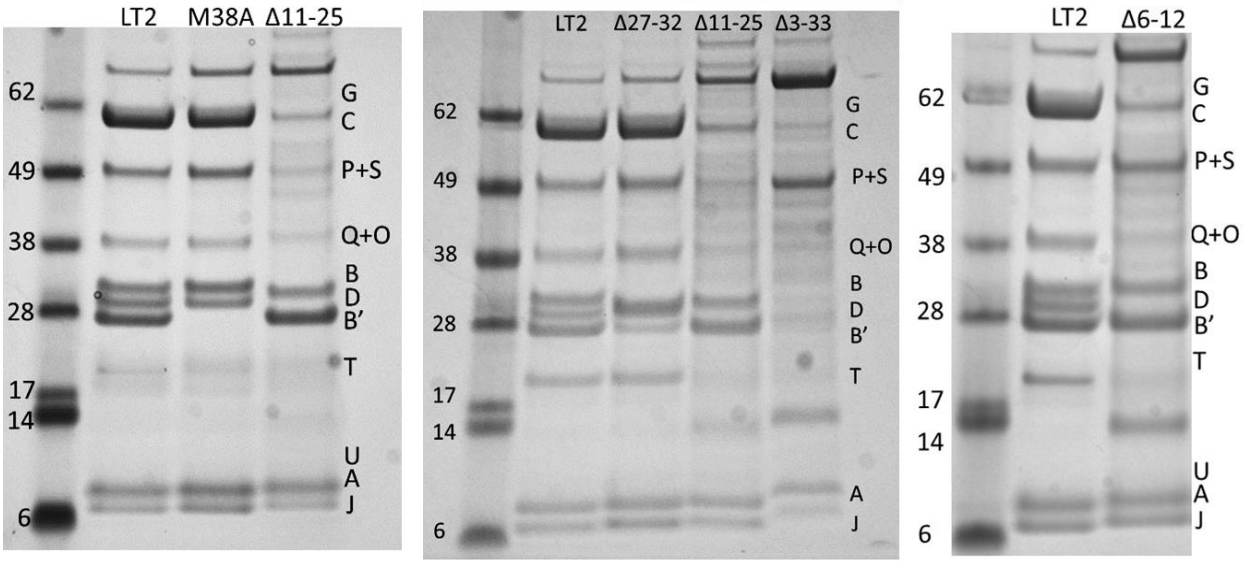

Figure 3. SDS-PAGE gels of purified deletion MCPs. Wild-type is LT2. 10µg of sample was loaded into each lane. Sample names are given at the top and the Pdu components are labeled on the right hand side as they are seen in wild-type.

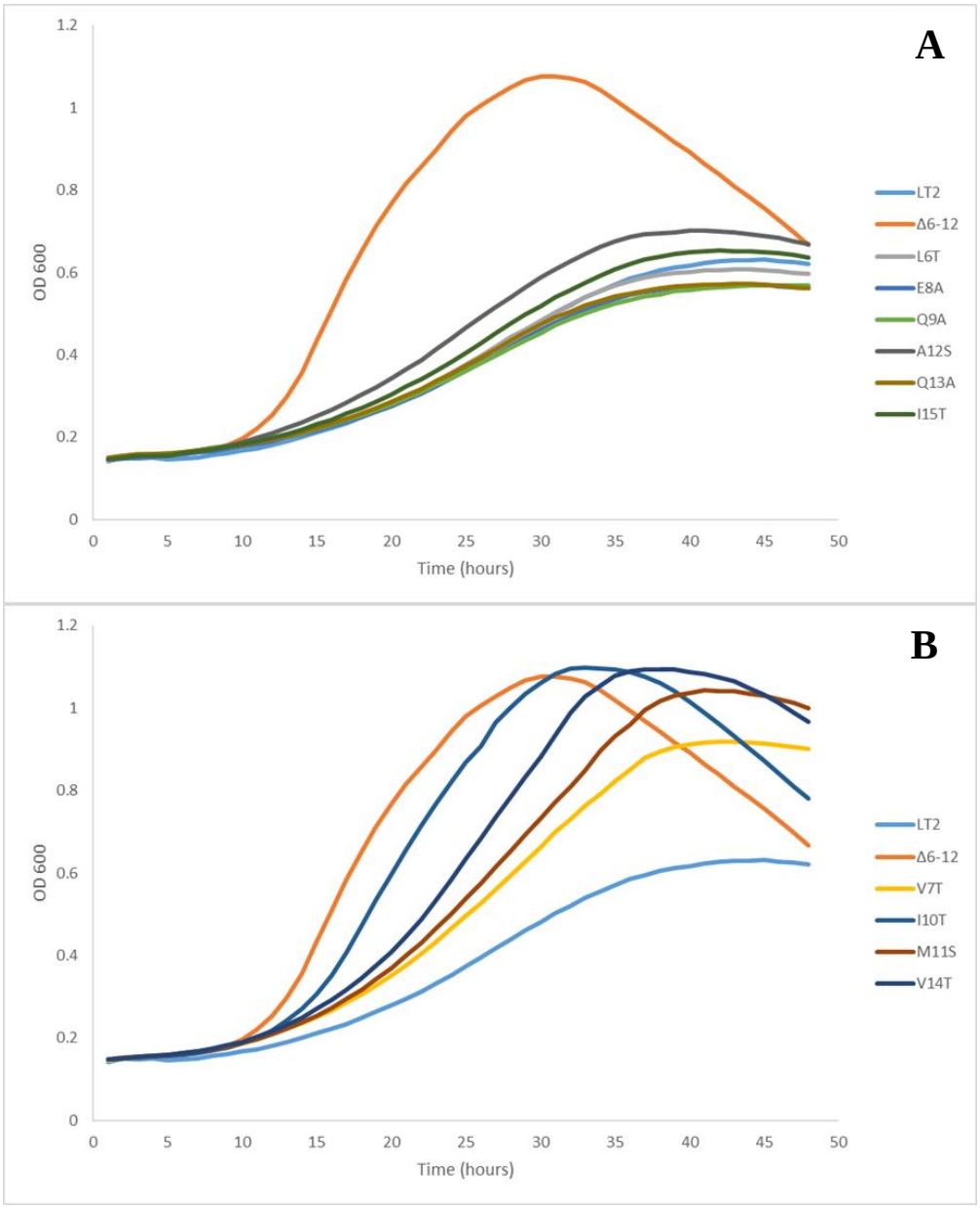

Figure 4. Growth curves of individual point mutants along the predicted α-helix on the N-terminus of PduB on minimal media (0.6% 1,2-PD, 50uM Fe, 20nm CN-B12). (A) Growth curves of mutants that have little to no growth difference from wild-type (LT2). (B) Mutants that show faster growth than wild-type (LT2) at a rate that approaches the phenotype of the α-helix deletion.

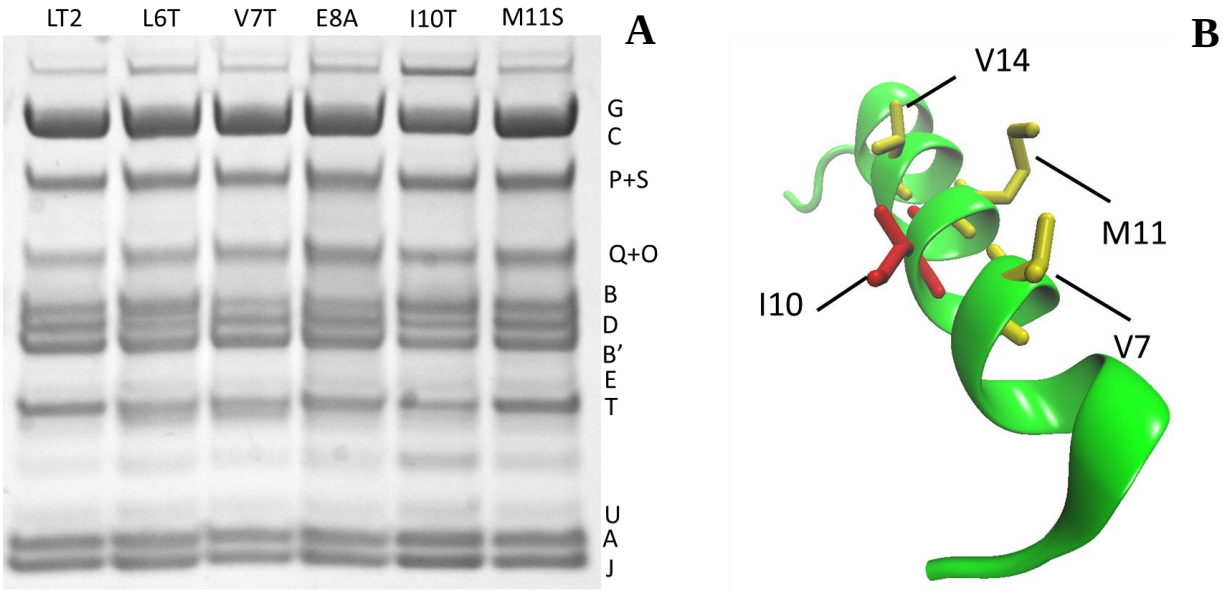

Figure 5. MCPs of select N-terminal points mutants. Labels on the left indicate the component of the Pdu MCP that corresponds to LT2. (B) PEP-FOLD predicted structure of the α-helix in the N-terminus of PduB with highlighted mutants that showed faster growth on minimal media and lower yields in MCP preps (except for V14T which was not purified). The I10 residue is colored red because it produces the most severe growth phenotype and has the lowest yield.

Materials and Methods

Multiple Sequence Alignment

The first 53 amino acids of the PduB sequence were inputted into NCBI PSI-Blast algorithm tool to searching the Reference Proteins (refseq_protein) database excluding *Salmonella enterica* (taxid:28901). The blast search was run for three cycles. 93 sequences were pulled together and a multiple sequence alignment was made using clustalomega and visualized using Jalview.

Generating chromosomal mutations

The same method was used as described in Chapter 2.

Growth assay on minimal media

The same method was used as described in Chapter 2.

Microcompartment Purification

The same method was used as described in Chapter 2.

DDH and PduP assays

The same method was used as described in Chapter2.

Peptide Prediction Software

The first 36 out of 37 residues of the N-terminal extension were inputted into the PEP-FOLD website (http://bioserv.rpbs.univ-paris-diderot.fr/services/PEP-FOLD/). The top rated model was used for structural analysis.

Chromosomal Oligos used in this study

All oligos used in this study were purchased from IDT

Sac-Cat Insetion oligos	Sequence
pduB_111_SC_F	tcacac cgatgtagaaaaaatcttaccgaagggaattagccaatgagcaatacattcaaatatgtatccg
pduB_111_SC_R	cgacaaattccgttaaactgcagctttttctgccatagccgtctctcgttacgccccgccctgccactc
pduB 27-32SC_F	tcatgg cgcaggtgattgcccgtgtggcaacgccggaacaacaggccatcaatacattcaaatatgtatccg
pduB 27-32SC_R	acaaattccgttaaactgcagctttttctgccatagccgtctctcgtatttacgccccgccctgccactc
pduB6_12SC F	gaa aaaatcttaccgaagggaattagccaatgagcagcaatgagaatacattcaaatatgtatccg
pduB6_12SC R	atggcctgttgttccggcgttgccacacgggcaatcacctgttacgccccgccctgccactc
Chromosomal mutation oligo	**Sequence**
PduB del 3-33	cgatgtagaaaaaatcttaccgaagggaattagccaatgagccgagagacggctatggcagaaaaaagctgcagtttaacggaattt
B del 27-32	gtggaacagatcatggcgcaggtgattgcccgtgtggcaacgccggaacaacaggccatcatacgagagacggctatggcagaaaaaagc
PduB M38A	gcaacgccggaacaacaggccatccctggtcaaccccaacctatacgagagacggctgcggcagaaaaaagctgcagtttaacggaattt
pduB del 11-25	gaagggaattagccaatgagcagcaatgagctggtggaacagatccctggtcaaccccaacctatacgagagacggctatggcagaaaaa
pduB del6_12	aaaatcttaccgaagggaattagccaatgagcagcaatgagcaggtgattgcccgtgtggcaacgccggaacaacaggccatccctggt
pduB L6T	tagccaatgagcagcaatgagacggtggaacagatcatggcgcaggtgattgcccgtgtggcaacgccgg
pduB V7T	tagccaatgagcagcaatgagctgacggaacagatcatggcgcaggtgattgcccgtgtggcaacgccgg
pduB E8A	tagccaatgagcagcaatgagctggtggcacagatcatggcgcaggtgattgcccgtgtggcaacgccgg
pduB Q9A	tagccaatgagcagcaatgagctggtggaagcgatcatggcgcaggtgattgcccgtgtggcaacgccgg
pduB I10T	tagccaatgagcagcaatgagctggtggaacagaccatggcgcaggtgattgcccgtgtggcaacgccgg
pduB M11S	tagccaatgagcagcaatgagctggtggaacagatctcggcgcaggtgattgcccgtgtggcaacgccgg
pduB A12S	tagccaatgagcagcaatgagctggtggaacagatcatgagtcaggtgattgcccgtgtggcaacgccgg
pduB Q13A	tagccaatgagcagcaatgagctggtggaacagatcatggcggcagtgattgcccgtgtggcaacgccgg
pduB V14T	tagccaatgagcagcaatgagctggtggaacagatcatggcgcagacgattgcccgtgtggcaacgccgg
pduB I15T	tagccaatgagcagcaatgagctggtggaacagatcatggcgcaggtgactgcccgtgtggcaacgccgg

Strains used in study

Strains used that were previously generated		
Name	**Genotype**	**Lab Strain Number**
LT2	wild-type salmonella lab strain LT2	
LT2/pKD46	LT2/pKD46	BE293
ΔBB'	LT2 ΔBB'	SS23
SC	p41a-Sac-Cat	CS693

Strains generated in this study			
Name	**Genotype**	**Mother/Father**	**BL Strain Number**
27-32SC	pduB 27-32 SC	BE293/SC oligo 27-32	54
27-32SC/pKD46	pduB 27-32 SC/pkD46	BL54/pKD46	55
Δ27-32	pduB Δ27-32	BL55/Bdel 27-32 oligo	56
3-107SC	pduB-SC3-107	BE293/Sc oligo 111	61
3-107SC/pKD46	pduB-SC3-107/PKd46	BL61/pKD46	62
Δ3-33	pduB Δ3-33	BL62/PduB del 3-33 oligo	66
M38A	PduB M38A	BL55/PduB M38A oligo	137
Δ11-25	PduB Δ11-25	BL62/pduB del 11-25 oligo	144
6-12SC	pduB SC 6-12	BE293/ SC oligo 6-12	154
6-12SC/pKD46	pduB SC 6-12/pkD46	BL154/pKD46	155
Δ6-12	PduB Δ6-12	BL155/pduB del6-12 oligo	156
L6T	pduB L6T	BL155/pduB L6T oligo	157
E8A	pduB E8A	BL155/pduB E8A oligo	158
I10T	pduB I10T	BL155/pduB I10T oligo	159
A12S	pduB A12S	BL155/pduB A12S oligo	160
V7T	pduB V7T	BL155/pduB V7T oligo	179
M11S	pduB M11S	BL155/pduB M11S oligo	180
V14T	pduB V14T	BL155/pduB V14T oligo	181
I15T	pduB I15T	BL155/pduB I15T oligo	182
Q9A	pduB Q9A	BL155/pduB Q9A oligo	183
Q13A	pduB Q13A	BL155/pduB Q13A oligo	184

Works Cited

Abdul-Rahman, F., *et al.* (2013). "The distribution of polyhedral bacterial microcompartments suggests frequent horizontal transfer and operon reassembly." J. Phylogen. Evolution. Biol. **1**(4): doi 10.4172/2329-9002.1000118

Axen, S. D., *et al.* (2014). "A taxonomy of bacterial microcompartment loci constructed by a novel scoring method." PLoS Comput. Biol. **10**(10): e1003898.

Bobik, T. A. (2006). "Polyhedral organelles compartmenting bacterial metabolic processes." Appl Microbiol Biotechnol **70**(5): 517-525.

Bobik, T. A., *et al.* (1999). "The propanediol utilization (*pdu*) operon of *Salmonella enterica* serovar Typhimurium LT2 includes genes necessary for formation of polyhedral organelles involved in coenzyme B_{12}-dependent 1, 2-propanediol degradation." J Bacteriol **181**(19): 5967-5975.

Bobik, T. A., *et al.* (1997). "Propanediol utilization genes (*pdu*) of *Salmonella typhimurium*: three genes for the propanediol dehydratase." J Bacteriol **179**(21): 6633-6639.

Cheng, S., *et al.* (2012). "The PduQ enzyme is an alcohol dehydrogenase used to recycle NAD^+ internally within the Pdu microcompartment of *Salmonella enterica*." PLoS One **7**(10): e47144.

Chowdhury, C., *et al.* (2015). "Selective molecular transport through the protein shell of a bacterial microcompartment organelle." Proc Natl Acad Sci U S A **112**(10): 2990-2995.

Chowdhury, C., *et al.* (2014). "Diverse bacterial microcompartment organelles." Microbiol. Mol. Biol. Rev. **78**(3): 438-468.

Fan, C. and T. A. Bobik (2011). "The N-terminal region of the medium subunit (PduD) packages adenosylcobalamin-dependent diol dehydratase (PduCDE) into the Pdu microcompartment." J Bacteriol **193**(20): 5623-5628.

Fan, C., *et al.* (2010). "Short N-terminal sequences package proteins into bacterial microcompartments." Proc Natl Acad Sci U S A **107**(16): 7509-7514.

Fan, C., *et al.* (2012). "Interactions between the termini of lumen enzymes and shell proteins mediate enzyme encapsulation into bacterial microcompartments." Proc Natl Acad Sci U S A **109**(37): 14995-15000.

Havemann, G. D. and T. A. Bobik (2003). "Protein content of polyhedral organelles involved in coenzyme B_{12}-dependent degradation of 1,2-propanediol in *Salmonella enterica* serovar Typhimurium LT2." J Bacteriol **185**(17): 5086-5095.

Havemann, G. D., *et al.* (2002). "PduA is a shell protein of polyhedral organelles involved in coenzyme B_{12}-dependent degradation of 1,2-propanediol in *Salmonella enterica* serovar typhimurium LT2." J Bacteriol **184**(5): 1253-1261.

Heldt, D., *et al.* (2009). "Structure of a trimeric bacterial microcompartment shell protein, EtuB, associated with ethanol utilization in *Clostridium kluyveri*." Biochem J **423**(2): 199-207.

Jorda, J., *et al.* (2013). "Using comparative genomics to uncover new kinds of protein-based metabolic organelles in bacteria." Protein Sci **22**(2): 179-195.

Kerfeld, C. A., *et al.* (2010). "Bacterial microcompartments." Annu Rev Microbiol **64**: 391-408.

Kinney, J. N., *et al.* (2012). "Elucidating essential role of conserved carboxysomal protein CcmN reveals common feature of bacterial microcompartment assembly." J Biol Chem **287**(21): 17729-17736.

Parsons, J. B., *et al.* (2010). "Synthesis of empty bacterial microcompartments, directed organelle protein incorporation, and evidence of filament-associated organelle movement." Mol Cell **38**(2): 305-315.

Rae, B. D., *et al.* (2013). "Functions, compositions, and evolution of the two types of carboxysomes: polyhedral microcompartments that facilitate CO_2 fixation in cyanobacteria and some proteobacteria." Microbiol. Mol. Biol. Rev. **77**(3): 357-379.

Sinha, S., *et al.* (2012). "The PduM protein is a structural component of the microcompartments involved in coenzyme B_{12}-dependent 1,2-propanediol degradation by *Salmonella enterica*." J Bacteriol **194**(8): 1912-1918.

Sinha, S., *et al.* (2014). "Alanine scanning mutagenesis identifies an asparagine-arginine-lysine triad essential to assembly of the shell of the Pdu microcompartment." J Mol Biol **426**(12): 2328-2345.